On Applications of Parity in Virtual Knot Theory

BY

AARON M KAESTNER
B.S., Indiana University, 2002
M.A., Saint Louis University, 2004

THESIS

Submitted in partial fulfillment of the requirements
for the degree of Doctor of Philosophy in Mathematics
in the Graduate College of the
University of Illinois at Chicago, 2011

Chicago, Illinois

Defense Committee:

Marc Culler
Louis Kauffman, Advisor and Chair
David Radford
C. Michael Tsau, Saint Louis University
John Wood

To my wife,

Carrie,

for supporting and encouraging me throughout this journey.

ACKNOWLEDGMENTS

It is my pleasure to thank my advisor Professor Louis Kauffman, without whose guidance and advice I would have not made it to the finish line. I am also indebted to my committee, who have graciously shared a great deal of wisdom and encouragement. Finally, my sincere gratitude goes out to Heather Dye for many mathematically stimulating conversations regarding virtual knot theory.

TABLE OF CONTENTS

TABLE OF CONTENTS (Continued)

CHAPTER **PAGE**

LIST OF TABLES

LIST OF FIGURES

SUMMARY

We investigate applications of parity in virtual knot theory which allow us to generalize previously known invariants - skein polynomials and biquandles. In the skein-theoretic direction we investigate a graphical application of parity to the bracket expansion of the Jones Polynomial as suggested by Manturov. In addition we consider its extension to the Arrow Polynomial as well as to the categorifications of both polynomials. In the process we show how known facts about minimal surface genus carry over to the new setting. Moreover, we provide calculators for these invariants and provide a list of the graphical polynomials for virtual knots with at most 4 real crossings.

Similarly for biquandles, we use crossing parity to construct a generalization which we call Parity Biquandles. These structures include all biquandles as a standard example referred to as the even parity biquandle. Additionally, we find all Parity Biquandles arising from the Alexander Biquandle and Quaternionic Biquandles. For a particular construction named the z-Parity Alexander Biquandle we show that the associated polynomial yields a lower bound on the number of odd crossings as well as the total number of real crossings and virtual crossings for the virtual knot. Moreover we extend this construction to links to produce a lower bound on the number of crossings between components of a virtual link.

CHAPTER 1

INTRODUCTION

Since the introduction of virtual knot theory crossing parity has provided valuable resource for creating invariants. For instance, given a virtual knot the odd writhe (1) (i.e. sum of the signs of the odd crossings) is an easily computable invariant. Recently, Manturov introduced a parity version of the bracket polynomial (2) and described how the construction can pass to Khovanov homology via a filtration on the space of virtual knots. Our first goal here is to investigate these constructions and show how we can apply a similar construction to the arrow polynomial. Along the way we show how known facts about minimal surface genus extend to the categorical setting. In this same vein we apply this philosophy of parity to biquandles and create a collection of new invariants for virtual knots.

We begin in Chapter 2 by giving a brief introduction to Virtual Knot Theory. This is followed by an investigation of the role of parity in virtual knots and links with an emphasis on parity in chord diagrams. This sets up a general approach to parity invariants which we apply in the following chapters. It should be noted that invariants for virtual knots arising from the analysis of chord diagrams were introduced in (3) and further explored by Goussarov, Polyak and Viro in (4). Similarly, virtual knot invariants arising from an analysis of parity have previously been constructed by Kauffman (1), (5), Manturov (6), Turaev (7) and Dye (8). Our approach to parity was inspired by Manturov's philosophy of parity (9),(10),(6) and the construction of the parity bracket polynomial (2), (5).

Chapter 3 recalls the bracket and arrow polynomials for virtual knots. We review Manturov's graphical parity bracket polynomial and show how we can use the same approach to create a parity arrow polynomial. Along the way we show how we can use these polynomials to produce lower bounds on the minimal surface genus for a virtual knot.

The history of the bracket polynomial (and Jones polynomial) as well as the arrow polynomial is rich. For an introduction to the bracket polynomial we point the reader to (11) and (12). Similarly, for the arrow polynomial we recommend the introductory paper (13) as well as the work of Dye and Kauffman in (14) (15).

Chapter 4 continues along the same vein as we review the categorifications of the bracket and arrow polynomials. We then investigate the categorified extensions of the graphical skein polynomials introduced in Chapter 3.

The Jones polynomial was categorified by Khovanov in (16). For an introduction to Khovanov homology we point the reader to (17) and (18). Since Khovanov's seminal work categorification in classical knot theory has been a fruitful topic of research. Notably, Rasmussen (19) used a spectral sequence introduced by Lee (20) to produce a lower bound on the slice genus for a classical knot. Recently it was also announced by Kronheimer and Mrowka (21) that Khovanov homology detects the unknot by showing there is a spectral sequence from (reduced) Khovanov homology to instanton Floer homology. This is exciting news as it provides support for the similar conjecture for the Jones polynomial.

The study of Khovanov homology in relation to virtual knot theory is still rather new. The introduction of the virtual crossing brings with it a new diagram for the unknot which has the property $d^2 = 0$ (using Khovanov's original definition) only for coefficients in $\mathbb{Z}_2$. A wonderful explanation of how far we can take Khovanov's original work is given by Viro in (22). To work around this new problem methods have been introduced by Asaeda, Przytycki, and Sikora (23) as well as Manturov (24). The Asaeda-Przytycki-Sikora approach requires not only a diagram but an embedding in a (fixed) thickened surface. On the other hand, Manturov's version introduces signed, oriented and ordered basis on the states of the cube complex to make all faces commute.

Other than its introduction in (25) and recent review in (5), little has been written about the categorifications of the arrow polynomial. In this regard we produce lower bounds for the homological width of the fully-graded categorification as well as extend bounds for the surface genus to the categorical setting. In the Appendix we provide an collection of programs for computing all of the invariants discussed in this paper. We hope these programs will increase the awareness and interest in the study of these categorifications.

Biquandles have a rich history in virtual knot theory including work by Sawollek (26), Nelson (27), Fenn, Kauffman and Jordan-Santana (28) Kauffman and Manturov (29), Kauffman and Hrencecin (30), Kauffman and Radford (31), and Bartholomew and Fenn (32), (33). In Chapter 5 we review the definition of biquandles for virtual knots and show how we can apply a similar philosophy to extend these invariants to parity biquandles. In particular we focus on the linear case and construct extensions of the generalized Alexander biquandle (31) as well as a family of quaternionic biquandles (33). We show how these new invariants produce lower bounds on the virtual crossing number, even and odd self-crossing numbers as well as virtual and classical link crossing numbers.

CHAPTER 2

PARITY AND VIRTUAL KNOTS AND LINKS

2.1 Virtual Knot Theory

In (3) Kauffman introduced virtual knots and links as a natural extension of classical knots and links. Virtual Knot Theory can be though of both as (1), equivalence classes of embeddings of closed curves in a thickened surface (possibly non-orientable) up to isotopy and handle stabilization on the surface and (2) the completion of the signed oriented Gauss codes (i.e. an arbitrary Gauss code corresponds to a virtual knot while not every Gauss code corresponds to a classical knot.)

We recall in Figure Figure 1 the Reidemeister Moves for classical knot diagrams. Figure Figure 2 displays the additional Virtual Reidemeister Moves for the theory in terms of planar diagrams. Here we have introduced the *virtual crossing* which is neither an under-crossing or over-crossing. We represent the virtual crossing by two arcs which cross and have a circle around the crossing point.

Note that the move in Figure Figure 3 is not an equivalence relation for diagrams of virtual knots and links. It can be shown that adding this relation to the Virtual Reidemeister Moves allows one to unknot any virtual knot. For this reason we refer to this move as the "Forbidden Move."

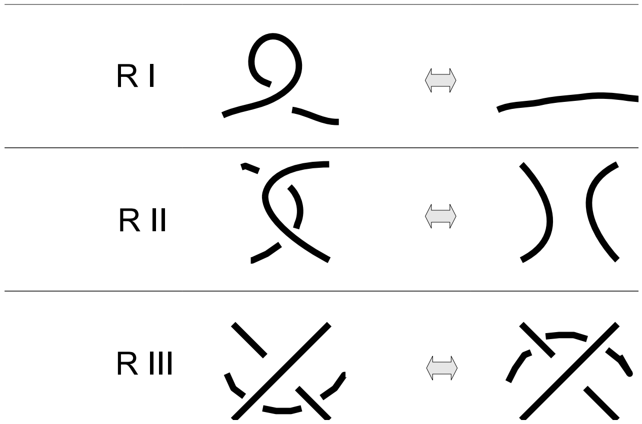

Figure 1. Reidemeister Moves

2.2 Parity, Virtual Knots and the Reidemeister Moves

Given a diagram D for a knot K label each crossing uniquely 1 through n, where n is the total number of crossings in D. Let P an arbitrary base-point on the knot. Starting at P and following the orientation of the knot we can construct a sequence of length $2n$ with terms corresponding to each crossing we encounter. Each term is a 3-tuple of the form (O or U, Crossing Number, $\pm$) where O or U corresponds to an over or under-crossing respectively and $\pm$ corresponds to the sign of the crossing. The resulting code is referred to as the (signed, oriented) *Gauss Code* for the diagram D of the knot K.

The Gauss code can be represented diagrammatically as follows. Given a circle (often refereed to as the *core circle*) place upon it in a counterclockwise fashion $2n$ points where each point is labeled by a crossing name (an integer between 1 and n) in the cyclic order corresponding

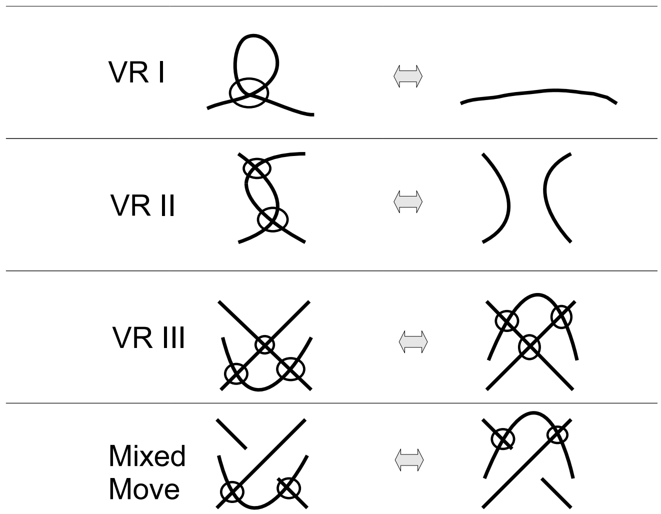

Figure 2. Virtual Reidemeister Moves

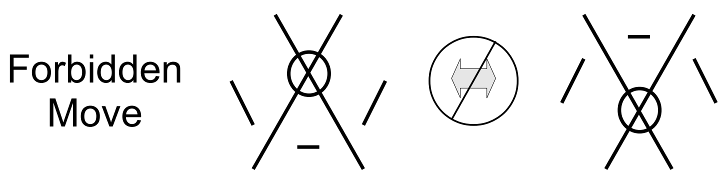

Figure 3. The "Forbidden Move"

to the Gauss code. Between the two occurrences of a crossing on the core circle, place an signed, oriented chord where the sign corresponds to the crossing sign and the orientation goes from the over crossing to the under crossing. We call this the *Chord Diagram* for D (4), (3). For example, the knot 3.1 in Figure Figure 44 has Gauss Code

$$``O1-, O2-, U1-, O3+, U2-, U3+''$$

and chord diagram as in Figure Figure 4.

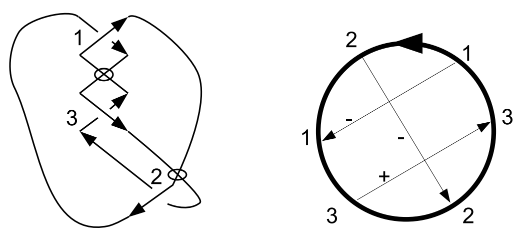

Figure 4. Chord Diagram for Virtual Knot 3.1

Definition 2.2.1. *Given a diagram D for a knot K we can label each crossing as even or odd in the following manner. For each crossing v locate the 2 occurrences of v in the Gauss code for D. If the number of crossing labels between the two occurrences of v is even then label the crossing even. Else it is labeled odd.*

Remark 2.2.1. *This parity is well-defined for a 1-component links (i.e. knots) as the number of crossing labels in the Gauss code is $2n$ where n is the number of crossings.*

It is important to notice how parity behaves under the classical Reidemeister moves. Note that virtual Reidemeister moves do not change the Gauss code or chord diagram and thus do not affect parity.

- **Reidemeister I**

  A first Reidemeister move is always even, as is shown in Figure Figure 5

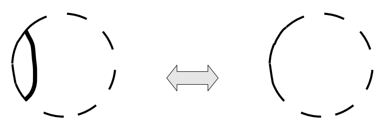

Figure 5. Reidemeister I equivalence for flat chord diagram

- **Reidemeister II**

  The two crossings involved in a second Reidemeister move are either both even or both odd. To see this, note that in Figure Figure 6 if the number of crossings before the second Reidemeister move is $n+2$ and a and b denote the number of markings on the core circle as labeled in the figure then $a+b=2n$ is even. Hence either a and b are both even or both odd.

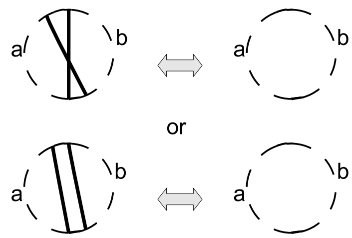

Figure 6. Reidemeister II equivalence for flat chord diagram

- **Reidemeister III**

  In a third Reidemeister move either all crossings are even or two are even and one is odd. To see this note that in Figure Figure 7 if the number of crossings not involved in the third Reidemeister move is n and a, b and c denote the number of markings on the core circle as labeled in the figure then $a + b + c = 2n$ is even. Hence either a, b and c are all even or two are odd and one is even.

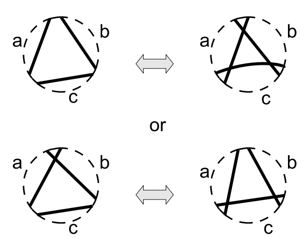

Figure 7. Reidemeister III equivalence for flat chord diagram

2.3 Parity and Virtual Links

For this subsection we will take a wider view and consider the space of virtual links (2 or more components). One should note that our definition of even and odd parity does not naturally extend. For example, the links in Figure Figure 8 illustrate some of the difficulty in the natural extension.

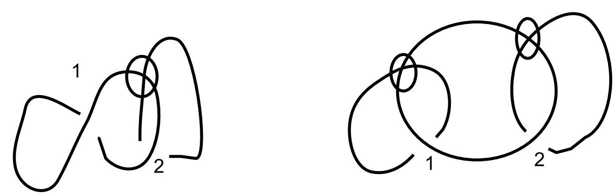

Figure 8. Examples of Difficulty in Extending the Definition to Links

Omitting signs, the left link in Figure 8 has Gauss code "$O1, U1, O2; U2$" while the other has Gauss code "$U1; O1, O2; U2$". In the first of these Crossing 1 is both even and odd in the first component while Crossing 1 is either even or odd depending upon whether you examine the first or second link component.

We may circumvent this pitfall by defining even and odd for self-crossings based on the parity of self-crossing in each component while labeling crossings shared by 2 components as link crossings.

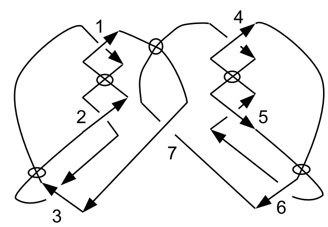

Figure 9. Link Parity Crossing Labelings

Example 2.3.1. *The link in Figure Figure 9 has Gauss Code*

$$``O1, O7, O3, U1, U2, U3, O2; U4, O5, U6, U5, O4, O6, U7''$$

Crossings 1, 2, 4 and 5 are odd, crossings 3, and 6 are even and crossing 7 is a link crossing.

As we did with odd crossings, we investigate the invariance of crossings between links to provide the framework for generalizing the parity polynomials. We will call a crossing where both arcs involved are in the same link component a self-crossing while a crossing whose arcs are in separate components a link-crossing.

- **Reidemeister I**

  In a Reidemeister I move only a single link component is involved hence is always an even self-crossing.

- **Reidemeister II**

  The two arcs involved in a second Reidemeister move are either both in the same component or each is in a different component. Thus either both crossings above are self-crossings or both crossings are link-crossings.

- **Reidemeister III**

  In a third Reidemeister move either all strands involved are in one component, or two in one component and one in another or all three in separate components. Thus either all crossings are self-crossings, or one self-crossing and two link-crossings or three link-crossings respectively.

CHAPTER 3

PARITY AND SKEIN POLYNOMIALS

3.1 The Normalized Bracket Polynomial

Recall the construction of the bracket polynomial introduced by Kauffman in (11).

Definition 3.1.1. *Given a diagram D for a virtual knot K the bracket polynomial of K is defined by the relations in Figures Figure 10.*

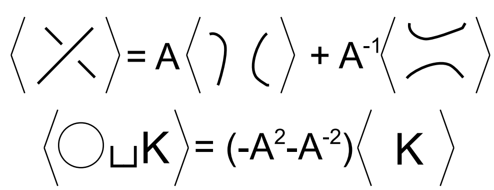

Figure 10. Bracket Polynomial Skein Relations

To be more precise, suppose D is an n-crossing diagram for the (virtual) knot K. We generate the polynomial by smoothing every crossing in each of the two ways possible.The result of each smoothing at a particular crossing is multiplication the term by, A or A^{-1}, following the conventions of Figure Figure 10. For a particular crossing we call these the *A-smoothing* and *B-smoothing* respectively.

Next let $s = (s_1, \ldots, s_n)$ where $s_i \in \{0, 1\}$. Define the *state* of D corresponding to s to be the result of applying an B-smoothing at crossing i when $s_i = 0$ and an A-smoothing at crossing i when $s_i = 1$. Furthermore define $\langle D \mid s \rangle$ to be the product of A's and A^{-1}'s that label the state s multiplied by the loop value $d^{\|s\|}$ where $d = (-A^2 - A^{-2})$ is the loop value. Here each state is a choice of smoothing for each crossing and is labeled with the type of smoothing at each of its sites.

Remark 3.1.1. *This definition of the bracket polynomial is renormalized from the standard definition. Here the value of a single loop is* $d = (-A^2 - A^{-2})$ *as opposed to* 1 *in the standard definition. This has the effect that our definition is* $d \times \langle\langle K \rangle\rangle$ *, where* $\langle\langle K \rangle\rangle$ *is the standard definition of the bracket polynomial as defined in (11).*

Definition 3.1.2. *Let* $\mathcal{S}$ *be the collection of all states of a diagram* D *for a knot* K*. We may define the* Bracket Polynomial of K *to be*

$$\langle K \rangle = \sum_{s \in \mathcal{S}} \langle D \mid s \rangle$$

It follows from this definition that the state sum is well defined and the expansion identities in Figure Figure 10 follow from the state sum definition.

Definition 3.1.3. *Given a virtual knot K with diagram D, the Normalized Bracket Polynomial of K is given by*

$$f_A(K) = f_A(D) = (-A)^{-3\omega(D)} \langle D \rangle$$

where $\langle D \rangle$ *is the bracket polynomial of* D *and*

$$\omega(D) = writhe(D) = (\#\ positive\ crossings\ in\ D) - (\#\ negative\ crossings\ in\ D).$$

Theorem 3.1.1. *The Normalized Bracket Polynomial is an invariant of (virtual) knots.*

Proof. Here each loop, regardless of virtual crossings, evaluates as the loop value d. See (11) ∎

3.2 The Arrow Polynomial

Similarly we recall the construction of the Arrow Polynomial introduced in (13).

Given a diagram D for a virtual knot K the (un-normalized) Arrow Polynomial of K is defined by the smoothing relations in Figure Figure 11 and reduction relations in Figure Figure 12 analogously to the prior construction of the Bracket Polynomial.

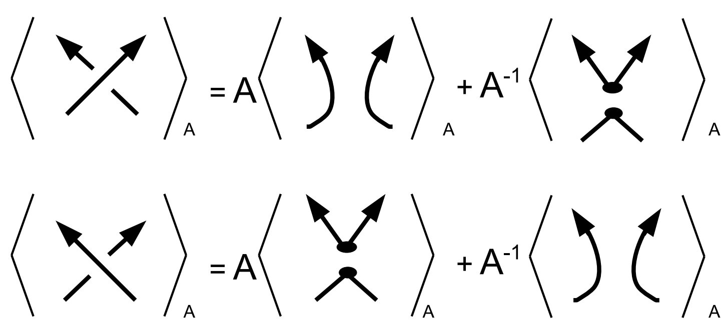

Figure 11. Arrow Polynomial Crossing Relations

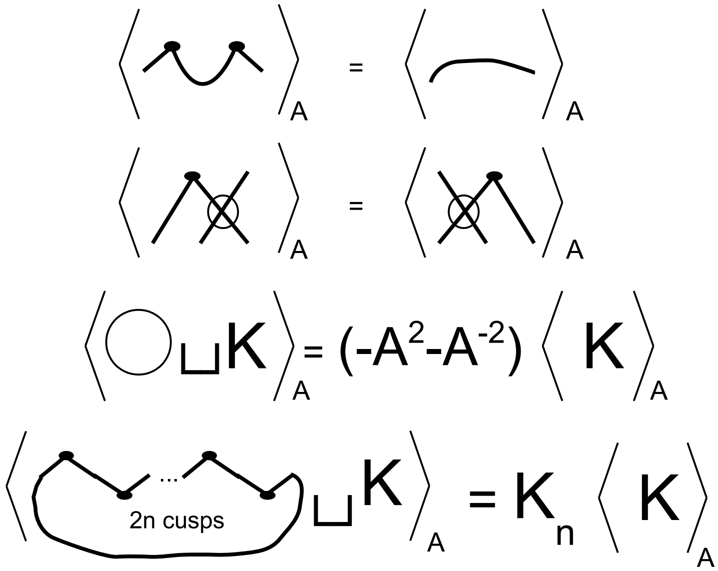

Figure 12. Arrow Polynomial Reduction Relations

Notice that the smoothing relations for the Arrow Polynomial are different depending on the sign of the crossing. While we still have an A-smoothing and B-smoothing and will refer to these choices, we may also differentiate the smoothings by whether-or-not they agree with the original (pre-smoothed) orientation of the knot diagram. If the orientations agree we call these *oriented smoothings* else they are *disoriented smoothings*. The disoriented smoothings create cusps in the state which satisfy the relations in Figure Figure 12. Moreover, these cusps introduce an infinite family of variables $\{K_n\}$,$n \in \mathbb{N}$ via the rules in Figure Figure 12. That is we cancel consecutive cusps pointing in the same direction (locally both inward or outward) and resolve virtual crossings as depicted in Figure Figure 12. The remaining $2n$ alternately-oriented cusps on a loop are counted and we assign the loop the value $\{K_n\}$ when $n > 0$. We refer to these variables as *Arrow Numbers* (15) (13).

Definition 3.2.1. *Given a virtual knot K with diagram D, the un-normalized Arrow Polynomial of K is given by*

$$\langle D \rangle_A = \sum_{s \in \mathcal{S}} \langle D \mid s \rangle_A$$

where $\mathcal{S}$ is the collection of all states of D.

Definition 3.2.2. *Given a virtual knot K with diagram D, the Normalized Arrow Polynomial of K is given by*

$$AP(K) = AP(D) = (-A)^{-3\omega(D)} \langle D \rangle_A$$

where $\langle D \rangle_A$ is the arrow polynomial of D and

$$\omega(D) = \mathit{writhe}(D) = (\#\ \mathit{positive\ crossings\ in}\ D) - (\#\ \mathit{negative\ crossings\ in}\ D).$$

Theorem 3.2.1. *The Normalized Arrow Polynomial is an invariant of virtual knots.*

Proof. See (13). ∎

Remark 3.2.1. *The Jordan Curve Theorem implies that the Arrow Polynomial is equivalent to the Normalized Bracket Polynomial for classical knots.*

3.2.1 The Arrow Polynomial and Surface Genus

Recall that virtual knots are in 1-1 correspondence with equivalence classes of knots in thickened oriented surfaces modulo 1-handle stabilization and Dehn twists. This raises the question, given a knot, what is the minimal genus for this embedding.

Definition 3.2.3. *Given a virtual knot K, the (orientable) surface genus of K, $s(K)$, is the minimal genus of the surface S_g such that $S^1 \hookrightarrow S_g \times I$ corresponds to K.*

Theorem 3.2.2. *(Theorem 4.5 of (15)) Let K be a virtual knot diagram with arrow polynomial $\langle K \rangle_A$. Suppose that $\langle K \rangle_A$ contains a summand with the monomial $K_{i_1}^{e_1} K_{i_2}^{e_2} \cdots K_{i_n}^{e_n}$ where $i_j \neq i_k$ for all j, k in the set $\{1, 2, \ldots, n\}$. Then n determines a lower bound on the genus g of the minimal genus surface in which K embeds. That is, if $n \geq 1$ then the minimum genus is 1 or greater and for $g \geq 2$ if $n > 3g - 3$ then $s(K) > g$.*

Proof. The proof follows from showing that non-zero arrow numbers correspond to essential curves on the surface. The bounds follow from considering the maximal number of non-intersecting essential curves on the surface which do not bound annuli. ∎

Remark 3.2.2. *In the $g = 1$ case it can be shown that if there is more than 1 non-intersecting essential curve then they must bound an annulus. Hence if $\langle L \rangle_A$ contains a summand with a monomial of the form $K_i K_j$ with $i \neq j$ then the minimal surface genus is at least 2.*

3.2.2 Examples

Following the naming conventions in Jeremy Green's Virtual Knot Tables (34) we consider virtual knot 3.1 as shown in Figure Figure 44. Figures Figure 14 and Figure 15 show how one

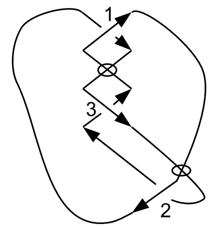

Figure 13. Virtual Knot 3.1

uses the state-sum formulas from the previous sections to arrive at the respective polynomials. Note that by the previous theorem the arrow polynomial gives that the surface genus of virtual knot 3.1 is at least one. The diagram above has surface genus 2.

3.3 Manturov's Graphified Parity Bracket Polynomial

Manturov (2) introduced the following graphical modification for the bracket polynomial.

Definition 3.3.1. *The parity bracket polynomial of a virtual knot K is defined by the rules in Figure Figure 16.*

Definition 3.3.2. *Given a virtual knot K with diagram D, The normalized parity bracket polynomial of K is given by*

$$PF_A(K) = PF_A(D) = (-A)^{-3\omega(D)}\langle D\rangle_P$$

where $\langle D\rangle_P$ *is the parity bracket polynomial of D and*

$$\omega(D) = writhe(D) = (\#\ positive\ crossings\ in\ D) - (\#\ negative\ crossings\ in\ D).$$

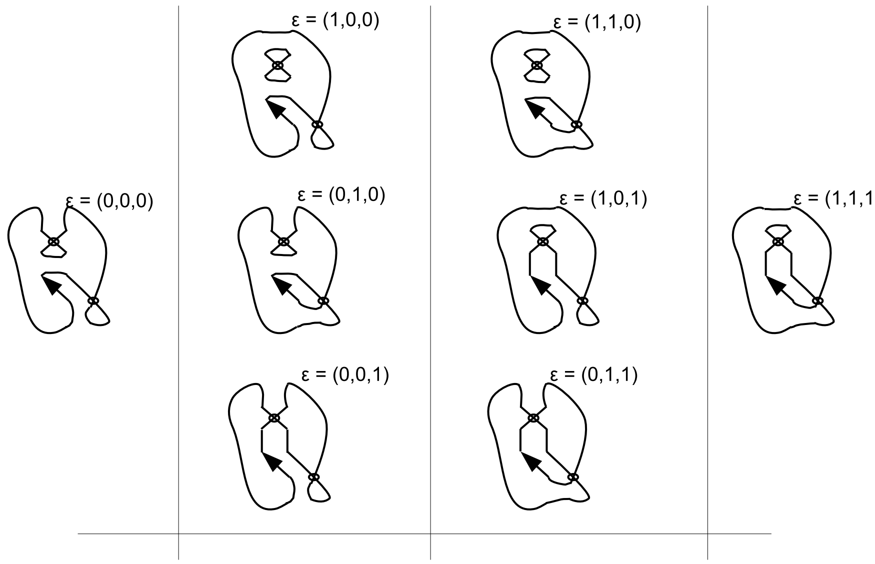

$$A^3(-A^2-A^{-2}) \quad + \quad A[(-A^2-A^{-2})^2 + (-A^2-A^{-2}) + (-A^2-A^{-2})] \quad + \quad A^{-1}[(-A^2-A^{-2})^2 + (-A^2-A^{-2}) + (-A^2-A^{-2})^2] \quad + \quad A^{-3}(-A^2-A^{-2})$$

$$<D>= (-A^{-1}-A^{-5}) \text{ and writhe}(D) = -1$$

$$F_K(A) = -A^3<D>= -A^3(-A^{-1}-A^{-5}) = -A^2-A^{-2}$$

Figure 14. Virtual Knot 3.1 Bracket Polynomial State-Sum

Theorem 3.3.1. *The parity bracket polynomial is an invariant of virtual knots.*

Proof. We give an outline of the proof. The majority of this proof follows from Kauffman's proof of invariance for the bracket polynomial (11). You can find a similar proof by Manturov in (2).

1. Reidemeister I follows from the writhe normalization.
2. Reidemeister II follows for even crossing as in the classical case and for odd crossing by the reduction relations.

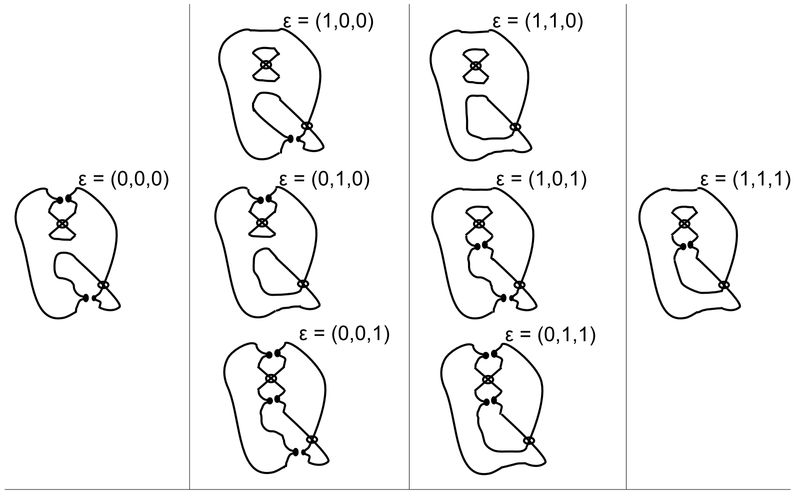

$$A^3K_1 + A[(-A^2-A^{-2})K_1 + (-A^2-A^{-2}) + K_2] + A^{-1}[(-A^2-A^{-2})^2 + K_1 + K_1^2] + A^{-3}(-A^2-A^{-2})$$

$$\langle D\rangle_A = (A^{-1}K_1^2 + AK_2) \text{ and writhe}(D) = -1$$

$$AP_K(A) = -A^3\langle D\rangle_A = -A^3(A^{-1}K_1^2 + AK_2) = -A^2K_1^2 - A^4K_2$$

Figure 15. Virtual Knot 3.1 Arrow Polynomial State-Sum

3. Reidemeister III follows by applying the “Kauffman Trick” at a single even crossing. (Note in the mixed case there is only 1 even crossing to choose.)

∎

Example 3.3.1. *Figure Figure 17 displays the calculation of the parity bracket polynomial for virtual knot 3.1 in Figure Figure 44.*

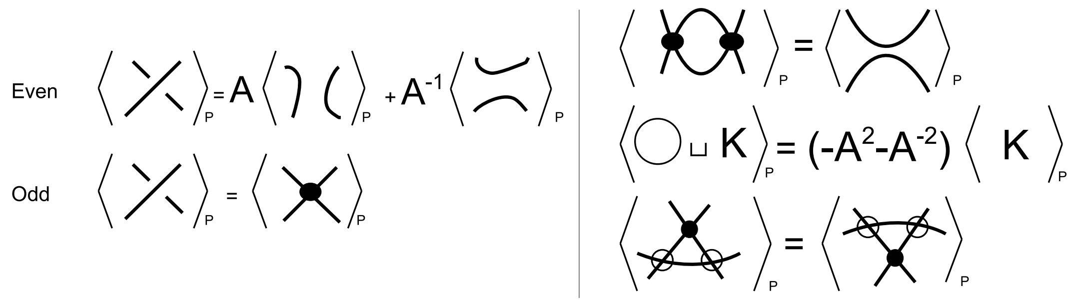

Figure 16. Parity Bracket Polynomial Skein Relations

Notice that the parity bracket polynomial contains graphical coefficients. Since all of the remaining crossings are virtual or graphical (i.e. coming from an odd crossing) the only skein relations we may apply to the graphical coefficients are the graphical Reidemeister II move as well as the graphical detour move.

3.3.0.1 The Parity Bracket Polynomial and Surface Genus

Definition 3.3.3. *Given a graphical coefficient D the minimal surface genus $s(D)$ is the minimal genus for an orientable surface S_g such that there is an embedding $D \to S_g$. Given the product of graphical coefficients $D_1 D_2 \cdots D_n$ the surface genus $s(D_1 D_2 \cdots D_n)$ is the minimal genus for an orientable surface S_g such that there exist disjoint embedding $D_i \to S_g$ for $i \in \{1, \ldots, n\}$.*

Remark 3.3.1. *Note that in the case of the parity bracket polynomial the minimal surface genus for a graphical coefficient is the same as the minimal surface genus for the underlying flat virtual knot. Hence for a graphical coefficient D, $s(D) \geq s(K)$ where K is any virtual knot arising from D by resolving all crossing in any manner.*

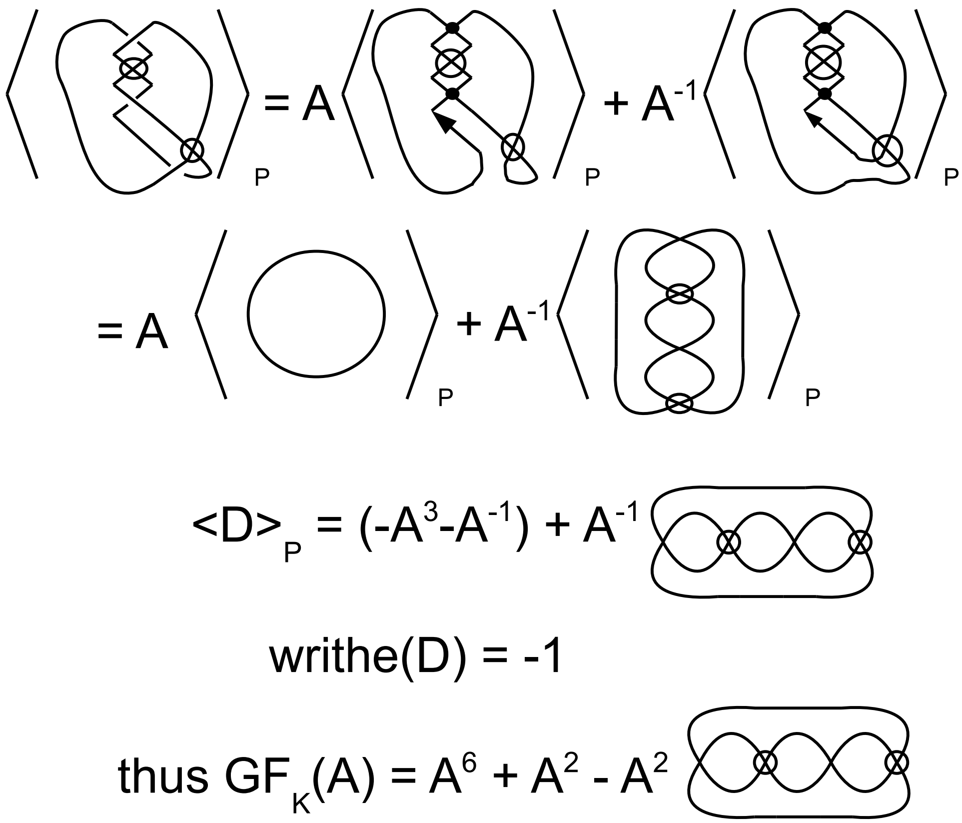

Figure 17. Virtual Knot 3.1 Graphical Parity Bracket Polynomial

Theorem 3.3.2. *Given a knot K, the parity bracket polynomial gives a lower bound on the surface genus of K, $s(K)$. More precisely, if $\langle D\rangle_P$ contains a monomial with graphical coefficients $D_1D_2\cdots D_n$ then*

$$s(D_1D_2\cdots D_n)\leq s(K)$$

Proof. Suppose K is given by an embedding $S^1\hookrightarrow S_g\times I$ and s' is the state of the parity bracket polynomial corresponding to the term with graphical coefficients $D_1D_2\cdots D_n$. Projecting s

down onto $S_g \times \{0\}$, we see that the minimal surface genus of s' is at least $s(D_1 D_2 \cdots D_n)$. Since the polynomial is an invariant of the knot this holds for every diagram and hence we get the result for the knot. ∎

Example 3.3.2. *Let K be virtual knot 4.72 in Figure Figure 18. It is a short exercise to show $\langle K \rangle_A = 1$ and that*

$$\langle K \rangle_P = -A^4 - A^2 + D_2[1] - 2 - \frac{1}{A^2} - \frac{1}{A^4}$$

where $D_2[1] =$ 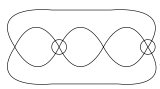*. Note that $s(D_2[1]) = 1$ (14) and hence $s(K) \geq 1$. Note that the diagram in Figure Figure 18 has genus 2. It is not currently known to us if the minimal surface genus is 1 or 2. Similarly the diagram in Figure Figure 18 has virtual crossing number 3. It is unclear if there is a diagram for this knot with a lower virtual crossing number.*

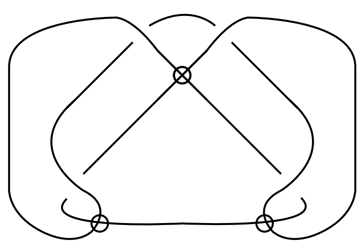

Figure 18. Virtual Knot 4.72

3.4 A Parity Arrow Polynomial

We use Manturov's idea of graphical coefficients (2) to extend the arrow polynomial via parity as follows.

Definition 3.4.1. *The (un-normalized) Parity Arrow Polynomial of a virtual knot K is defined by the relations in Figures Figure 19 and Figure 20.*

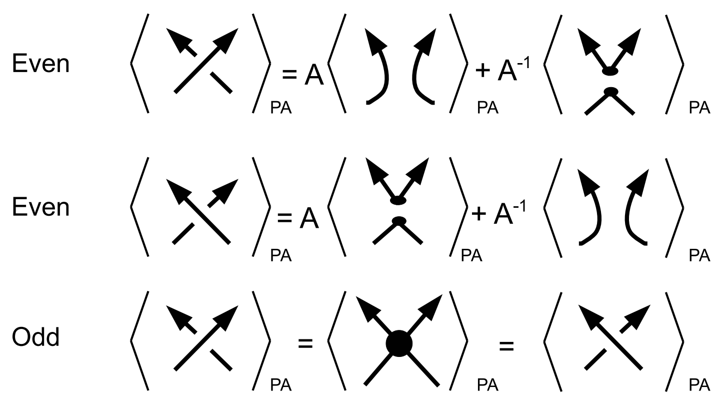

Figure 19. Parity Arrow Polynomial Crossing Skein Relations

Definition 3.4.2. *Given a virtual knot K with diagram D, The Normalized Parity Arrow Polynomial of K is given by*

$$PAP_A(K) = PAP_A(D) = (-A)^{-3\omega(D)} \langle D \rangle_{PA}$$

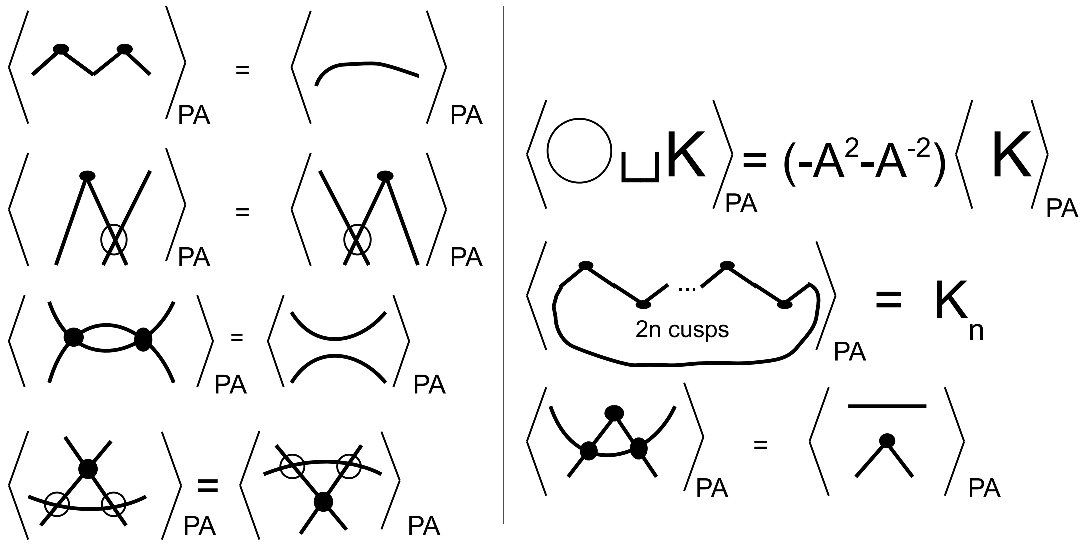

Figure 20. Parity Arrow Polynomial Reduction Skein Relations

where $\langle D \rangle_{PA}$ *is the parity arrow polynomial of* D *and*

$$\omega(D) = writhe(D) = (\#\ positive\ crossings\ in\ D) - (\#\ negative\ crossings\ in\ D).$$

Theorem 3.4.1. *The Normalized Parity Arrow Polynomial is an invariant of virtual knots.*

Proof. As in the case of the parity bracket polynomial much of the proof is the same here as in the non-parity version.

1. Reidemeister I follows from the writhe normalization.

2. Reidemeister II follows for even crossing by the equivalent proof for the arrow polynomial and for odd crossing by the reduction relations.

3. Reidemeister III follows by applying the "Kauffman Trick" at a single even crossing in conjunction with the cusped 'Reidemeister II'-like relation. (Note in the mixed case there is only 1 even crossing to choose.) See Figure Figure 21 for one of diagramatic proofs. The others follow similarly.

∎

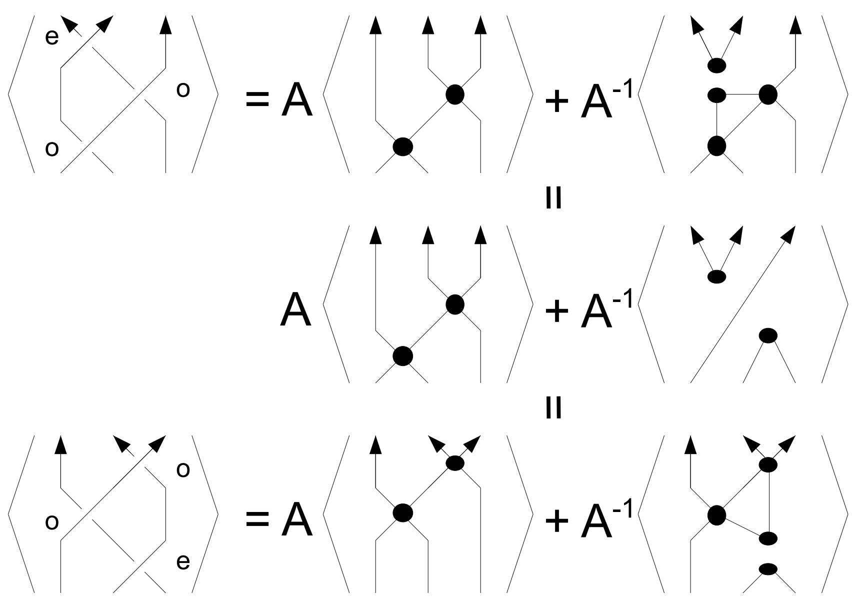

Figure 21. Invariance for one of the mixed Reidemeister III move.

Example 3.4.1. *The normalized parity arrow polynomial for virtual knot 4.70 in Figure Figure 22 is equal*

$$D_2[3]A^8 + 2K_1A^6 - A^6 - A^2$$

where $D_2[3]$ *is the graphical coefficient* 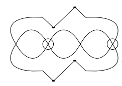*. We should note that the parity bracket polynomial of virtual knot 4.70 also contains a graphical coefficient.*

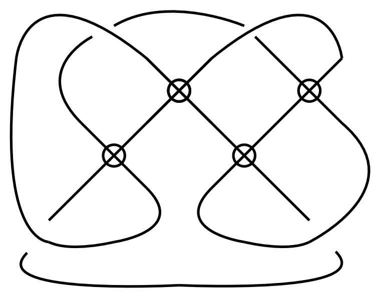

Figure 22. Virtual Knot 4.70

Remark 3.4.1. *In (13) Kauffman introduced a polynomial called with extended bracket polynomial which is a generalization of the arrow polynomial. One key difference between these two polynomials is that the cusps in the extended bracket polynomial are maintained in associated pairs. One can extend the parity arrow polynomial in a similar fashion by replacing the mixed 'Reidemeister II'-like relation with a similar relation* 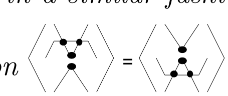*.*

3.4.0.2 The Parity Arrow Polynomial and Surface Genus

Similar to the parity bracket polynomial we have the following lower bound on the surface genus.

Theorem 3.4.2. *Given a knot K, the parity bracket polynomial gives a lower bound on the surface genus of K, $s(K)$. More precisely, if $\langle D\rangle_{PA}$ contains a monomial with graphical coefficients $D_1 D_2 \cdots D_n$ then*

$$s(D_1 D_2 \cdots D_n) \leq s(K)$$

Proof. This is identical to the proof for the parity bracket polynomial. ∎

Example 3.4.2. *The virtual knot 5.5 in Figure Figure 23 has arrow polynomial*

$$A^{10} K1^2 - A^{10} K1 - 3A^6 K1^2 + 3A^6 K1 + A^6 - \frac{1}{A^6} - 2A^4 K2 - 3A^2 K1 + \frac{K1}{A^2} + 2A^2$$

and parity arrow polynomial

$$-A^4 D_4[1] - A^6 - 2A^2 - \frac{1}{A^2}$$

Where $D_4[1] =$ 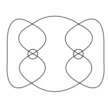 *Note that by (15) the arrow polynomial gives a minimal surface genus, $s(K) \geq 1$. However, in (14) Dye and Kauffman show that a Kishino knot lying under $D_4[1]$ (in the sense of resolving graphical nodes into knot crossings) has surface genus 2. Hence the parity arrow polynomial gives the lower bound $s(K) \geq 2$.*

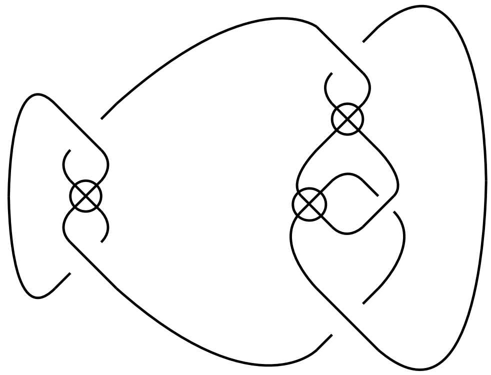

Figure 23. Virtual Knot 5.5

3.4.1 Z-Equivalence and Graphical Parity Polynomials

When computing the normalized bracket polynomial for virtual knots the relation of Z-Equivalence, depicted in Figure Figure 24, goes undetected. Passing to the parity bracket polynomial we have the option to add the corresponding graphical relation to the coefficients (i.e. including the relation in Figure Figure 24 when the classical crossings are replaced by graphical nodes.)

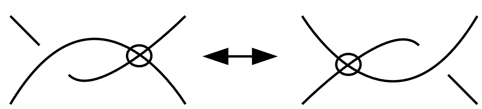

Figure 24. Z-Equivalence and the Bracket Polynomial

We will call the version with a minimal set of relations the *parity bracket polynomial* and the version taken up to Z-Equivalence on the odd crossings the *z-parity bracket polynomial.* Going a step further, we can choose to completely ignore the graphical coefficients by sending the graphical nodes to virtual crossings. This leads to the following *forgetful parity bracket polynomial.*

Lemma 3.4.3. *The parity bracket polynomial is strictly stronger than the z-parity bracket polynomial which in turn is strictly stronger than the forgetful parity bracket polynomial.*

Proof. For the parity bracket polynomial and z-parity bracket polynomial the follows immediately from the definition. For the forgetful parity bracket polynomial and z-parity bracket polynomial, notice that the action of swapping an odd crossing for a virtual crossing in the Z-Equivalence relation yields an identity. ∎

3.4.2 Manturov's Parity Filtration

In (2) Manturov introduced the following descending filtration on the category of virtual knots. Given a virtual knot K with chord diagram D. Let $D_0 = D$ be the equivalence class of D up to Reidemeister moves and define D_{i+1} to be the equivalence class of D_i after removing all odd chords (or equivalently, turning odd crossings into virtual crossings.)

This is well-defined since parity is invariant under the Reidemeister moves as shown above, most notably this filtration does not introduce the "forbidden move" from Figure Figure 3 when applied to the mixed-parity Reidemeister III move. Hence for 2 representatives $D_i, D_i' \in [D_i] :=$ Equivalence Class of D_i we have $[D_{i+1}] \equiv [D'_{i+1}]$.

Diagrammatically this filtration is described by the map sending odd crossing to virtual crossing and hence the forgetful parity polynomials are precisely an application of the respective polynomial on the filtration.

Theorem 3.4.4. *1. For any virtual knot this filtration is finite. (i.e. there exists n such that $D_n = D_i$ for $n \leq i$.)*

2. For any classical knot this filtration is of the form$D_0 = D_1 = \ldots$.

Proof. 1. This follows from the finiteness of crossings.

2. Every classical knot is equivalent to a knot with all even crossings.

∎

It is not difficult to construct a family of virtual knots for which given an n, $D_n = D_i$ for $n \leq i$. Consider the family in Figure Figure 25. Here the knot F_1 is the 2-crossing virtual knot (hence not equivalent to the unknot.) Each additional member of the family is produced from its predecessor by the addition of two odd positive crossing arcs and which become the only odd arcs in the new diagram. Since we are unable to cancel the two new odd crossings with one another we see each new virtual knot created in this way is unique from its predecessor. Moreover for F_n it is easy to verify that for $D_n = D_i = \text{Unknot}$ for $n \leq i$.

3.4.3 Graphical Link Parity Polynomials

This motivates the following definitions for link parity polynomials.

Definition 3.4.3. *Given a diagram D for a virtual knot K the (Link) Parity Bracket Polynomial of K is defined by the relations in Figures Figure 26 and Figure 27.*

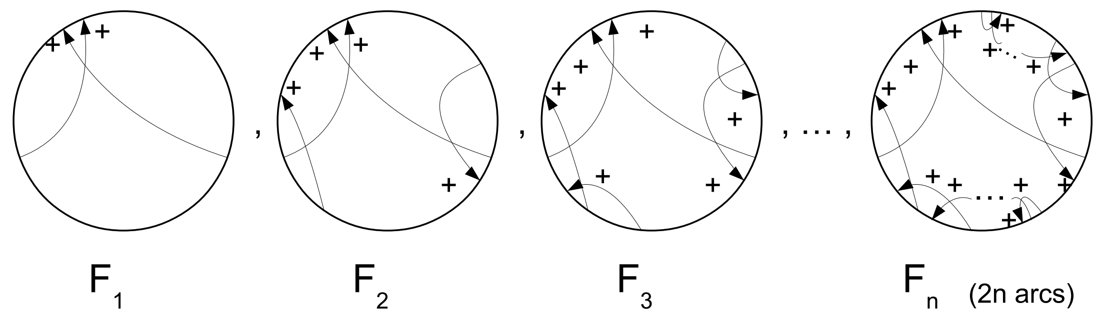

Figure 25. A Parity Filtration Family

Definition 3.4.4. *Given a virtual knot K with diagram D, The Normalized (Link) Parity Bracket Polynomial of K is given by*

$$PF_A(K) = PF_A(D) = (-A)^{-3\omega(D)}\langle D\rangle_P$$

where $\langle D\rangle_P$ is the parity bracket polynomial of D and

$$\omega(D) = writhe(D) = (\#\ positive\ crossings\ in\ D) - (\#\ negative\ crossings\ in\ D).$$

Theorem 3.4.5. *The (link) parity bracket polynomial is an invariant of virtual knots.*

Proof. 1. **RI:** A crossing involved in a Reidemeister I move is always an even self-crossing, hence invariance follows from the writhe normalization as in the normalized bracket polynomial.

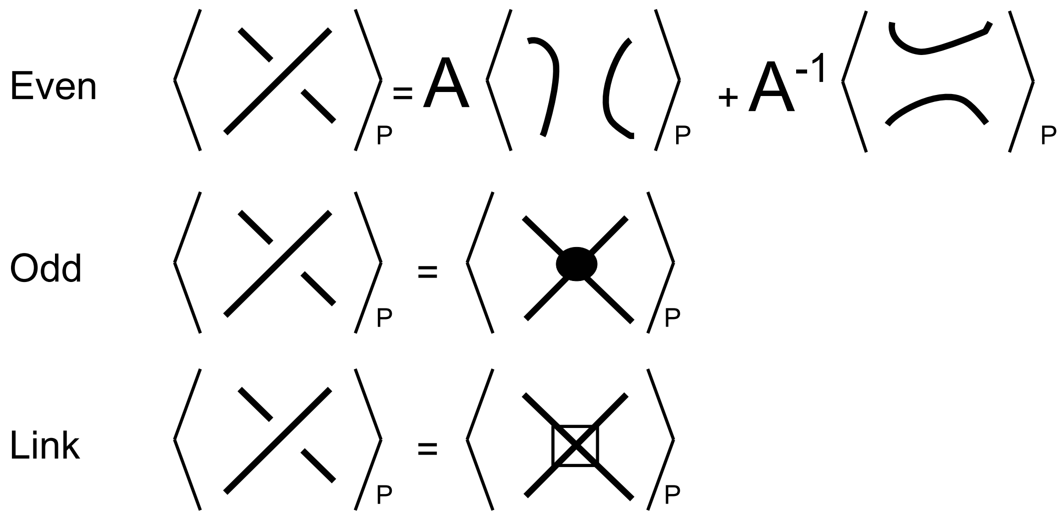

Figure 26. Link Parity Bracket Polynomial Smoothing Relations

2. **RII:** Reidemeister II follows for even self-crossing as in the classical case and for odd self-crossing and link-crossings by the reduction relations.

3. **RIII:** Here we have three cases to consider:

   (a) Reidemeister III for three self-crossings follows by applying the "Kauffman Trick" at a single even crossing.

   (b) For a Reidemeister III involving one self-crossings and two link crossings, if the self-crossing is even then the "Kauffman Trick" with the RII-like move for link crossings gives invariance. If the self-crossing is odd then the result is immediate by the reduction relations.

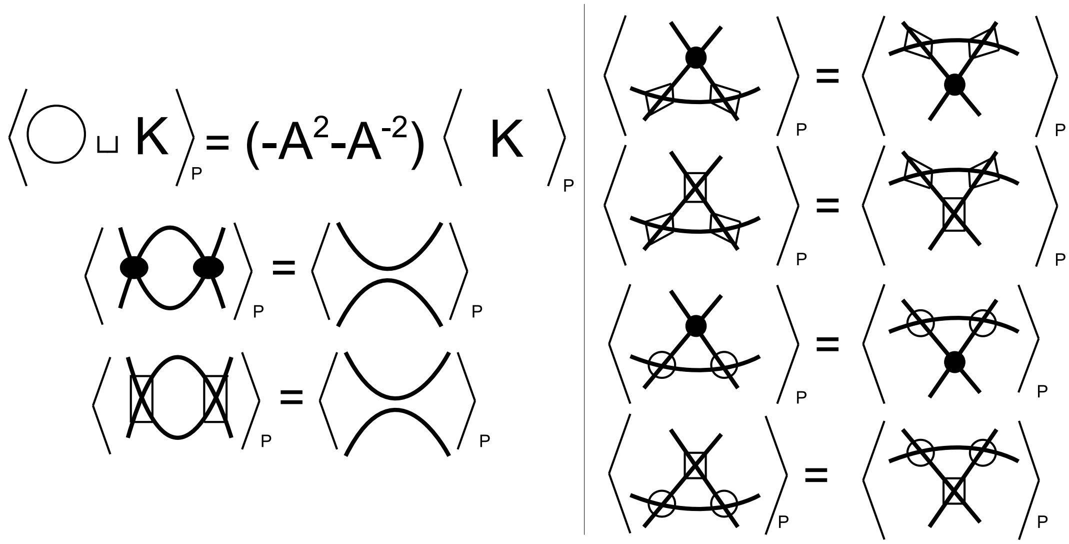

Figure 27. Link Parity Bracket Polynomial Reduction Relations

(c) Reidemeister II for three link-crossings also follows immediately from the reduction relations.

4. **Mixed Move:** For an even self-crossing this is the standard proof and for an odd self-crossing or link-crossing it follows from the reduction relations.

∎

Example 3.4.3. *Figure Figure 28 displays the calculation for the (link) parity bracket polynomial for the given 2-component link.*

Similarly for the parity arrow polynomial we have:

Definition 3.4.5. *Given a diagram D for a virtual knot K the (link) parity arrow polynomial of K is defined by the relations in Figures Figure 26 and Figure 27.*

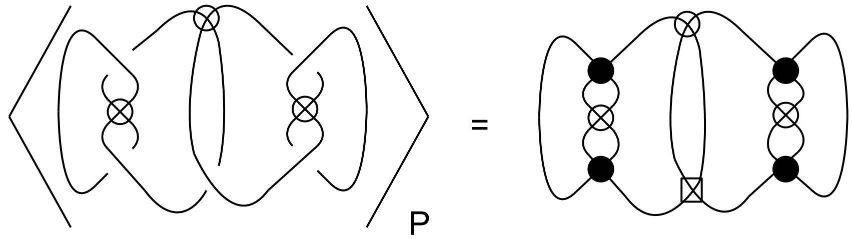

Figure 28. Graphical Link Parity Bracket Polynomial Example

Definition 3.4.6. *Given a virtual knot K with diagram D, The Normalized (Link) Parity Arrow Polynomial of K is given by*

$$PAP_A(K) = PAP_A(D) = (-A)^{-3\omega(D)}\langle D\rangle_{PA}$$

where $\langle D\rangle_{PA}$ *is the parity arrow polynomial of D and*

$$\omega(D) = writhe(D) = (\#\ positive\ crossings\ in\ D) - (\#\ negative\ crossings\ in\ D).$$

Theorem 3.4.6. *The (link) parity arrow polynomial is an invariant of virtual knots.*

Proof. This proof is nearly identical to the one above. The only difference is the proof for the Reidemeister III move involving an even self-crossing and two link crossings. Here we use a cusped RII-like move for link crossing in the "Kauffman Trick". ∎

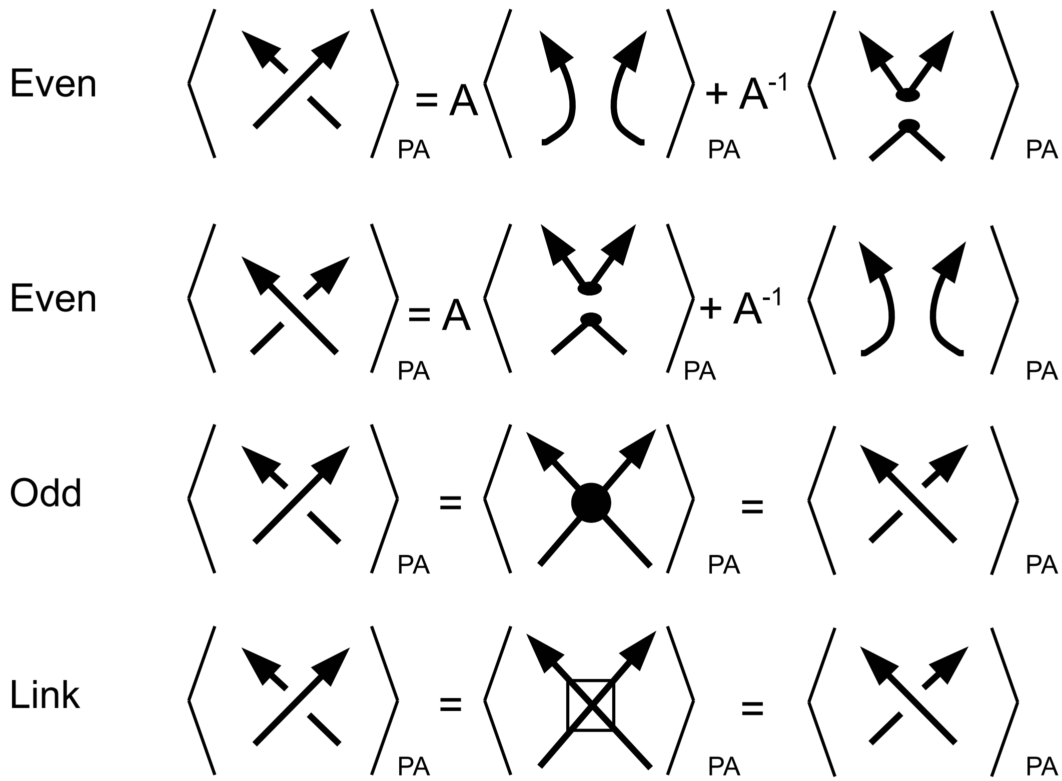

Figure 29. Link Parity Arrow Polynomial Smoothing Relations

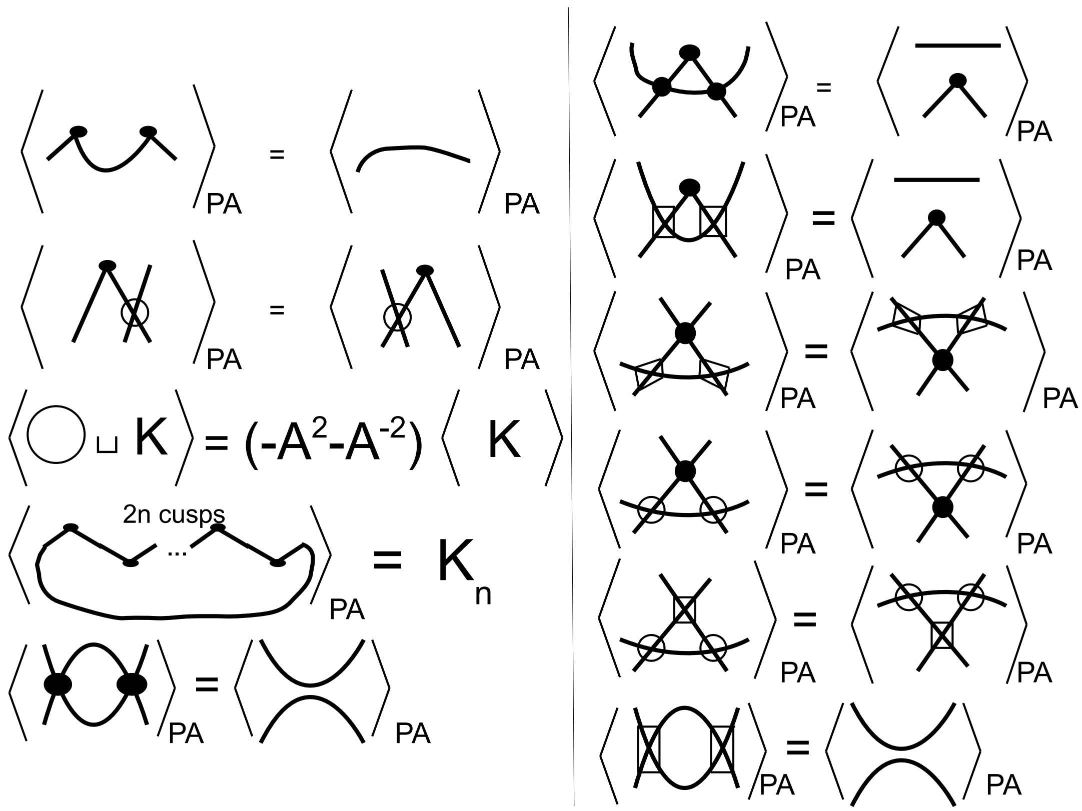

Figure 30. Link Parity Arrow Polynomial Reduction Relations

CHAPTER 4

PARITY AND CATEGORIFICATION

4.1 Khovanov Homology for Virtual Knots

For completeness we recall the definition of Khovanov Homology (16) (35). Our construction follows closely that of Dror Bar-Natan (17) and Kauffman (5). For other descriptions of the construction we point the reader to Khovanov (16) (35), Wehrli (36), Viro (22), Shumakovitch (37), Elliott (38) Kauffman(5), and Manturov (24). For technical reasons involving the construction of the categorification of the arrow polynomial we will take coefficients over the field $\mathbb{Z}_2$. It should be noted that the construction of Khovanov Homology for virtual knots can be extended to arbitrary coefficients following the construction of Manturov in (24). As one would expect, Manturov's definition is homologous to that of Khovanov for classical knots.

Before we recall the construction, we first re-normalize the Normalized Bracket Polynomial in order to simplify the definition. For a given a virtual knot or link K with corresponding diagram D, let $c(K)$ denote the crossing number of D. Sending $\langle K \rangle$ to $A^{-c(K)}\langle K \rangle$ and A to $-q^{-1}$ we get the following definition of the bracket polynomial:

$$\langle \emptyset \rangle = 1 \ ; \ \langle \bigcirc K \rangle = (q+q^{-1})\langle K \rangle \ ; \ \langle \times \rangle = \langle \asymp \rangle - q \langle) (\rangle$$

And, as is pointed out in Bar-Natan (17) we can summarize the Khovanov Bracket via the axioms:

$$[\![\emptyset]\!] = 0 \to \mathbb{Z}_2 \to 0 \ ; \ [\![\bigcirc K]\!] = V \otimes [\![K]\!] \ ; \ [\![\times]\!] = Cone([\![\asymp]\!] \xrightarrow{d} [\![)(]\!]\{1\})$$

where $V = \mathbb{Z}_2[X]/(X^2)$, $\{1\}$ is the "degree shift by one" operation on the quantum grading and *Cone* is the mapping cone over the differential d which we have yet to define. Note that we will use the enhanced state definition common in the literature, where each enhanced state corresponds to a labeling of the circle by 1 or X. This has the correspondence

$$1 \Leftrightarrow q^{+1} \text{ and } X \Leftrightarrow q^{-1}.$$

Remark 4.1.1. *For convenience we will continue to use the terms A-smoothing and B-smoothing as defined earlier.*

More constructively, consider the collection of enhanced states S arising from applying an A-smoothing and B-smoothing at each crossing and furthermore labeling each of the resulting circles by either 1 or X. Define the *Khovanov complex* $\mathcal{C}^{\bullet,\bullet}$ by setting $\mathcal{C}^{i,j}$ to be the linear span of states $s \in S$ where $i = n_B(s) =$ "the number of B-smoothings in s" and $j = j(s) = n_B(s) + \lambda(s)$ where $\lambda(s) =$ "the number of loops in s labeled 1 minus the number of loops labeled X". We will refer to i as the *homological grading* and j as the *quantum grading.*

For any two states s, s' that differ by replacing an A-smoothing by a B-smoothing at a single site respectively we would like to define a *local differential*, $d_{s,s'}$, such that the homological grading is increased by 1 and the quantum grading is preserved. Once this is defined, we then have the differential

$$d : \mathcal{C}^{i,j} \to \mathcal{C}^{i+1,j}$$

defined by

$$d(s) = \sum_{s'} d_{s,s'}$$

All that remains is to determine the possible values for $d_{s,s'}$. Since we are only concerned with resmoothing at a single site there are 3 possible scenarios relating s and s' in the setting of virtual knots.

Circle Annihilation

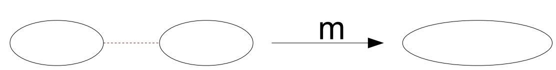

Circle Creation

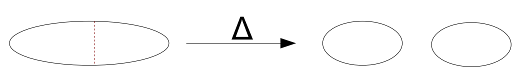

Single-Cycle Smoothing

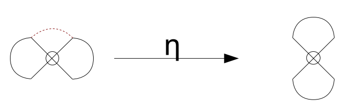

For any circles in state s not involved in resmoothing we set $d_{s,s'}$ to act as the identity on the enhanced states. For the enhanced circles involved in the resmoothing we define m, Δ and η as follows:

$$m: \begin{array}{ccc} 1 \otimes 1 & \rightarrow & 1 \\ 1 \otimes X & \rightarrow & X \\ X \otimes 1 & \rightarrow & X \\ X \otimes X & \rightarrow & 0 \end{array}$$

$$\Delta: \begin{array}{ccc} 1 & \rightarrow & 1 \otimes X + X \otimes 1 \\ X & \rightarrow & X \otimes X \end{array}$$

$$\eta: \begin{array}{ccc} 1 & \rightarrow & 0 \\ X & \rightarrow & 0 \end{array}$$

We are now in a position to define the *Khovanov Homology of a knot or link* K,

$$\mathcal{H}(K) = [\![K]\!][-n_-]\{n_+ - 2n_-\}$$

where $[l]$ is the shift operator on the homological grading and $\{l\}$ is the shift operator on the quantum grading. Moreover we can define the *Khovanov invariant* to be the Poincaré Polynomial:

$$Kh(K) := \sum_{i,j} t^i q^j dim\mathcal{H}^{i,j}(K)$$

Example 4.1.1. *Consider the virtual knot 3.1 in Figure Figure 44. The Khovanov complex for the unenhanced states is shown in Figure Figure 31. It is a small exercise to show* $Kh(VK_{3.1}) = q + q^{-1}$

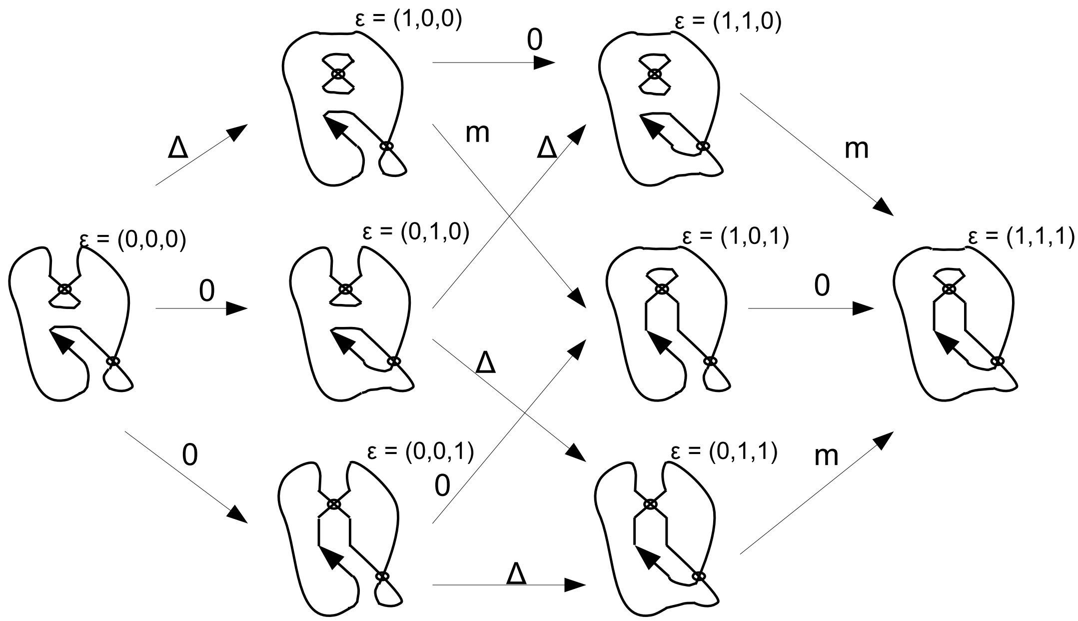

Figure 31. Virtual Knot 3.1 Khovanov Homology Complex

We will omit the well known proof that $d^2 = 0$, which amounts to checking all cases in the virtual setting, as well as the proof of invariance under the Reidemeister Moves. Missing details can be found in (16), (17), (18), (24), and (22).

If not for the self-imposed $\mathbb{Z}_2$ setting, we could also discuss applications of Lee's spectral sequence (20), (19) in the virtual setting. We plan to return to this subject in a future paper.

4.2 Categorifications of the Arrow Polynomial

In 2009 Dye, Kauffman and Manturov (25) introduced two categorifications of the Arrow Polynomial for virtual knots. Both constructions are homology theories defined over $\mathbb{Z}_2$ and agree with Khovanov homology over $\mathbb{Z}_2$ for classical knots. We remark that this construction is similar in flavor to the construction of Khovanov homology described in the previous section. The major difference in the constructions presented here are the considerations of additional gradings arising from the arrow numbers. We will use the same renormalization for categorification of the arrow polynomial as we did in Khovanov Homology, namely sending $\langle K\rangle$ to $A^{-c(K)}\langle K\rangle$ and A to $-q^{-1}$, where $c(K)$ is the crossing number for the diagram of K.

We first recall the construction introduced in (25) introducing the multiple grading and vector grading. Consider the collection of enhanced states S arising from applying an A-smoothing and B-smoothing at each crossing, where A- and B-smoothings are defined as in Figure Figure 11, and furthermore labeling each of the resulting circles by either 1 or X. Define the *Arrow complex* $\mathcal{C}_A^{\bullet,\bullet,\bullet,\bullet}$ by setting $\mathcal{C}_A^{i,j,m,v}$ to be the linear span of enhanced states $s \in S$ where $i = n_B(s) =$ "the number of B-smoothings in s" and $j = j(s) = n_B(s) + \lambda(s)$ where $\lambda(s) =$ "the number of loops in s labeled 1 minus the number of loops labeled X". We will refer to i as the *homological grading* and j as the *quantum grading.*

Given a state s define the *multiple grading of s*, $mg(s)$, to be the set of arrow numbers of s.

Given an enhanced state s, consider the collection Λ_s of enhanced circles carrying nonzero arrow numbers. For a circle $c \in \Lambda$ with arrow number p let the *order* of c, $o(c)$, be the value of k such that $p = 2^{k-1} * l$ with $gcd(2, l) = 1$. Define the function $vg(c)$ by $vg(c) = e_{o(c)}$ if c is labeled by X and $vg(c) = -e_{o(c)}$ if c is labeled by 1, where $e_1, e_2, \ldots$ is the standard basis for $\mathbb{R}^\infty$. Then the *vector grading*, $vg(s)$, is given by

$$vg(s) = \sum_{c \in \Lambda} vg(c)$$

Example 4.2.1. *The state* $s =$ 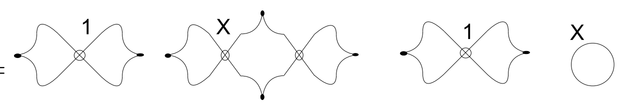

has

$$mg(s) = \{K_1, K_2\} \text{ and } vg(s) = (-2, 1, 0, 0, 0, ...)$$

As before, for any two states s, s' that differ by an A- to B- resmoothing at a single site it remains to define a *local differential*, $d_{s,s'}$, such that the homological grading is increased by 1 and the quantum grading, multiple grading and vector grading are all preserved. Once this is defined, we then have the differential

$$d : \mathcal{C}_A^{i,j,m,v} \to \mathcal{C}_A^{i+1,j,m,v}$$

defined by

$$d(s) = \sum_{s'} d_{s,s'}$$

Finally, The local differential $d_{s,s'}$ is defined by $d_{s,s'} = \tilde{\partial}_{s,s'} \circ \partial_{s,s'}$ where $\partial_{s,s'}$ is the Khovanov local differential between the corresponding states and $\tilde{\partial}_{s,s'}$ is the projection map preserving the multiple grading and vector grading. It is a short exercise to show that this satisfies the requisite $d^2 = 0$ through checking all possible cases. A key observation for the proof is noting that for circle annihilation and circle creation arrow number are $\pm$-additive while a single cycle resmoothing causes the arrow number to change by 1 as is shown in Figure Figure 32.

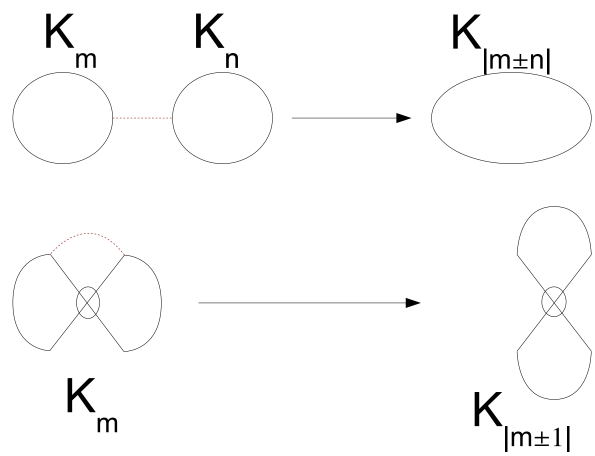

Figure 32. The Effect of Resmoothing on Arrow Numbers

We are now in a position to define the homology for the fully-graded categorification of the arrow polynomial of a knot or link K, $\mathcal{H}_A(K)$, by renormalizing analogously to Khovanov

Homology. Moreover we can define the *fully-graded arrow categorification invariant* to be the Poincaré Polynomial:

$$AKh(K) := \sum_{i,j\in\mathbb{Z},m\in M(D),v\in V(D)} m \times v \times t^i \times q^j \times dim\mathcal{H}_A{}^{i,j,m,v}(K)$$

where

$$S(D) = \{\text{enhanced states of D}\}\ ,\ M(D) = \bigcup_{s\in S} mg(s) \text{ and } V(D) = \bigcup_{s\in S} vg(s)$$

for a diagram D of K.

Example 4.2.2. *Consider the virtual knot 3.1 in Figure Figure 44. The cube complex for the unenhanced states is shown in Figure Figure 33. It is a small exercise to show*

$$AKh(VK_{3.1}) = \frac{vg(2,1)K[2]}{q^3 t} + \frac{vg(1,2)K[1]}{q^3} + \frac{vg(2,-1)K[2]}{qt} + qvg(1,-2)K[1] + \frac{2K[1]}{q}$$

Remark 4.2.1. *To translate the polynomial into the form of the definition one only has to see how to read the multiple grading and vector grading for a given monomial. The multiple grading is simply the collection of coefficients of the form* $K[i](= K_i)$*. The vector grading is obtained as follows. Each coefficient of the form* $vg(i,a)$ *corresponds to having coefficient* $a_i = a$ *when the vector grading is written as* $\sum_{i\in\mathbb{N}} a_i e_i$*. The product of vector gradings corresponds to the sum of the individual gradings. For example* $vg(2,1)vg(1,-1)$ *corresponds to the vector grading* $(-1,1,0,0,0,\ldots)$.

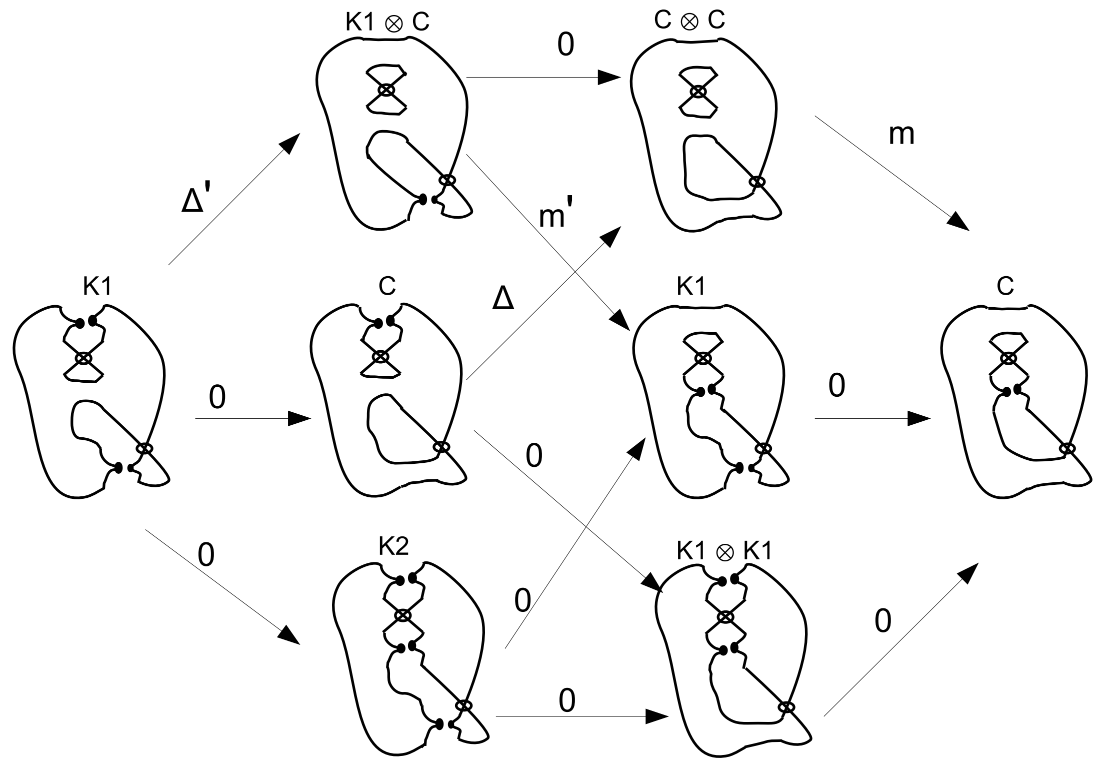

Figure 33. Virtual Knot 3.1 Arrow Polynomial Categorification Complex

We will again omit the proof of invariance under the Reidemeister Moves, which is similar to the equivalent proof for Khovanov homology. Similarly we leave out most of the proof that $d^2 = 0$ other than to point out why we work over $\mathbb{Z}_2$. As with Khovanov homology, the proof follows by showing that the differential commutes for every possible face with every possible grading configuration in the cube complex. Much of this is follows from the additivity relations for arrow numbers under resmoothing. However, the face in Figure Figure 34 is an example of a general type necessitating working over $\mathbb{Z}_2$.

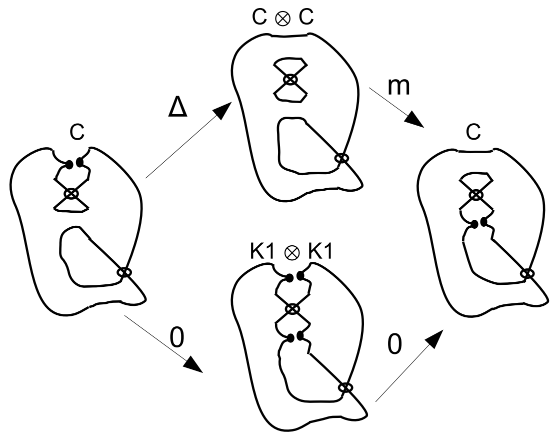

Figure 34. An example of the necessity of working over $\mathbb{Z}_2$

In (25) a simpler categorification for the arrow polynomial is introduced. We can arrive at this construction through a simple modification of the differential $\tilde{\partial}_{s,s'}$. Suppose we represent the vector grading as $vg(s) = \sum_{i \in \mathbb{N}} a_{i_s} * e_i$ where $e_1, e_2, \ldots$ is the standard basis for $\mathbb{R}^\infty$. Rather than preserving the multiple grading and vector grading, $\tilde{\partial}_{s,s'}$ is define by

$$\tilde{\partial}_{s,s'} = \{ \begin{array}{ll} 1 & \text{, if } a_{1_s} \equiv a_{1_{s'}} \bmod 2 \\ 0 & \text{, if } a_{1_s} \not\equiv a_{1_{s'}} \bmod 2 \end{array}$$

We have constructed a Mathematica program to calculate all of the categorifications mentioned in this section for knots with at most 6 classical crossings based on Jeremy Green's table (34). We have been unable to find two virtual knots that are distinguished by the fully-graded categorification and not by the simpler categorification. Additionally, there are no knots which are distinguished from the unknot by the categorification and not by the arrow polynomial.

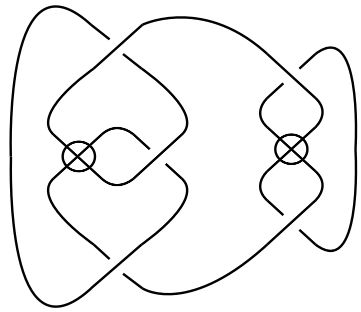

Figure 35. Virtual Knot 5.129

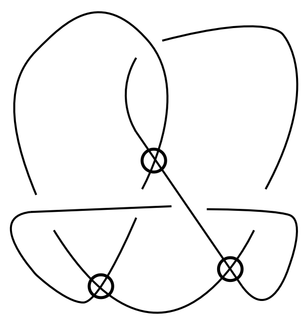

Figure 36. Virtual Knot 5.267

4.2.1 Knots Distinguished by the Arrow Categorification Invariant

Example 4.2.3. *Virtual Knots 5.129 in Figure Figure 35 and 5.267 in Figure Figure 36 both have Khovanov invariant*

$$Kh(5.129) = Kh(5.267) = \frac{1}{q^5t^2} + \frac{1}{q^3t^2} + \frac{1}{q^3t} + q^2t + \frac{1}{q^2} + \frac{1}{qt} + q + \frac{1}{q} + t + 1$$

and Arrow Polynomial

$$AP(5.129) = AP(5.267) = -A^{10} + A^6 - A^4 K2 - 2A^2 K1^2 - A^2 K1 + \frac{K1}{A^2} + 2A^2 - K2$$

However,

$$\begin{aligned} AKh(5.129) = &\frac{vg(2,1)K[2]}{q^3 t} + \frac{2vg(1,2)K[1]}{q^3} + q^2 tvg(1,-1)K[1] + \frac{vg(1,1)K[1]}{q^2} \\ &+ qtvg(2,-1)K[2] + \frac{vg(2,-1)K[2]}{qt} + \frac{tvg(2,1)K[2]}{q} \\ &+ 2qvg(1,-2)K[1] + tvg(1,1)K[1] + vg(1,-1)K[1] + \frac{4K[1]}{q} \\ &+ \frac{1}{q^5 t^2} + \frac{1}{q^3 t^2} + \frac{2}{q^3 t} + \frac{2}{qt} + qt + \frac{t}{q} + q + \frac{1}{q} \end{aligned}$$

and

$$\begin{aligned} AKh(5.267) = &\frac{vg(2,1)K[2]}{q^3 t} + \frac{2vg(1,2)K[1]}{q^3} + q^2 tvg(1,-1)K[1] + \frac{vg(1,1)K[1]}{q^2} \\ &+ qtvg(2,-1)K[2] + \frac{vg(2,-1)K[2]}{qt} + \frac{tvg(2,1)K[2]}{q} \\ &+ 2qvg(1,-2)K[1] + tvg(1,1)K[1] + vg(1,-1)K[1] + \frac{4K[1]}{q} \\ &+ \frac{1}{q^5 t^2} + \frac{1}{q^3 t^2} + \frac{2}{q^3 t} + \frac{2}{qt} \end{aligned}$$

4.2.2 The Fully-Graded Arrow Categorification and Surface Genus

We may extend Theorem 3.2.2 on surface genus bounds produced by the arrow polynomial to the fully-graded categorification as follows.

Theorem 4.2.1. *Let K be a virtual knot diagram with fully-graded arrow categorification invariant $AKh(K)$. Suppose that $AKh(K)$ contains a summand having non-empty multiple grading $\mathcal{M}$, a nonempty set of arrow numbers, with $|\mathcal{M}| = n$. Then n determines a lower bound on the genus g of the minimal genus surface in which K embeds. That is, if $n = 1$ then the minimum genus is at least 1, if $n = 2$ then the minimum genus is 2 or greater and for $n \geq 3$ if $n > 3g - 3$ then $s(K) > g$.*

We add a bit more detail to the earlier sketch to highlight why we only get the extension in the fully-graded categorification. The proof relies on the following fact from (39).

Lemma 4.2.2. *Consider a collection $\mathcal{A}$ of non-intersecting essential curves (i.e. not contractible) on an orientable surface S_g of genus g no pair of which co-bound an annulus. If $g = 1$ then $|\mathcal{A}| \leq 1$ and if $g \geq 2$ then $|\mathcal{A}| \leq 3g - 3$.*

Proof of 4.2.1: The proof follows by the above lemma once we show that multiple grading corresponds to n non-intersecting essential curves of which no pair co-bound an annulus. Since the multiple grading is an invariant of the knot we have that any embedding into $S_g \times I$ for K must contain a state s with $mg(s) = \mathcal{A}$.

To see that each element of $\mathcal{A}$ is an essential curve suppose for contradiction $K_{i_l} \in \mathcal{A}$ bounds a disk. By the disoriented smoothing relation each cusp in K_{i_l} is paired with another cusp somewhere in s corresponding to the other half of the smoothing. Since K_{i_l} bounds a disk (in the projection to S_g) the Jordan Curve Theorem implies the interior and exterior cusps cannot be paired. If we consider only the internal cusps in K_{i_l} they too cannot be paired with one-another (for odd arrow numbers this follows from parity and for even arrow numbers this follows from orientation.) Thus an inner cusp of K_{i_l} must be paired with the cusp either of another K_{i_j} or of circle with an even number of canceling cusps. In either case we produce another cusps with which to repeat the argument. Since our knot has a finite number of crossing (hence a finite number of cusps) this is a contradiction. A similar argument shows that given $K_{i_l}, K_{i_j} \in \mathcal{A}$ with $i_l \neq i_j$ they cannot co-bound an annulus.∎

4.2.3 Categorification and Width

The subject of the width of Khovanov homology for various classes of knots has been of interest since Khovanov's seminal work (16). Here we produce a definition of width for the virtual setting, recall known results in the classical setting and give some basic results in the virtual knot setting.

In the classical case it was noticed early on that when plotting the homological degree versus the quantum degree for the support of the Khovanov invariant the majority of small knots were supported on 2 diagonals corresponding to the signature of the knot ± 1. In the classical case we say that a knot is *H-thin* if its Khovanov homology is supported on 2 diagonals corresponding to lines $t - 2q = constant$, else it is called *H-thick*. In the case of alternating knots Lee (20) proved that they are H-thin. Since all alternating knots are of even parity (which we will define shortly), Lee's proof extends to virtual alternating knots as was pointed our by Viro (22). The thickness of a number of other classes of classical knots is known and a recent summary of the known results can be found in (38).

In the virtual case we need to re-examine our definition of H-thick and H-thin. If we wish to use the thickness of the homology to determine if the Khovanov homology holds additional information over the Jones Polynomial we quickly run into trouble in the virtual case. It is no longer enough to determine if the homology is supported on 2 diagonals to determine if the homology contains more information than the polynomial (not to mention that the signature is not well-defined). For instance Virtual Knot 2.1 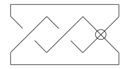 has bracket polynomial

$$(A^4 + A^6 - A^{10})(-A^2 - A^{-2})$$

and Khovanov Invariant

$$(q^6 + q^4)t^2 + (q^4 + q^2)t + q^3 + q$$

. By the classical definition Virtual Knot 2.1 is H-thick as it is supported on 4 diagonals. However, the Khovanov homology does not hold any additional information.

Two good questions to ask are (1) for a given virtual knot, on how many diagonals is the homology $\mathcal{H}(K)$ supported and (2) what is the maximal width between the diagonals (i.e. $c_{max} - c_{min}$ for the supported diagonals $t - 2q = c$.) We call the solution to the first the *thickness* of the homology and denote it by $Th(\mathcal{H}(K))$ for a given knot K. The second is referred to as the *width* of the homology and denoted by $W(\mathcal{H}(K))$.

More can be said about knots with orientable atoms. We recall from Manturov (40) that for a given knot K, an atom for K is a pair (M, Γ) where M is a surface without boundary (not necessarily connected or orientable) and Γ is a 4-valent graph on M such that (M, Γ) admits a checkerboard coloring. We say an atom is orientable if M is orientable.

In (41) Manturov proves that for knots with orientable atoms we have:

Theorem 4.2.3. *For a knot K with orientable atom, $Th(Kh(K)) \leq g(K) + 2$ where $g(K)$ is the Turaev genus (or atom genus) of the knot.*

The proof require a careful examination of the interplay between the Turaev genus of the knot and the number of crossings in the knot diagram. Note that the orientable condition is important. Virtual knot 2.1 has $Th(Kh(K)) = 4$ (as shown above), however $g(K) = 1/2$ since K can be placed on the projective plane in a checkerboard fashion.

Asking the same questions for the fully-graded arrow categorification we immediately see:

Theorem 4.2.4. *Given a virtual knot K suppose the arrow polynomial $\langle K \rangle_A$ contains a monomial with non-zero arrow number $K_{i_1}^{e_1} \dots K_{i_n}^{e_n}$ then*

$$W(AKh(K))) \geq 2(\sum_{i=1,\dots,n} e_i)$$

Proof. This is an immediate consequence of categorification. Since we have categorified up to multiple grading and vector grading the monomial with non-zero arrow number $K_{i_1}^{e_1} \dots K_{i_n}^{e_n}$ corresponds to a term in $AKh(K)$. If we consider the vector gradings related to the corresponding unenhanced state in the cube complex we see the the largest and smallest correspond to the "all 1" labeling and the"all X" labeling. The corresponding width between these states is $2(\sum_{i=1,\dots,n} e_i)$ giving the theorem. ∎

The above proof actually gives more if we consider all possible labelings.

Theorem 4.2.5. *Given a virtual knot K suppose the arrow polynomial $\langle K \rangle_A$ contains a monomial with non-zero arrow number $K_{i_1}^{e_1} \ldots K_{i_n}^{e_n}$, then*

$$Th(AKh(K))) \geq \sum_{i=1,\ldots,n} e_i$$

4.2.4 Rational Virtual Knots

Lee (20) showed that the Khovanov homology of an alternating knot is completely determined by its Jones polynomial. Recall that every classical rational knot is isotopic to an alternating knot (see Theorem 3.5 of (42)). Hence the Khovanov homology of every classical rational knot is completely determined by its Jones Polynomial.

This is not the case for virtual knots and the categorifications of the arrow polynomial. The following examples were found with the help of Slavik Jablan and the program LinKnot (43).

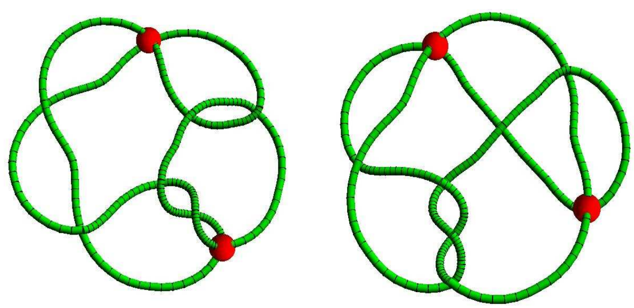

Figure 37. Virtual Rational Knots Distinguished by Categorification

Both of the knots in Figure Figure 37 have identical normalized bracket polynomial

$$\frac{1}{A^{26}}+\frac{1}{A^{24}}-\frac{1}{A^{20}}-\frac{1}{A^{18}}+\frac{1}{A^{12}}-\frac{1}{A^{10}}-\frac{1}{A^{8}}-\frac{1}{A^{6}}$$

and normalized arrow polynomial

$$A^{10}+A^{8}\mathrm{K1}-\frac{1}{A^{6}}-2A^{4}\mathrm{K1}-\frac{\mathrm{K1}}{A^{4}}+\frac{1}{A^{2}}+2\mathrm{K1}$$

The knot on the left hand side has Khovanov invariant

$$\begin{aligned} q^{13}t^{5}+q^{12}t^{4}+q^{11}t^{5}+q^{11}t^{4}+q^{10}t^{4}+2q^{10}t^{3} \\ +q^{9}t^{4}+2q^{8}t^{3}+2q^{8}t^{2}+2q^{6}t^{2}+q^{6}t+q^{5}+q^{4}t+q^{3} \end{aligned}$$

and fully-graded arrow categorification invariant

$$\begin{aligned} q^{12}t^{4}\mathrm{vg}(1,-1)K[1]+q^{10}t^{4}\mathrm{vg}(1,1)K[1] \\ +2q^{10}t^{3}\mathrm{vg}(1,-1)K[1]+2q^{8}t^{3}\mathrm{vg}(1,1)K[1] \\ +2q^{8}t^{2}\mathrm{vg}(1,-1)K[1]+2q^{6}t^{2}\mathrm{vg}(1,1)K[1] \\ +q^{6}t\mathrm{vg}(1,-1)K[1]+q^{4}t\mathrm{vg}(1,1)K[1]+q^{13}t^{5} \\ +q^{11}t^{5}+q^{11}t^{4}+q^{9}t^{4}+q^{5}+q^{3} \end{aligned}$$

while the knot on the right hand side has Khovanov invariant

$$
\begin{aligned}
q^{13}t^5 + q^{12}t^4 + q^{11}t^5 + q^{11}t^4 + q^{10}t^4 + 2q^{10}t^3 \\
+q^9t^4 + q^9t^3 + q^9t^2 + 2q^8t^3 + 2q^8t^2 + q^7t^3 + 2q^7t^2 + q^7t \\
+2q^6t^2 + q^6t + q^5t^2 + q^5t + q^5 + q^4t + q^3
\end{aligned}
$$

and fully-graded arrow categorification invariant

$$
\begin{aligned}
q^{12}t^4\mathrm{vg}(1,-1)K[1] + q^{10}t^4\mathrm{vg}(1,1)K[1] \\
+2q^{10}t^3\mathrm{vg}(1,-1)K[1] + 2q^8t^3\mathrm{vg}(1,1)K[1] \\
+2q^8t^2\mathrm{vg}(1,-1)K[1] + 2q^6t^2\mathrm{vg}(1,1)K[1] \\
+q^6t\mathrm{vg}(1,-1)K[1] + q^4t\mathrm{vg}(1,1)K[1] + q^{13}t^5 \\
+q^{11}t^5 + q^{11}t^4 + q^9t^4 + q^9t^3 + q^9t^2 + q^7t^3 + 2q^7t^2 \\
+q^7t + q^5t^2 + q^5t + q^5 + q^3.
\end{aligned}
$$

4.3 Graphical Parity and Categorifications

We would like to categorify the parity polynomials in an analogous manner to the original polynomials by adding an additional grading, similarly to the construction of the categorification of the arrow polynomial, based on the equivalence classes of graphified flat knot diagrams.

However, it is fairly simple to construct an example showing this to be naive. For instance, consider the virtual knot in Figure Figure 38.

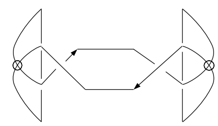

Figure 38. Kishino Knot

Performing the available Reidemeister II move, the resulting diagram is one of three virtual knots often referred to as Kishino knots. Figure Figure 39 shows that both the parity bracket polynomial and parity arrow polynomial of the knot is the graphified version of the diagram as there are no graphical Reidemeister II moves or detour moves available.

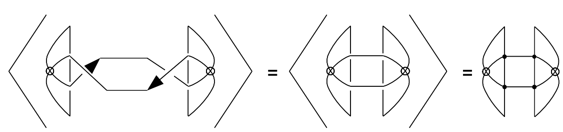

Figure 39. Graphical Parity Bracket Polynomial of a Kishino Knot

However, when we consider the Khovanov complex (the arrow polynomial categorifications have equivalent complexes) as in Figure Figure 40 we can see that $d^2 \neq 0$. In particular, the all-A and all-A^{-1} states are both graphically equivalent to two circles while in the middle we have the top state graphically equivalent to a graphified Kishino knot and the bottom state graphically equivalent to 3 circles. Hence, as shown in the figure, the upper differentials are both the 0-map. Considering the element $(x \otimes 1)$, we see

$$d^2(x \otimes 1) = (1 \otimes m) \circ (\Delta \otimes 1)(x \otimes 1) = (1 \otimes m)(x \otimes x \otimes 1) = x \otimes x \neq 0$$

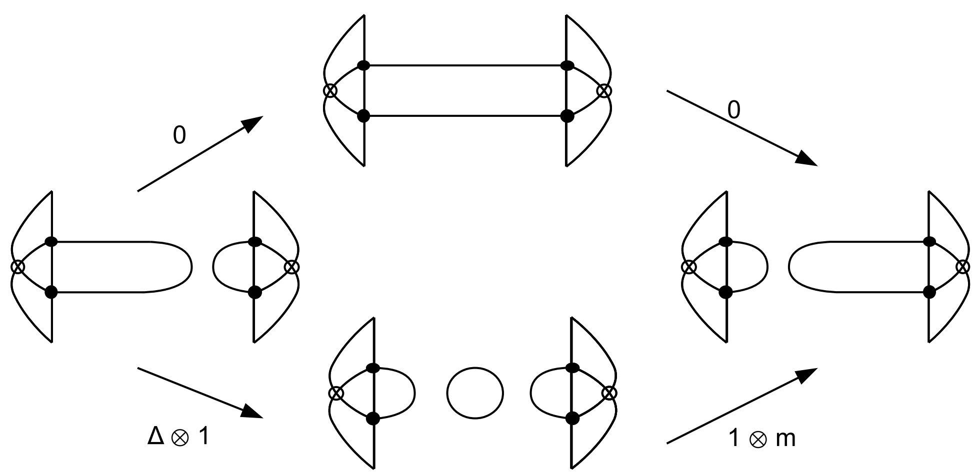

Figure 40. Graphical Parity Kishino Complex

However, this does not prevent us from applying Manturov's parity filtration along with the forgetful version of the parity categorifications. In doing so we clearly lose some of the power of the parity polynomial (for instance the Kishino knot is no longer detected) but we still retain an invariant which is capable of detecting non-classicality. We can define the *parity Khovanov homology* (respectively, *parity arrow categorification*) to be the homology theory produced by first applying Manturov's parity filtration to the given knot and then computing the Khovanov homology (respectively, the arrow categorification) of the resulting knot. Similarly, define the *parity Khovanov invariant* (respectively, *parity arrow invariant*) to be the resulting Poincaré Polynomial as produced previously.

For instance, consider the knot in Figure Figure 41. Applying the parity Khovanov homology we have that the original knot has Khovanov invariant

$$\frac{1}{q^9t^3}+\frac{1}{q^8t^2}+\frac{1}{q^7t^3}+\frac{1}{q^7t^2}+\frac{1}{q^6t^2}+\frac{1}{q^6t}+\frac{1}{q^5t^2}+\frac{1}{q^5}+\frac{1}{q^4t}+\frac{1}{q^3}$$

Applying the filtration and turning crossings 1 and 4 into virtual crossings we have that the underlying knot at this level of the filtration is the two crossing virtual knot. Hence virtual knot 4.9 has parity Khovanov invariant

$$\frac{1}{q^6t^2}+\frac{1}{q^4t^2}+\frac{1}{q^4t}+\frac{1}{q^3}+\frac{1}{q^2t}+\frac{1}{q}$$

and moreover is non-classical.

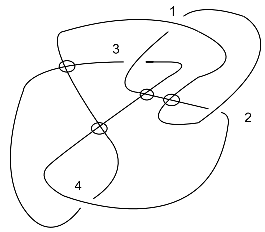

Figure 41. Virtual Knot 4.9

Using Jeremy Green's virtual knot table (34) we have been able to calculate the parity categorifications on knots with at most 6 real crossings. Table Table I is a collection of planar diagram codes for 8 knots which are not distinguished from the unknot via the bracket polynomial, arrow polynomial or their categorifications, but are distinguished from the unknot via the parity arrow categorification. Please see the Appendix for an explanation of our planar diagram conventions. The top four knots have parity arrow invariant

$$\frac{\mathrm{vg}(2,1)K[2]}{q^3t}+\frac{\mathrm{vg}(1,2)K[1]}{q^3}+\frac{\mathrm{vg}(2,-1)K[2]}{qt}+q\mathrm{vg}(1,-2)K[1]+\frac{2K[1]}{q}$$

while the lower four have parity arrow invariant

$$q^3t\mathrm{vg}(2,-1)K[2]+q^3\mathrm{vg}(1,-2)K[1]+qt\mathrm{vg}(2,1)K[2]+\frac{\mathrm{vg}(1,2)K[1]}{q}+2qK[1]$$

6.5508	PD[X[4, 2, 5, 1], X[7, 4, 8, 3], X[10, 6, 11, 5], Y[12, 3, 1, 2], Y[9, 7, 10, 6], Y[8, 12, 9, 11]]
6.5627	PD[X[4, 2, 5, 1], X[7, 4, 8, 3], X[10, 6, 11, 5], Y[12, 3, 1, 2], Y[9, 7, 10, 6], Y[11, 9, 12, 8]]
6.7613	PD[X[4, 2, 5, 1], X[7, 4, 8, 3], X[9, 7, 10, 6], Y[12, 3, 1, 2], Y[10, 6, 11, 5], Y[8, 12, 9, 11]]
6.7701	PD[X[4, 2, 5, 1], X[7, 4, 8, 3], X[9, 7, 10, 6], Y[12, 3, 1, 2], Y[10, 6, 11, 5], Y[11, 9, 12, 8]]
6.24828	PD[X[6, 4, 7, 3], X[9, 5, 10, 4], X[11, 8, 12, 7], Y[12, 3, 1, 2], Y[1, 11, 2, 10], Y[8, 6, 9, 5]]
6.37012	PD[X[6, 4, 7, 3], X[8, 6, 9, 5], X[11, 8, 12, 7], Y[12, 3, 1, 2], Y[1, 11, 2, 10], Y[9, 5, 10, 4]]
6.60677	PD[X[3, 7, 4, 6], X[9, 5, 10, 4], X[11, 8, 12, 7], Y[12, 3, 1, 2], Y[1, 11, 2, 10], Y[8, 6, 9, 5]]
6.65816	PD[X[3, 7, 4, 6], X[8, 6, 9, 5], X[11, 8, 12, 7], Y[12, 3, 1, 2], Y[1, 11, 2, 10], Y[9, 5, 10, 4]]

TABLE I

Undistinguished by Categorification but Distinguished by Parity

4.3.1 Link Parity Polynomials and Categorification

Following the construction presented in Section 3.4.3 we can extend the graphical polynomials to links. However, the graphical coefficients for links suffer a similar problem to that of knots when categorified. As with knots we map use the forgetful map to send the graphical link coefficients to virtual crossings. The effect of this for links is rather unfortunate as it reduces a link to the disjoint union of its components. (This is easiest to see by thinking of the chord diagram.) Hence it reduces the link parity categorification back to the knot parity categorification setting.

CHAPTER 5

PARITY AND BIQUANDLES

5.1 Biquandles

Following (27) and (31) we recall the definition of a Biquandle.

Definition 5.1.1. *A biquandle* (X, B) *is a set* X *and a map* $B : X \times X \to X \times X$ *which satisfies the following conditions:*

1. B *is invertible, i.e there exists a map* $B^{-1} : X \times X \to X \times X$ *satisfying* $B \circ B^{-1} = Id_{X \times X} = B^{-1} \circ B$,

2. *For all* $a, b \in X$ *there exists* $x \in X$ *such that*

   $x = B_2^{-1}(a, B_2(b, x))$, $a = B_1(b, x)$ *and* $b = B_1^{-1}(a, B_2(b, x))$

   For all $a, b \in X$ *there exists* $x \in X$ *such that*

   $x = B_1(B_1^{-1}(x, b), a)$, $a = B_2^{-1}(x, b)$ *and* $b = B_2(B_1^{-1}(x, b), a)$

3. B *satisfies the set-theoretic Yang-Baxter equation* $(B \times Id) \circ (Id \times B) \circ (B \times Id) = (Id \times B) \circ (B \times Id) \circ (Id \times B)$

4. *Given* $a \in X$ *there exists* $x \in X$ *such that* $a = B_1(a,x)$ *and* $x = B_2(a,x)$

   Given $a \in X$ *there exists* $x \in X$ *such that* $a = B_1^{-1}(a,x)$ *and* $x = B_2^{-1}(a,x)$

Diagrammatically B and B^{-1} corresponds to a crossing as in Figure Figure 42. Reinterpreting the above definition in this diagrammatic form we see that the Axioms 1 and 2 for B are equivalent to the same-oriented and opposite-oriented Reidemeister II Moves, Axiom 4 corresponds to a Reidemeister I Move and Axiom 3 corresponds to a same-oriented, positive crossing Reidemeister III Move. It is a simple exercise (44) to show that this is enough to ensure invariance under all remaining oriented Reidemeister Moves.

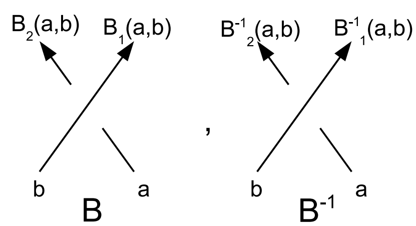

Figure 42. Representation of the Biquandle

Given a knot K, the biquandle of the knot K, $BQ(K)$, is the non-associative algebra generated by the arcs in any planar diagrams of K and relations given by the map B.

Lemma 5.1.1. *$BQ(K)$ is an invariant of the virtual knot K.*

Remark 5.1.1. *Those familiar with the subject will note that the removal of Axiom 4 from the above list gives the definition of a birack. This omission, along with the following section, yields the appropriate definition of parity birack. We will not discuss parity biracks further other than to remark that, just as every biquandle is a birack, every parity biquandle is a parity birack.*

Some common examples of biquandles are the Generalized Alexander Biquandle (31), (26) and the Quaternionic Biquandles with integral coefficients (33).

The Generalized Alexander Biquandle is defined by the diagram in Figure Figure 43 where $a, b \in X$, where s and t are commuting variables in the ground ring, and results in a $\mathbb{Z}\left[s^{\pm 1}, t^{\pm 1}\right]$-module. The following example shows how to use this definition to arrive at the Sawollek Polynomial (31), (26) , a Laurent Polynomial in $\mathbb{Z}\left[s^{\pm 1}, t^{\pm 1}\right]$. Note this polynomial is unique up to a multiple of $t^{\pm 1}$.

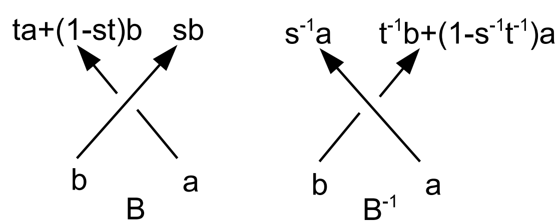

Figure 43. Generalized Alexander Biquandle

Example 5.1.1. *Consider the 3-Crossing Knot* 3.1 *(our naming conventions follow Jeremy Green's Knot Tables (34)) in Figure Figure 44.*

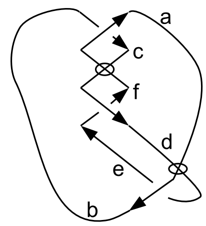

Figure 44. Virtual Knot 3.1 with Labeled Chords

Following the convention of Figure Figure 43 we obtain the following system of equations:

$$\begin{aligned} a &= s^{-1}f \\ b &= s^{-1}a \\ c &= t^{-1}b + (1 - s^{-1}t^{-1})f \\ d &= sc \\ e &= t^{-1}d + (1 - s^{-1}t^{-1})a \\ f &= te + (1 - st) \end{aligned}$$

Or equivalently:

$$\begin{aligned}
-a + s^{-1}f &= 0\\
s^{-1}a - b &= 0\\
t^{-1}b - c + (1 - s^{-1}t^{-1})f &= 0\\
sc - d &= 0\\
(1 - s^{-1}t^{-1})a + t^{-1}d - e &= 0\\
(1 - st)c + te - f &= 0
\end{aligned}$$

Fixing the basis $\{a, b, c, d, e, f\}$ *of* $X^{\times 6}$ *we obtain the matrix:*

$$\begin{pmatrix}
-1 & 0 & 0 & 0 & 0 & s^{-1}\\
s^{-1} & -1 & 0 & 0 & 0 & 0\\
0 & t^{-1} & -1 & 0 & 0 & (1 - s^{-1}t^{-1})\\
0 & 0 & s & -1 & 0 & 0\\
(1 - s^{-1}t^{-1}) & 0 & 0 & t^{-1} & -1 & 0\\
0 & 0 & (1 - st) & 0 & t & -1
\end{pmatrix}$$

Taking the determinant and multiplying by $(-1)^{\omega(K)}$, *where*

$$\omega(K) = \mathit{writhe}(K) = (\#\ \mathit{positive\ crossings\ in}\ K) - (\#\ \mathit{negative\ crossings\ in}\ K)$$

we find, up to multiples of $s^n t^m$, $n, m \in \mathbb{Z}$, *the Sawollek Polynomial of virtual knot* 3.1 *is*

$$\frac{1-\frac{1}{s^2}}{t}+\frac{1}{s^2}+\left(s-\frac{1}{s}\right)t-s+\frac{1}{s}-1$$

For a more systematic description of the matrix construction see (26). It should be noted that the Sawollek polynomial and the generalizations presented later in this paper are well-defined following the proof given in (33) and in the spirit of (45). When working over a gcd-ring, including a polynomial ring over $\mathbb{Z}$, the determinant of the presentation matrix generates a principle ideal and is an invariant of the knot (33). Recall that for a classical knot one of the relations in the matrix above will always be a consequence of the others, hence the Sawollek polynomial will be identically zero on classical knots.

As described in (33) the Quaternionic Biquandles with integral coefficients are a defined as in Figure Figure 45 where $U, V \in \{\pm i, \pm j, \pm k\}, U \perp V$.

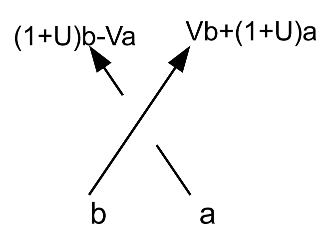

Figure 45. Quaternionic Biquandle with Integral Coefficients

5.2 Parity Biquandles

Definition 5.2.1. *A Parity Biquandle* (X, B, P) *is biquandle* (X, B) *and a map* $P : X \times X \to X \times X$ *which satisfies*

1. P *is invertible, i.e there exists a map* $P^{-1} : X \times X \to X \times X$ *satisfying* $P \circ P^{-1} = Id_{X\times X} = P^{-1} \circ P$,

2. *For all* $a, b \in X$ *there exists* $x \in X$ *such that*

   $x = P_2^{-1}(a, P_2(b, x))$, $a = P_1(b, x)$ *and* $b = P_1^{-1}(a, P_2(b, x))$

   For all $a, b \in X$ *there exists* $x \in X$ *such that*

   $x = P_1(P_1^{-1}(x, b), a)$, $a = P_2^{-1}(x, b)$ *and* $b = P_2(P_1^{-1}(x, b), a)$

3. B *and* P *satisfy the set-theoretic Yang-Baxter equations*

   $(P \times Id) \circ (Id \times P) \circ (B \times Id) = (Id \times B) \circ (P \times Id) \circ (Id \times P)$

   $(P \times Id) \circ (Id \times B) \circ (P \times Id) = (Id \times P) \circ (B \times Id) \circ (Id \times P)$

   $(B \times Id) \circ (Id \times P) \circ (P \times Id) = (Id \times P) \circ (P \times Id) \circ (Id \times B)$

Definition 5.2.2. *Given a biquandle* (X, B) *the even parity biquandle of* (X, B) *is the parity biquandle* (X, B, B).

Given a knot K and diagram D, the parity biquandle of the knot K, $PBQ(K)$, is the non-associative algebra generated by the arcs in D and relations given by applying the maps B at even crossings of D and P at odd crossings of D.

Lemma 5.2.1. *$PBQ(K)$ is an invariant of the virtual knot K.*

5.2.1 The Parity Alexander Biquandle

Given that $B : X \times X \to X \times X$ as described in Figure Figure 43 is linear we can represent B by the matrix

$$\begin{bmatrix} 0 & s \\ t & 1-st \end{bmatrix}$$

Representing P by a 2 matrix, we utilized the linear algebra functionality of Mathematica to determine the following possible values for P.

1. Even Parity Alexander Biquandle

$$P_1 = B = \begin{bmatrix} 0 & s \\ t & 1-st \end{bmatrix}$$

2.

$$P_2 = \begin{bmatrix} 0 & s \\ t & st-1 \end{bmatrix}$$

3. z-Parity Alexander Biquandle

$$P_3 = \begin{bmatrix} 0 & z \\ z^{-1} & 0 \end{bmatrix}$$

or diagrammatically:

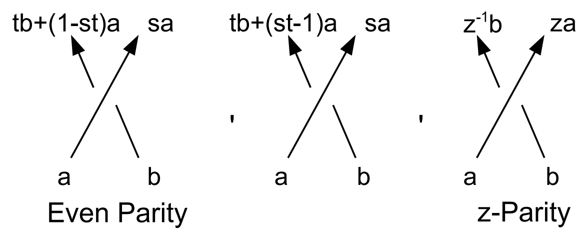

Figure 46. Representations for P in the Parity Alexander Biquandle

Thus (X, B, P_1), (X, B, P_2) and (X, B, P_3) are each parity biquandles. Note (X, B, P_1) and (X, B, P_2) generate $\mathbb{Z}\left[s^{\pm 1}, t^{\pm 1}\right]$-modules while (X, B, P_3), the z-Parity Alexander Biquandle, generates a $\mathbb{Z}\left[s^{\pm 1}, t^{\pm 1}, z^{\pm 1}\right]$-module.

Note that $P_2 = \begin{bmatrix} 0 & s \\ t & 1 - st \end{bmatrix} \times \begin{bmatrix} 1 & 2(s - t^{-1}) \\ 0 & 1 \end{bmatrix}$. Although the polynomial invariant induced by P_2 appears distinct from the Sawollek polynomial, we have yet to find any computational benefit resulting from its calculation. P_3 is a different matter. Namely we have the following theorems:

Theorem 5.2.2. *1. If the polynomial associated to any Parity Alexander Biquandle for a virtual knot K is nonzero, then K is nonclassical.*

2. *If the z-Parity Alexander Polynomial for a virtual knot K is unequal to the Sawollek Polynomial for K then any diagram of K contains an odd crossing.*

Proof. 1. Suppose K is (equivalent to) a classical knot. By the Jordan Curve Theorem K is equivalent to a knot with no odd crossings. Thus any Parity Alexander Biquandle for K is equivalent to the Generalized Alexander Biquandle for K. Thus the respective polynomial is equivalent to the Sawollek polynomial which is identically 0 on classical knots. (See Theorem 3 in (26) or (46))

2. Similarly, if K has a diagram D with no odd crossings, then the z-Parity Alexander Biquandle of D is equivalent to the Generalized Alexander Biquandle of D. Since the Parity Biquandle is invariant under the Reidemeister moves we have the z-Parity Alexander Polynomial of K is equal to the Sawollek Polynomial for K.

∎

Moreover, the z-Parity Alexander Polynomial provides a lower bound on the minimum number of odd crossings in a virtual knot.

Theorem 5.2.3. *Given a virtual knot K, let n_o be the minimum number of odd crossings in any diagram of K, and suppose $z^{e_{max}}$ and $z^{e_{min}}$ are, respectively, the highest and lowest powers* *of z appearing in the z-Parity Alexander Polynomial of K, and set* $e = \max(|e_{max}|, |e_{min}|)$ *then*

$$\begin{cases} e \leq n_o, & \textit{if } e \textit{ is even} \\ \\ (e+1) \leq n_o, & \textit{if } e \textit{ is odd} \end{cases}$$

Proof. Suppose D is a diagram for K with a minimal number of odd crossings and let n be the number of odd crossings in D. Then the matrix of relations contains n entries of value z (and z^{-1}). Thus the highest and lowest power of z in any term of the determinant is $\pm n$. This gives the inequality $e \leq n_o$. Since the number of odd crossings in any knot is always even (Prop. 1.2 (8)) we get the theorem. ∎

Corollary 5.2.4. *Given a virtual knot K let n be the minimum number of real (non-virtual) crossings in any diagram of K and define e as in the previous theorem. If $e > 0$ then $(e+1) \leq n$.*

Proof. Let D be any diagram for K. Suppose for contradiction $e > 0$ and D has no even crossings. Then every relation is of the form $a = z^{\pm 1}b$ where a and b are consecutive arc labels of D. Moreover, starting at any arc and traversing D creates a cycle of relations of the above form with n occurrences of z and z^{-1}. Hence the z-Parity Alexander Biquandle of K is trivial and thus $e = 0$. ∎

Example 5.2.1. *Following the same procedure as earlier with knot* 3.1 *we see it has z-Parity Alexander Polynomial*

$$\frac{\frac{1}{st} - 1}{z^2} - \frac{1}{st} + 1$$

Hence the diagram in Figure Figure 44 is minimal for virtual knot 3.1 *in the sense that it contains the minimum number of odd crossings and the minimum number of total crossing for any diagram of the knot.*

Using Jeremy Green's tables (34) we have calculated the Sawollek Polynomial and the z-Parity Alexander Polynomial for knots with at most 6 real crossings. The knots in Figure Figure 47 and Figure Figure 48 are special in that they are not distinguished from the unknot via the Sawollek Polynomial, z-Parity Sawollek Polynomial, Arrow Polynomial and Parity Arrow Polynomial. Knot 6.32008 has 4 odd crossings while Knot 6.73583 has no odd crossings and both knots are trivial as flats. Using a 2-cable Jones Polynomial calculator adapted from Dror Bar-Natan's "faster" Jones Polynomial Calculator (47) we have been able to distinguish each of these knots from one-another and from the unknot.

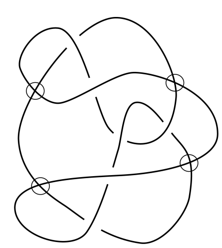

Figure 47. Knot 6.32008

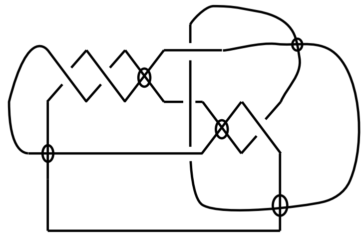

Figure 48. Knot 6.73583

See the Appendix for calculations on knots with at most 4 real crossings following the conventions of (34) along with their Sawollek Polynomials. Note that of the 19 knots with Sawollek polynomial equal 0, 3 are detected (nonzero) by z-Parity. Similarly, of the 54 knots with z-Parity polynomial equal 0, 38 are detected by Sawollek.

While investigating computations for the z-Parity Alexander polynomial we have verified the following conjecture on virtual knots with less than 6 real crossings.

Conjecture 5.2.5. *Given a virtual knot K let n be the minimum number of real (non-virtual) crossings in any diagram of K and suppose $z^{e_{max}}$ and $z^{e_{min}}$ are, respectively, the highest and lowest powers of z appearing in the z-Parity Alexander Polynomial of K. Then $(e_{max} - e_{min}) \leq n$*

The lower bound in this conjecture rarely appears to be tight. The following example is one of five knots with 4-crossings where the bound equals the minimum real crossing number.

Example 5.2.2. *Knot 4.96, given by Gauss Code*

$$\text{“}O1-, O2-, U3+, U1-, O4-, U2-, O3+, U4-''$$

and having 2 odd crossings, has z-Parity Alexander Polynomial

$$z^2\left(\frac{1}{st}-\frac{1}{s^2t^2}\right)+\frac{\frac{1}{st}-\frac{1}{s^2t^2}}{z^2}+\frac{2}{s^2t^2}-\frac{2}{st}$$

5.2.2 Parity Quaternionic Biquandles

In the same fashion as the Parity Alexander Biquandle we utilized Mathematica along with the matrix representation to determine the following values for P, when (X, B) is a Quaternionic Biquandle with integral coefficients.

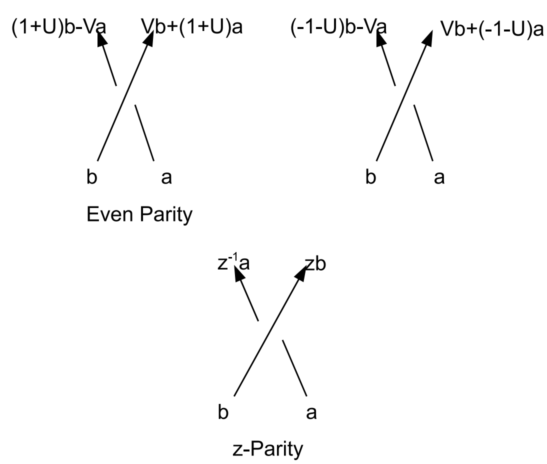

Figure 49. Values for P for the Parity Quaternionic Biquandle

To create an polynomial invariant from the quaternionic biquandle we follow the construction in (33). We first perform a change of basis on the map B which corresponds to extending the ground ring by commuting variables t, t^{-1} . This can be represented diagrammatically as in Figure Figure 50. The construction follows analogously to the Sawollek polynomial. However, before taking the determinant we replace each element of the presentation matrix with its corresponding $SU(2)$ matrix representation. For an n-crossing knot this produces a $4n \times 4n$ matrix over $\mathbb{C}$ whose determinant, called the Study Determinant in (33), is an invariant of the knot.

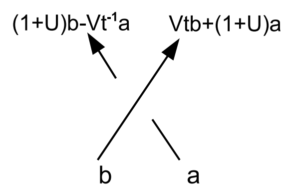

Figure 50. Representation for B in the Integral Quaternionic Biquandle

Example 5.2.3. *Setting $U = i$ and $V = j$ in Figure Figure 45 the virtual knot* 3.1 *in Figure Figure 44 has z-Parity Quaternionic polynomial*

$$2z^4 + \frac{2}{z^4} - 4z^2 - \frac{4}{z^2} + 4$$

5.2.3 Link Parity Biquandles

Following the framework presented earlier we obtain the following extension to links.

Definition 5.2.3. *A Link Parity Biquandle* (X, B, P, L) *is biquandle* (X, B, P) *and a map* $L : X \times X \to X \times X$ *which satisfies*

1. *L is invertible, i.e there exists a map* $L^{-1} : X \times X \to X \times X$ *satisfying* $P \circ P^{-1} = Id_{X \times X} = P^{-1} \circ P$*,*

2. *For all* $a, b \in X$ *there exists* $x \in X$ *such that*

   $x = L_2^{-1}(a, L_2(b, x)),\ a = L_1(b, x)$ *and* $b = L_1^{-1}(a, L_2(b, x))$

   For all $a, b \in X$ *there exists* $x \in X$ *such that*

   $x = L_1(L_1^{-1}(x, b), a),\ a = L_2^{-1}(x, b)$ *and* $b = L_2(L_1^{-1}(x, b), a)$

3. *B, P,and L satisfy the set-theoretic Yang-Baxter equations*

   $(L \times Id) \circ (Id \times L) \circ (B \times Id) = (Id \times B) \circ (L \times Id) \circ (Id \times L)$

   $(L \times Id) \circ (Id \times B) \circ (L \times Id) = (Id \times L) \circ (B \times Id) \circ (Id \times L)$

   $(B \times Id) \circ (Id \times L) \circ (L \times Id) = (Id \times L) \circ (L \times Id) \circ (Id \times B)$

   $(L \times Id) \circ (Id \times L) \circ (P \times Id) = (Id \times P) \circ (L \times Id) \circ (Id \times L)$

   $(L \times Id) \circ (Id \times P) \circ (L \times Id) = (Id \times L) \circ (P \times Id) \circ (Id \times L)$

   $(P \times Id) \circ (Id \times L) \circ (L \times Id) = (Id \times L) \circ (L \times Id) \circ (Id \times P)$

   $(L \times Id) \circ (Id \times L) \circ (L \times Id) = (Id \times L) \circ (L \times Id) \circ (Id \times L)$

Given a link K and diagram D, the link parity biquandle of the knot K, $LPBQ(K)$, is the non-associative algebra generated by the arcs in D and relations given by applying the maps B at even crossings of D, P at odd crossings of D and L at link crossings of D.

Lemma 5.2.6. *$LPBQ(K)$ is an invariant of the virtual link K.*

Furthermore, since at most one even or odd crossing can be involved in any Reidemeister move, we get the following generalization:

Definition 5.2.4. *A Generalized Link Parity Biquandle*

$$(X, \{B_\lambda\}_{\lambda\in\Lambda}, \{P_\lambda\}_{\lambda\in\Lambda}, \{L_{\{\lambda,\rho\}}\})$$

is a family where for every $\lambda, \rho, \gamma \in \Lambda = \{1, \ldots, n\}, \lambda \neq \rho \neq \gamma$, $(X, B_\lambda, P_\lambda)$ is a parity biquandle, $(X, B_\lambda, P_\lambda, L_{\{\lambda,\rho\}})$ is a link parity biquandle and the maps satisfy the following condition:

$$(L_{\{\lambda,\rho\}} \times Id) \circ (Id \times L_{\{\lambda,\gamma\}}) \circ (L_{\{\rho,\gamma\}} \times Id) = (Id \times L_{\{\rho,\gamma\}}) \circ (L_{\{\lambda,\gamma\}} \times Id) \circ (Id \times L_{\{\lambda,\rho\}})$$

Given an n-component link K with diagram D, and components labeled $1, \ldots, n$ the generalized link parity biquandle of the link K, $GPBQ(K)$, is the non-associative algebra generated by the arcs in D and relations given by applying the map B_λ at even crossings of component λ, the map P_λ at odd crossings of component λ, and the map $L_{\{\lambda,\rho\}}$ at crossings between components λ and ρ for $\lambda \neq \rho \in \{1, \ldots, n\}$

Lemma 5.2.7. *$GPBQ(K)$ is an invariant of the virtual link K.*

5.2.3.1 The Generalized Link Parity Alexander Biquandle

Suppose (X, B) is the Generalized Alexander Biquandle described in Figure Figure 43. We have shown that for a single component we may generalize via parity to the z-Parity Alexander Biquandle by applying the relation in Figure Figure 46 at odd crossings. Since it is not possible to have self-crossings from more than one component involved in a Reidemeister move we can instead use separate variables z_i for each component i of a link as shown in Figure Figure 51. We utilized Mathematica to determine the values for maps for $L_{\{i,j\}} : X \times X \to X \times X$ which satisfy the definition of a Generalized Link Parity Biquandle pictured diagrammatically as in Figure Figure 51.

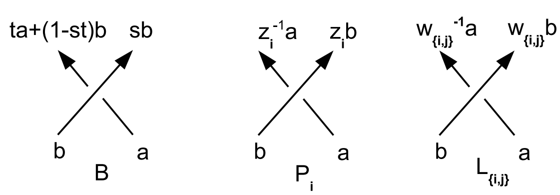

Figure 51. Relations for the Link Parity Alexander Biquandle

Once again we may define a polynomial as above which we refer to as the Generalized Link Parity Alexander Polynomial. An analogous proof to that of Theorem 5.2.3 gives the following:

Theorem 5.2.8. *Given a virtual link K with components labeled $1, \ldots, k$. For $i \in \{1, \ldots, k\}$ let o_i be the minimum number of odd crossings in component i of any diagram of K, and suppose $z_i^{e_{max}}$ and $z_i^{e_{min}}$ are, respectively, the highest and lowest powers of z_i appearing in the Generalized Link Parity Alexander Polynomial of K. Then* $\max(|e_{max}|, |e_{min}|) \leq o_i$.

Theorem 5.2.9. *Given a virtual link K with components labeled $1, \ldots, k$. For $i \neq j \in \{1, \ldots, k\}$ let $l_{\{i,j\}}$ be the minimum number of link crossings between components i and j of any diagram of K, and suppose $w_{\{i,j\}}^{e_{max}}$ and $w_{\{i,j\}}^{e_{min}}$ are, respectively, the highest and lowest powers of $w_{\{i,j\}}$ appearing in the Generalized Link Parity Alexander Polynomial of K. Then* $\max(|e_{max}|, |e_{min}|) \leq l_{\{i,j\}}$.

Example 5.2.4. *The virtual link in Figure Figure 9 has Generalized Link Parity Alexander Polynomial.*

$$\frac{st}{wz_1^2} + \frac{st}{wz_2^2} - \frac{st}{wz_1^2 z_2^2} - \frac{1}{stwz_1^2 z_2^2} - \frac{st}{w} - \frac{w}{st} + \frac{1}{stz_1^2} + \\ \frac{1}{stz_2^2} - \frac{1}{wz_1^2} - \frac{1}{wz_2^2} + \frac{2}{wz_1^2 z_2^2} - \frac{1}{z_1^2} - \frac{1}{z_2^2} + 2$$

Note that Theorems 5.2.8 and 5.2.9 prove the diagram in Figure Figure 9 is minimal both in the number of odd crossings in each component as well as in the number of crossing between components.

5.2.4 Extensions to Virtual Crossings

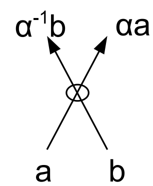

Figure 52. Manturov's Virtual Crossing Biquandle Relation

Manturov's twist relation for virtual crossings (48), (31) for the Generalized Alexander Biquandle as shown in Figure Figure 52 allows us to further extend the Alexander Biquandle and the Generalized Link Parity Alexander Biquandle to what we call the α-Alexander Biquandle and α-Generalized Link Parity Alexander Biquandle. Denote the relation and associated map from $X \times X \to X \times X$ in Figure Figure 52 by V. Notice that replacing α by w in V we have the link parity relation L for the Generalized Link Parity Alexander Biquandle. Thus V satisfies the axioms of L. In other words, the α-Alexander Biquandle and α-Generalized Link Parity Alexander Biquandle are invariant under both oriented virtual Reidemeister II moves, the oriented virtual Reidemeister III move as well as the oriented Mixed Moves (Figure Figure 53). Moreover, it is easy to check that V satisfies Axiom 4 of the Biquandle map B implying the α-Alexander Biquandle and α-Generalized Link Parity Alexander Biquandle are invariant under the Virtual Reidemeister I Move. Hence the α-Alexander Biquandle and α-Generalized Link Parity Alexander Biquandle are invariants of virtual knots.

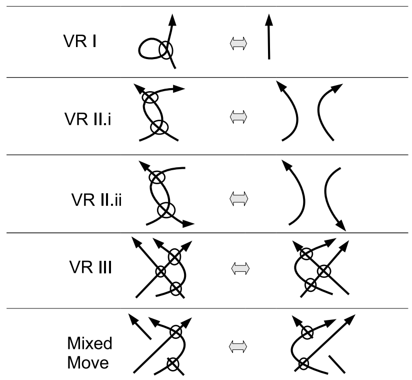

Figure 53. Oriented Virtual Reidemeister Moves

Starting with the Generalized Alexander Biquandle incorporating Manturov's Twist creates the α-Generalized Alexander Biquandle and the α-Generalized Link Parity Alexander Biquandle with respective polynomials we refer to as α-Sawollek and α-Generalized Link Parity Alexander. An analogous proof to that of Theorem 5.2.3 gives the following:

Theorem 5.2.10. *Given a virtual link K, let n_v be the minimum number of virtual crossings in any diagram of K, and suppose $\alpha^{e_{max}}$ and $\alpha^{e_{min}}$ are, respectively, the highest and lowest powers of α appearing in the α-Sawollek polynomial (or (α-Generalized Link Parity Alexander polynomial) of K. Then* $\max\left(|e_{max}|, |e_{min}|\right) \leq n_v$.

Example 5.2.5. *Calculating the α-Sawollek polynomial and the α-Generalized Link Parity Alexander polynomial for the virtual knot* 3.1 *in Figure Figure 44 we get the respectively:*

$$\alpha^{-1}(-s+t^{-1})+(-1+st)+\alpha(s^{-1}-s^{-2}t^{-1})+\alpha^2(s^{-2}-ts^{-1})$$

and

$$s^{-1}t^{-1}(\alpha^2 z^{-2}-1)$$

It follows from Theorem 5.2.3, Corollary 5.2.4 and Theorem 5.2.10 that the diagram in Figure Figure 44 is minimal in virtual crossing number, odd crossing number and total crossing number.

Example 5.2.6. *The virtual link in Figure Figure 9 has α-Generalized Link Parity Alexander Polynomial.*

$$-\frac{st\alpha^5}{z_2^2wz_1^2}-\frac{\alpha^5}{stz_2^2wz_1^2}+\frac{st\alpha^3}{z_2^2w}+\frac{\alpha^2}{stz_2^2}+\frac{st\alpha^3}{wz_1^2}+\frac{\alpha^2}{stz_1^2}-$$
$$\frac{st\alpha}{w}-\frac{w}{st\alpha}+\frac{2\alpha^5}{z_2^2wz_1^2}-\frac{\alpha^3}{z_2^2w}-\frac{\alpha^2}{z_2^2}-\frac{\alpha^3}{wz_1^2}-\frac{\alpha^2}{z_1^2}+2$$

Thus Theorems 5.2.8 and 5.2.9 prove the diagram in Figure Figure 9 is minimal both in the number of odd crossings in each component as well as in the number of crossing between components and Theorem 5.2.10 shows that the diagram is minimal with respect to virtual crossing number.

CHAPTER 6

CONCLUSION

The philosophy of generalizations based on parity presented here appears adaptable to a number of classical and virtual knot invariants. Following (31) the z-parity Alexander polynomial should motivate additional parity generalizations of bi-oriented quantum algebras. Additionally, these methodologies should generate solutions to a parity version of the algebraic Yang-Baxter equation in the same fashion as those found by Dye (49).

The application of parity to the skein polynomials has produced non-trivial flat virtual diagrams which yield lower bounds on the minimal surface genus as shown earlier. We have classified these for knots with at most four classical crossings in Appendix A. A similar analysis for virtual knots with at most six real crossings should generate another collection of virtual flats to examine.

We have only begun to scratch the surface in our search for parity biquandles. In the linear case, Bartholomew and Fenn have shown in (33) there are additional quaternionic biquandles with coefficients in the Hurwitz ring. One would expect to find similar results to the linear biquandle structures studied here. Additionally, Bartholomew and Fenn (32) point out the nonlinear biquandles of Wada (50) and Silver and Williams (51). It is hopeful that additional useful examples will arise from these structures.

APPENDICES

Appendix A

PARITY BRACKET AND PARITY ARROW POLYNOMIALS FOR KNOTS WITH AT MOST FOUR CLASSICAL CROSSINGS

The following table displays the parity bracket polynomial and parity arrow polynomial for virtual knots with at most four crossings. Naming conventions are as in (34). Graphical coefficients are labeled by $D_2[1], D_2[2], D_2[3]$ and $D_4[1], \ldots, D_4[4]$ corresponding to the following diagrams.

$D_2[1] =$ 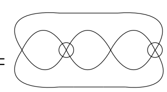 $D_2[2] =$ 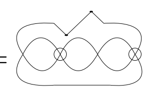

$D_2[3] =$ 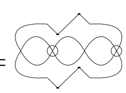

$D_4[1] =$ 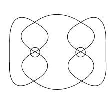 $D_4[2] =$ 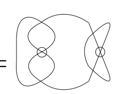

$D_4[3] =$ 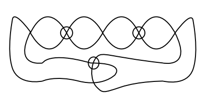 $D_4[4] =$ 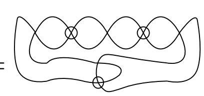

It has been shown by Dye and Kauffman (Theorem 4.1 of (14)) that graphical coefficients $D_4[1]$ and $D_4[2]$ have surface genus $s(D_4[1]) = 2$ and $s(D_4[2]) = 2$. Using this fact we can see

Appendix A (Continued)

that the parity polynomials are able to give a better bound on the genus than that of the arrow polynomial (15) for certain knots. In particular we have

$$s(K) \geq 2 \text{ for } K \in \{4.1, 4.2, 4.4, 4.5, 4.7, 4.8, 4.55, 4.56, 4.76, 4.77\}.$$

TABLE II: Parity Bracket and Parity Arrow Polynomial Calculations

Knot	Parity Bracket	Parity Arrow
2.1	$-A^2 - \frac{1}{A^2}$	$-A^2 - \frac{1}{A^2}$
3.1	$A^6 - \mathrm{D}_2[1]A^2 + A^2$	$A^6 - \mathrm{D}_2[1]A^2 + A^2$
3.2	$-A^2 - \frac{1}{A^2}$	$-A^2 - \frac{1}{A^2}$
3.3	$A^6 - \mathrm{D}_2[1]A^2 + A^2$	$A^6 - \mathrm{D}_2[1]A^2 + A^2$
3.4	$-\frac{\mathrm{D}_2[1]}{A^2} + \frac{1}{A^2} + \frac{1}{A^6}$	$-\frac{\mathrm{D}_2[1]}{A^2} + \frac{1}{A^2} + \frac{1}{A^6}$
3.5	$A^{18} - A^{10} - A^6 - A^2$	$\mathrm{K}_1^2 A^{14} - A^{14} - \mathrm{K}_1^2 A^{10} - A^2$
3.6	$A^{18} - A^{10} - A^6 - A^2$	$A^{18} - A^{10} - A^6 - A^2$
3.7	$-A^2 - \frac{1}{A^2}$	$-A^{10} + \mathrm{K}_1^2 A^6 - A^6 - \mathrm{K}_1^2 A^2$
4.1	$\mathrm{D}_4[1]$	$\mathrm{D}_4[1]$
4.2	$\mathrm{D}_4[2]$	$\mathrm{D}_4[2]$
4.3	$-A^2 - \frac{1}{A^2}$	$-A^2 - \frac{1}{A^2}$
4.4	$\mathrm{D}_4[1]$	$\mathrm{D}_4[1]$
4.5	$\mathrm{D}_4[2]$	$\mathrm{D}_4[2]$
4.6	$-A^2 - \frac{1}{A^2}$	$-A^2 - \frac{1}{A^2}$

Appendix A (Continued)

Knot	Parity Bracket	Parity Arrow
4.7	$\mathrm{D}_4[2]$	$\mathrm{D}_4[2]$
4.8	$\mathrm{D}_4[1]$	$\mathrm{D}_4[1]$
4.9	$\mathrm{D}_2[1]A^8 - 2A^8 - A^6 - 2A^4 - A^2$	$\mathrm{D}_2[2]A^8 + 2\mathrm{K}_1A^6 - A^6 - A^2$
4.10	$A^{12} - A^6 - A^4 - A^2$	$-\mathrm{K}_1A^{10} + \mathrm{K}_1A^6 - A^6 - A^2$
4.11	$-A^4 - A^2 + \mathrm{D}_2[1] - 2 - \frac{1}{A^2} - \frac{1}{A^4}$	$\mathrm{K}_1A^2 - A^2 + \mathrm{D}_2[3] + \frac{\mathrm{K}_1}{A^2} - \frac{1}{A^2}$
4.12	$-A^2 - \frac{1}{A^2}$	$-A^2 - \frac{1}{A^2}$
4.13	$-A^2 - \frac{1}{A^2}$	$-A^2 - \frac{1}{A^2}$
4.14	$\frac{\mathrm{D}_2[1]}{A^8} - \frac{1}{A^2} - \frac{2}{A^4} - \frac{1}{A^6} - \frac{2}{A^8}$	$\frac{2\mathrm{K}_1}{A^6} + \frac{\mathrm{D}_2[2]}{A^8} - \frac{1}{A^2} - \frac{1}{A^6}$
4.15	$A^{12} - A^6 - A^4 - A^2$	$-\mathrm{K}_1A^{10} + \mathrm{K}_1A^6 - A^6 - A^2$
4.16	$\mathrm{D}_2[1]A^8 - 2A^8 - A^6 - 2A^4 - A^2$	$\mathrm{D}_2[2]A^8 + 2\mathrm{K}_1A^6 - A^6 - A^2$
4.17	$-A^4 - A^2 + \mathrm{D}_2[1] - 2 - \frac{1}{A^2} - \frac{1}{A^4}$	$\mathrm{K}_1A^2 - A^2 + \mathrm{D}_2[3] + \frac{\mathrm{K}_1}{A^2} - \frac{1}{A^2}$
4.18	$-A^2 - \frac{1}{A^2}$	$-A^2 - \frac{1}{A^2}$
4.19	$-A^4 - A^2 + \mathrm{D}_2[1] - 2 - \frac{1}{A^2} - \frac{1}{A^4}$	$\mathrm{K}_1A^2 - A^2 + \mathrm{D}_2[2] + \frac{\mathrm{K}_1}{A^2} - \frac{1}{A^2}$
4.20	$-\frac{1}{A^2} - \frac{1}{A^4} - \frac{1}{A^6} + \frac{1}{A^{12}}$	$\frac{\mathrm{K}_1}{A^6} - \frac{\mathrm{K}_1}{A^{10}} - \frac{1}{A^2} - \frac{1}{A^6}$
4.21	$\frac{\mathrm{D}_2[1]}{A^8} - \frac{1}{A^2} - \frac{2}{A^4} - \frac{1}{A^6} - \frac{2}{A^8}$	$\frac{2\mathrm{K}_1}{A^6} + \frac{\mathrm{D}_2[2]}{A^8} - \frac{1}{A^2} - \frac{1}{A^6}$
4.22	$-\frac{1}{A^2} - \frac{1}{A^4} - \frac{1}{A^6} + \frac{1}{A^{12}}$	$\frac{\mathrm{K}_1}{A^6} - \frac{\mathrm{K}_1}{A^{10}} - \frac{1}{A^2} - \frac{1}{A^6}$
4.23	$A^{12} - A^6 - A^4 - A^2$	$-\mathrm{K}_1A^{10} + \mathrm{K}_1A^6 - A^6 - A^2$
4.24	$-\frac{1}{A^2} - \frac{1}{A^4} - \frac{1}{A^6} + \frac{1}{A^{12}}$	$\frac{\mathrm{K}_1}{A^6} - \frac{\mathrm{K}_1}{A^{10}} - \frac{1}{A^2} - \frac{1}{A^6}$
4.25	$-A^2 - \frac{1}{A^2}$	$-A^2 - \frac{1}{A^2}$
4.26	$\mathrm{D}_4[3]$	$\mathrm{D}_4[3]$
4.27	$-A^2 - \frac{1}{A^2}$	$-A^2 - \frac{1}{A^2}$
4.28	$\mathrm{D}_4[4]$	$\mathrm{D}_4[4]$

Appendix A (Continued)

Knot	Parity Bracket	Parity Arrow
4.29	$\mathrm{D}_2[1]A^8 - 2A^8 - A^6 - 2A^4 - A^2$	$\mathrm{D}_2[3]A^8 + 2\mathrm{K}_1A^6 - A^6 - A^2$
4.30	$-A^4 - A^2 + \mathrm{D}_2[1] - 2 - \frac{1}{A^2} - \frac{1}{A^4}$	$\mathrm{K}_1A^2 - A^2 + \mathrm{D}_2[2] + \frac{\mathrm{K}_1}{A^2} - \frac{1}{A^2}$
4.31	$A^{12} - A^6 - A^4 - A^2$	$-\mathrm{K}_1A^{10} + \mathrm{K}_1A^6 - A^6 - A^2$
4.32	$-A^2 - \frac{1}{A^2}$	$-A^2 - \frac{1}{A^2}$
4.33	$-A^4 - A^2 + \mathrm{D}_2[1] - 2 - \frac{1}{A^2} - \frac{1}{A^4}$	$\mathrm{K}_1A^2 - A^2 + \mathrm{D}_2[2] + \frac{\mathrm{K}_1}{A^2} - \frac{1}{A^2}$
4.34	$\frac{\mathrm{D}_2[1]}{A^8} - \frac{1}{A^2} - \frac{2}{A^4} - \frac{1}{A^6} - \frac{2}{A^8}$	$\frac{2\mathrm{K}_1}{A^6} + \frac{\mathrm{D}_2[2]}{A^8} - \frac{1}{A^2} - \frac{1}{A^6}$
4.35	$-A^2 - \frac{1}{A^2}$	$-A^2 - \frac{1}{A^2}$
4.36	$-\frac{1}{A^2} - \frac{1}{A^4} - \frac{1}{A^6} + \frac{1}{A^{12}}$	$\frac{\mathrm{K}_1}{A^6} - \frac{\mathrm{K}_1}{A^{10}} - \frac{1}{A^2} - \frac{1}{A^6}$
4.37	$A^{12} - A^6 - A^4 - A^2$	$-\mathrm{K}_1A^{10} + \mathrm{K}_1A^6 - A^6 - A^2$
4.38	$-A^2 - \frac{1}{A^2}$	$-A^2 - \frac{1}{A^2}$
4.39	$-A^2 - \frac{1}{A^2}$	$-A^2 - \frac{1}{A^2}$
4.40	$-\frac{1}{A^2} - \frac{1}{A^4} - \frac{1}{A^6} + \frac{1}{A^{12}}$	$\frac{\mathrm{K}_1}{A^6} - \frac{\mathrm{K}_1}{A^{10}} - \frac{1}{A^2} - \frac{1}{A^6}$
4.41	$A^{12} - A^6 - A^4 - A^2$	$-\mathrm{K}_1A^{10} + \mathrm{K}_1A^6 - A^6 - A^2$
4.42	$-A^2 - \frac{1}{A^2}$	$-A^2 - \frac{1}{A^2}$
4.43	$-A^2 - \frac{1}{A^2}$	$-A^2 - \frac{1}{A^2}$
4.44	$-A^2 - \frac{1}{A^2}$	$-A^2 - \frac{1}{A^2}$
4.45	$\mathrm{D}_4[3]$	$\mathrm{D}_4[3]$
4.46	$-A^2 - \frac{1}{A^2}$	$-A^2 - \frac{1}{A^2}$
4.47	$\mathrm{D}_4[4]$	$\mathrm{D}_4[4]$
4.48	$\mathrm{D}_2[1]A^8 - 2A^8 - A^6 - 2A^4 - A^2$	$\mathrm{D}_2[2]A^8 + 2\mathrm{K}_1A^6 - A^6 - A^2$
4.49	$-A^4 - A^2 + \mathrm{D}_2[1] - 2 - \frac{1}{A^2} - \frac{1}{A^4}$	$\mathrm{K}_1A^2 - A^2 + \mathrm{D}_2[3] + \frac{\mathrm{K}_1}{A^2} - \frac{1}{A^2}$
4.50	$A^{12} - A^6 - A^4 - A^2$	$-\mathrm{K}_1A^{10} + \mathrm{K}_1A^6 - A^6 - A^2$

Appendix A (Continued)

Knot	Parity Bracket	Parity Arrow
4.51	$-A^2 - \frac{1}{A^2}$	$-A^2 - \frac{1}{A^2}$
4.52	$\frac{\mathrm{D}_2[1]}{A^8} - \frac{1}{A^2} - \frac{2}{A^4} - \frac{1}{A^6} - \frac{2}{A^8}$	$\frac{2\mathrm{K}_1}{A^6} + \frac{\mathrm{D}_2[2]}{A^8} - \frac{1}{A^2} - \frac{1}{A^6}$
4.53	$-A^2 - \frac{1}{A^2}$	$-A^2 - \frac{1}{A^2}$
4.54	$-A^2 - \frac{1}{A^2}$	$-A^2 - \frac{1}{A^2}$
4.55	$\mathrm{D}_4[1]$	$\mathrm{D}_4[1]$
4.56	$\mathrm{D}_4[2]$	$\mathrm{D}_4[2]$
4.57	$\mathrm{D}_2[1]A^8 - 2A^8 - A^6 - 2A^4 - A^2$	$\mathrm{D}_2[3]A^8 + 2\mathrm{K}_1A^6 - A^6 - A^2$
4.58	$-A^4 - A^2 + \mathrm{D}_2[1] - 2 - \frac{1}{A^2} - \frac{1}{A^4}$	$\mathrm{K}_1A^2 - A^2 + \mathrm{D}_2[2] + \frac{\mathrm{K}_1}{A^2} - \frac{1}{A^2}$
4.59	$-A^4 - A^2 + \mathrm{D}_2[1] - 2 - \frac{1}{A^2} - \frac{1}{A^4}$	$\mathrm{K}_1A^2 - A^2 + \mathrm{D}_2[2] + \frac{\mathrm{K}_1}{A^2} - \frac{1}{A^2}$
4.60	$-\frac{1}{A^2} - \frac{1}{A^4} - \frac{1}{A^6} + \frac{1}{A^{12}}$	$\frac{\mathrm{K}_1}{A^6} - \frac{\mathrm{K}_1}{A^{10}} - \frac{1}{A^2} - \frac{1}{A^6}$
4.61	$A^{12} - A^6 - A^4 - A^2$	$-\mathrm{K}_1A^{10} + \mathrm{K}_1A^6 - A^6 - A^2$
4.62	$-A^2 - \frac{1}{A^2}$	$-A^2 - \frac{1}{A^2}$
4.63	$-A^2 - \frac{1}{A^2}$	$-A^2 - \frac{1}{A^2}$
4.64	$-\frac{1}{A^2} - \frac{1}{A^4} - \frac{1}{A^6} + \frac{1}{A^{12}}$	$\frac{\mathrm{K}_1}{A^6} - \frac{\mathrm{K}_1}{A^{10}} - \frac{1}{A^2} - \frac{1}{A^6}$
4.65	$A^{12} - A^6 - A^4 - A^2$	$-\mathrm{K}_1A^{10} + \mathrm{K}_1A^6 - A^6 - A^2$
4.66	$-A^2 - \frac{1}{A^2}$	$-A^2 - \frac{1}{A^2}$
4.67	$-A^2 - \frac{1}{A^2}$	$-A^2 - \frac{1}{A^2}$
4.68	$-\frac{1}{A^2} - \frac{1}{A^4} - \frac{1}{A^6} + \frac{1}{A^{12}}$	$\frac{\mathrm{K}_1}{A^6} - \frac{\mathrm{K}_1}{A^{10}} - \frac{1}{A^2} - \frac{1}{A^6}$
4.69	$A^{12} - A^6 - A^4 - A^2$	$-\mathrm{K}_1A^{10} + \mathrm{K}_1A^6 - A^6 - A^2$
4.70	$\mathrm{D}_2[1]A^8 - 2A^8 - A^6 - 2A^4 - A^2$	$\mathrm{D}_2[3]A^8 + 2\mathrm{K}_1A^6 - A^6 - A^2$
4.71	$-A^4 - A^2 + \mathrm{D}_2[1] - 2 - \frac{1}{A^2} - \frac{1}{A^4}$	$\mathrm{K}_1A^2 - A^2 + \mathrm{D}_2[2] + \frac{\mathrm{K}_1}{A^2} - \frac{1}{A^2}$
4.72	$-A^4 - A^2 + \mathrm{D}_2[1] - 2 - \frac{1}{A^2} - \frac{1}{A^4}$	$\mathrm{K}_1A^2 - A^2 + \mathrm{D}_2[2] + \frac{\mathrm{K}_1}{A^2} - \frac{1}{A^2}$

Appendix A (Continued)

Knot	Parity Bracket	Parity Arrow
4.73	$-A^2 - \frac{1}{A^2}$	$-A^2 - \frac{1}{A^2}$
4.74	$-A^2 - \frac{1}{A^2}$	$-A^2 - \frac{1}{A^2}$
4.75	$-A^2 - \frac{1}{A^2}$	$-A^2 - \frac{1}{A^2}$
4.76	$\mathrm{D}_4[2]$	$\mathrm{D}_4[2]$
4.77	$\mathrm{D}_4[1]$	$\mathrm{D}_4[1]$
4.78	$A^{12} - A^6 - A^4 - A^2$	$-\mathrm{K}_1 A^{10} + \mathrm{K}_1 A^6 - A^6 - A^2$
4.79	$A^{12} - A^6 - A^4 - A^2$	$-\mathrm{K}_1 A^{10} + \mathrm{K}_1 A^6 - A^6 - A^2$
4.80	$\mathrm{D}_4[3]$	$\mathrm{D}_4[3]$
4.81	$\mathrm{D}_4[4]$	$\mathrm{D}_4[4]$
4.82	$-A^{10} + \mathrm{D}_2[1]A^6 - A^6 - \mathrm{D}_2[1]A^2$	$-A^{10} + \mathrm{D}_2[1]A^6 - A^6 - \mathrm{D}_2[1]A^2$
4.83	$-A^2 - \frac{1}{A^2}$	$-A^2 - \frac{1}{A^2}$
4.84	$-A^{10} + \mathrm{D}_2[1]A^6 - A^6 - \mathrm{D}_2[1]A^2$	$-A^{10} + \mathrm{D}_2[1]A^6 - A^6 - \mathrm{D}_2[1]A^2$
4.85	$-A^2 - \frac{1}{A^2}$	$-A^{10} + \mathrm{K}_1^2 A^6 - A^6 - \mathrm{K}_1^2 A^2$
4.86	$-A^{10} - \frac{1}{A^{10}}$	$-A^{10} - A^2 + \frac{\mathrm{K}_1^2}{A^2} - \frac{1}{A^2} - \frac{\mathrm{K}_1^2}{A^6} + \frac{1}{A^6}$
4.87	$-A^{10} + \mathrm{D}_2[1]A^6 - A^6 - \mathrm{D}_2[1]A^2$	$-A^{10} + \mathrm{D}_2[1]A^6 - A^6 - \mathrm{D}_2[1]A^2$
4.88	$-A^{10} + \mathrm{D}_2[1]A^6 - A^6 - \mathrm{D}_2[1]A^2$	$-A^{10} + \mathrm{D}_2[1]A^6 - A^6 - \mathrm{D}_2[1]A^2$
4.89	$A^{18} - A^{10} - A^6 - A^2$	$-A^{18} + 2\mathrm{K}_1^2 A^{14} - 2A^{14} - 2\mathrm{K}_1^2 A^{10} + A^{10} + A^6 - A^2$
4.90	$-A^{10} - \frac{1}{A^{10}}$	$-\mathrm{K}_1^2 A^6 + A^6 + \mathrm{K}_1^2 A^2 - 2A^2 + \frac{\mathrm{K}_1^2}{A^2} - \frac{2}{A^2} - \frac{\mathrm{K}_1^2}{A^6} + \frac{1}{A^6}$
4.91	$-A^2 - \frac{1}{A^2}$	$-A^2 - \frac{1}{A^2}$
4.92	$-A^2 - \frac{1}{A^2}$	$-A^2 - \frac{1}{A^2}$

Appendix A (Continued)

Knot	Parity Bracket	Parity Arrow
4.93	$-A^{10}+\mathrm{D}_2[1]A^6-A^6-\mathrm{D}_2[1]A^2$	$-A^{10}+\mathrm{D}_2[1]A^6-A^6-\mathrm{D}_2[1]A^2$
4.94	$-A^2-\frac{1}{A^2}$	$-A^2-\frac{1}{A^2}$
4.95	$-A^2-\frac{1}{A^2}$	$-A^2-\frac{1}{A^2}$
4.96	$-A^{10}+\mathrm{D}_2[1]A^6-A^6-\mathrm{D}_2[1]A^2$	$-A^{10}+\mathrm{D}_2[1]A^6-A^6-\mathrm{D}_2[1]A^2$
4.97	$-A^2-\frac{1}{A^2}$	$-A^2-\frac{1}{A^2}$
4.98	$-A^2-\frac{1}{A^2}$	$-A^2-\frac{1}{A^2}$
4.99	$-A^{10}-\frac{1}{A^{10}}$	$-A^{10}-\frac{1}{A^{10}}$
4.100	$-A^2-\frac{1}{A^2}$	$-A^2-\frac{1}{A^2}$
4.101	$-A^2-\frac{1}{A^2}$	$-A^2-\frac{1}{A^2}$
4.102	$-A^2-\frac{1}{A^2}$	$-A^2-\frac{1}{A^2}$
4.103	$-A^{10}+\mathrm{D}_2[1]A^6-A^6-\mathrm{D}_2[1]A^2$	$-A^{10}+\mathrm{D}_2[1]A^6-A^6-\mathrm{D}_2[1]A^2$
4.104	$-A^2-\frac{1}{A^2}$	$-A^2-\frac{1}{A^2}$
4.105	$A^{18}-A^{10}-A^6-A^2$	$A^{18}-A^{10}-A^6-A^2$
4.106	$-A^2-\frac{1}{A^2}$	$-A^{10}+\mathrm{K}_1^2A^6-A^6-\mathrm{K}_1^2A^2$
4.107	$-A^2-\frac{1}{A^2}$	$-A^2-\frac{1}{A^2}$
4.108	$-A^{10}-\frac{1}{A^{10}}$	$-A^{10}-\frac{1}{A^{10}}$

Appendix B

PARITY AND NON-PARITY BRACKET AND ARROW POLYNOMIAL CALCULATORS

B.1 Planar Diagram Conventions

The the Planar Diagram code conventions given in Figure Figure 54 are used for the skein polynomial, categorification and biquandle calculators.

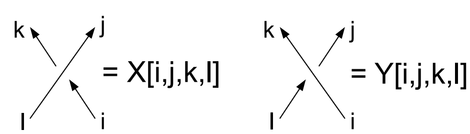

Figure 54. Planar Diagram Code Conventions

Example B.1.1. *Virtual Knot 3.1 as labeled in Figure Figure 55 has planar diagram code:*

$$PD[X[1,5,2,4], X[5,4,6,3], Y[6,3,1,2]]$$

Appendix B (Continued)

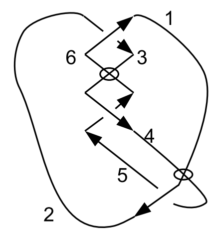

Figure 55. Planar Diagram Code for Virtual Knot 3.1

B.2 Normalized Parity Bracket Polynomial Calculator

The following program computes the normalized parity bracket polynomial. The program is based on Kauffman's original construction of the bracket polynomial (11) (12). A more detailed description of the original construction, as well as improvements to its efficiency, can also be found at The Knot Atlas (47).

```
SetAttributes[del, Orderless]


EvenParityPD[L_PD] :=
 L /. {X[i_, j_, k_, l_] :> Odd[i, j, k, l] /; OddQ[i - j]} /. {Y[i_,
     j_, k_, l_] :> Odd[i, j, k, l] /; OddQ[i - j]}


np[L_PD] := Count[L, _X];
nm[L_PD] := Count[L, _Y];


rule1 = {X[i_, j_, k_, l_] :> A del[i, j] del[k, l] +
```

Appendix B (Continued)

```
      B del[l, i] del[j, k],
   Y[i_, j_, k_, l_] :> B del[i, j] del[k, l] +
      A del[l, i] del[j, k]};

rule2 = {del[a_, b_] del[b_, c_] :> del[a, c]};

rule3 = {(del[a_, a_]) :> J, (del[a_, b_])^2 :> J};

ruleGraphical = {Odd[a_, b_, c_, d_] Odd[b_, c_, d_, a_] :> D2[1],
   Odd[c_, b_, d_, a_] Odd[d_, a_, c_, b_] :> D2[1],
   Odd[a_, d_, b_, c_] Odd[d_, g_, e_, f_] Odd[e_, h_, f_, g_] Odd[h_,
       c_, a_, b_] :> D4[1],
   Odd[e_, d_, f_, c_] Odd[f_, e_, g_, d_] Odd[g_, b_, h_, a_] Odd[h_,
       c_, a_, b_] :> D4[2],
   Odd[a_, f_, b_, e_] Odd[f_, e_, g_, d_] Odd[g_, d_, h_, c_] Odd[h_,
       c_, a_, b_] :> D4[3],
   Odd[e_, b_, f_, a_] Odd[f_, e_, g_, d_] Odd[g_, d_, h_, c_] Odd[h_,
       c_, a_, b_] :> D4[4]};

ruleParity1 = {Odd[a_, b_, c_, d_] del[a_, x_] :> Odd[x, b, c, d],
   Odd[a_, b_, c_, d_] del[b_, x_] :> Odd[a, x, c, d],
   Odd[a_, b_, c_, d_] del[c_, x_] :> Odd[a, b, x, d],
   Odd[a_, b_, c_, d_] del[d_, x_] :> Odd[a, b, c, x]};
```

Appendix B (Continued)

```
ruleParityR2Equiv = {

   Odd[a_, b_, y_, x_] Odd[c_, d_, x_, y_] :> del[a, d] del[b, c],

   Odd[b_, y_, x_, a_] Odd[c_, d_, x_, y_] :> del[a, d] del[b, c],

   Odd[a_, b_, y_, x_] Odd[d_, x_, y_, c_] :> del[a, d] del[b, c],

   Odd[b_, y_, x_, a_] Odd[d_, x_, y_, c_] :> del[a, d] del[b, c],

   Odd[c_, d_, x_, y_] Odd[x_, a_, b_, y_] :> del[a, d] del[b, c],

   Odd[d_, x_, y_, c_] Odd[x_, a_, b_, y_] :> del[a, d] del[b, c],

   Odd[a_, b_, y_, x_] Odd[x_, y_, c_, d_] :> del[a, d] del[b, c],

   Odd[b_, y_, x_, a_] Odd[x_, y_, c_, d_] :> del[a, d] del[b, c],

   Odd[x_, a_, b_, y_] Odd[x_, y_, c_, d_] :> del[a, d] del[b, c],

   Odd[a_, b_, y_, x_] Odd[y_, c_, d_, x_] :> del[a, d] del[b, c],

   Odd[b_, y_, x_, a_] Odd[y_, c_, d_, x_] :> del[a, d] del[b, c],

   Odd[x_, a_, b_, y_] Odd[y_, c_, d_, x_] :> del[a, d] del[b, c],

   Odd[c_, d_, x_, y_] Odd[y_, x_, a_, b_] :> del[a, d] del[b, c],

   Odd[d_, x_, y_, c_] Odd[y_, x_, a_, b_] :> del[a, d] del[b, c],

   Odd[x_, y_, c_, d_] Odd[y_, x_, a_, b_] :> del[a, d] del[b, c],

   Odd[y_, c_, d_, x_] Odd[y_, x_, a_, b_] :> del[a, d] del[b, c]};


RawBracket[K__] :=

 Simplify[(K //. rule1 // Expand) //.

    Union[ruleParity1, ruleParityR2Equiv, rule2] /.

   Union[rule3, ruleGraphical]]

rule4 = {B :> 1/A, J :> -A^2 - 1/A^2};

B[K_PD] :=
```

Appendix B (Continued)

```
 Expand[Simplify[
    RawBracket[RawBracket[K /. (PD[z___] :> Times[z])]] /.
     rule4]*((-(A^3))^(-(np[K] - nm[K])))]
(*F[t_] := B[t]/.A:>1*)
ParityJones[K_PD] := B[EvenParityPD[K]]
```

B.3 Normalized Parity Arrow Polynomial Calculator

The following program for the normalized parity arrow polynomial is based on the program by Kauffman in (13).

```
EvenParityPD[L_PD] :=
 L /. {X[i_, j_, k_, l_] :> Odd[i, j, k, l] /; OddQ[i - j]} /. {Y[i_,
     j_, k_, l_] :> Odd[i, j, k, l] /; OddQ[i - j]}

SetAttributes[del, Orderless]
rule1 = {X[i_, j_, k_, l_] :>
    A del[i, j] del[k, l] + B led[l, i] led[j, k],
   Y[i_, j_, k_, l_] :> B del[i, j] del[k, l] + A led[l, i] led[j, k]};

rule2 = {del[a_, b_] del[b_, c_] :> del[a, c],
   del[a_, b_] del[c_, b_] :> del[a, c],
   del[a_, b_] led[b_, c_] :> led[a, c],
   del[a_, b_] led[c_, b_] :> led[c, a],
   del[b_, a_] led[b_, c_] :> led[a, c],
```

Appendix B (Continued)

```
   del[b_, a_] led[c_, b_] :> led[c, a],
   led[a_, b_] del[b_, c_] :> led[a, c],
   led[a_, b_] del[c_, b_] :> led[a, c],
   led[b_, a_] del[c_, b_] :> led[c, a],
   led[b_, a_] del[b_, c_] :> led[c, a],
   led[a_, b_] led[b_, c_] :> del[a, c]
   };

rule3 = {(del[a_, a_]) :> J, (del[a_, b_])^2 :> J,
   led[a_, b_]^2 :> K1,
   led[a_, b_] led[c_, b_] led[c_, d_] led[a_, d_] :> K2,
    led[a_, g_] led[a_, i_] led[c_, g_] led[c_, k_] led[e_, i_] led[
      e_, k_] :>  K3};

ruleGraphical = { Odd[c_, b_, d_, a_] Odd[d_, a_, c_, b_] :> D2[1],
   led[a_, d_] led[b_, e_] Odd[e_, d_, f_, c_] Odd[f_, c_, a_, b_] :>
    J, led[d_, a_] led[e_, b_] Odd[e_, d_, f_, c_] Odd[f_, c_, a_,
      b_] :> J,
   led[e_, h_] led[f_, a_] Odd[c_, f_, b_, e_] Odd[h_, c_, a_, b_] :>
    D2[2], led[e_, b_] led[f_, c_] Odd[e_, h_, f_, a_] Odd[h_, c_, a_,
       b_] :> D2[2],
   led[c_, h_] led[d_, a_] led[d_, g_] led[e_, h_] Odd[a_, f_, b_,
      e_] Odd[b_, g_, c_, f_] :> J,
   led[c_, h_] led[d_, a_] led[d_, g_] led[e_, h_] Odd[e_, b_, f_,
```

```
    a_] Odd[f_, c_, g_, b_] :> J,
  led[a_, f_] led[b_, g_] led[d_, g_] led[e_, h_] Odd[c_, f_, d_,
    e_] Odd[h_, c_, a_, b_] :> D2[2],
  led[f_, a_] led[g_, b_] led[g_, d_] led[h_, e_] Odd[c_, f_, d_,
    e_] Odd[h_, c_, a_, b_] :> D2[3],
  Odd[a_, d_, b_, c_] Odd[d_, g_, e_, f_] Odd[e_, h_, f_, g_] Odd[h_,
     c_, a_, b_] :> D4[1],
  Odd[e_, d_, f_, c_] Odd[f_, e_, g_, d_] Odd[g_, b_, h_, a_] Odd[h_,
     c_, a_, b_] :> D4[2],
  Odd[a_, f_, b_, e_] Odd[f_, e_, g_, d_] Odd[g_, d_, h_, c_] Odd[h_,
     c_, a_, b_] :> D4[3],
  Odd[e_, b_, f_, a_] Odd[f_, e_, g_, d_] Odd[g_, d_, h_, c_] Odd[h_,
     c_, a_, b_] :> D4[4]};

ruleParity1 = {Odd[a_, b_, c_, d_] del[a_, x_] :> Odd[x, b, c, d],
  Odd[a_, b_, c_, d_] del[b_, x_] :> Odd[a, x, c, d],
  Odd[a_, b_, c_, d_] del[c_, x_] :> Odd[a, b, x, d],
  Odd[a_, b_, c_, d_] del[d_, x_] :> Odd[a, b, c, x]};

ruleParityR2Equiv = {
  Odd[a_, b_, y_, x_] Odd[c_, d_, x_, y_] :> del[a, d] del[b, c],
  Odd[b_, y_, x_, a_] Odd[c_, d_, x_, y_] :> del[a, d] del[b, c],
  Odd[a_, b_, y_, x_] Odd[d_, x_, y_, c_] :> del[a, d] del[b, c],
  Odd[b_, y_, x_, a_] Odd[d_, x_, y_, c_] :> del[a, d] del[b, c],
```

Appendix B (Continued)

```
   Odd[c_, d_, x_, y_] Odd[x_, a_, b_, y_] :> del[a, d] del[b, c],
   Odd[d_, x_, y_, c_] Odd[x_, a_, b_, y_] :> del[a, d] del[b, c],
   Odd[a_, b_, y_, x_] Odd[x_, y_, c_, d_] :> del[a, d] del[b, c],
   Odd[b_, y_, x_, a_] Odd[x_, y_, c_, d_] :> del[a, d] del[b, c],
   Odd[x_, a_, b_, y_] Odd[x_, y_, c_, d_] :> del[a, d] del[b, c],
   Odd[a_, b_, y_, x_] Odd[y_, c_, d_, x_] :> del[a, d] del[b, c],
   Odd[b_, y_, x_, a_] Odd[y_, c_, d_, x_] :> del[a, d] del[b, c],
   Odd[x_, a_, b_, y_] Odd[y_, c_, d_, x_] :> del[a, d] del[b, c],
   Odd[c_, d_, x_, y_] Odd[y_, x_, a_, b_] :> del[a, d] del[b, c],
   Odd[d_, x_, y_, c_] Odd[y_, x_, a_, b_] :> del[a, d] del[b, c],
   Odd[x_, y_, c_, d_] Odd[y_, x_, a_, b_] :> del[a, d] del[b, c],
   Odd[y_, c_, d_, x_] Odd[y_, x_, a_, b_] :> del[a, d] del[b, c]};


ruleParityArrowR3Equiv = {
   led[x_, y_] Odd[a_, z_, x_, b_] Odd[c_, d_, y_, z_] :>
    del[b, d] led[a, c],
   led[x_, y_] Odd[b_, a_, z_, x_] Odd[c_, d_, y_, z_] :>
    del[b, d] led[a, c],
   led[x_, y_] Odd[a_, z_, x_, b_] Odd[d_, y_, z_, c_] :>
    del[b, d] led[a, c],
   led[x_, y_] Odd[b_, a_, z_, x_] Odd[d_, y_, z_, c_] :>
    del[b, d] led[a, c],
   led[x_, y_] Odd[c_, d_, y_, z_] Odd[x_, b_, a_, z_] :>
    del[b, d] led[a, c],
```

Appendix B (Continued)

```
led[x_, y_] Odd[d_, y_, z_, c_] Odd[x_, b_, a_, z_] :>
 del[b, d] led[a, c],
led[x_, y_] Odd[a_, z_, x_, b_] Odd[y_, z_, c_, d_] :>
 del[b, d] led[a, c],
led[x_, y_] Odd[b_, a_, z_, x_] Odd[y_, z_, c_, d_] :>
 del[b, d] led[a, c],
led[x_, y_] Odd[x_, b_, a_, z_] Odd[y_, z_, c_, d_] :>
 del[b, d] led[a, c],
led[x_, y_] Odd[a_, z_, x_, b_] Odd[z_, c_, d_, y_] :>
 del[b, d] led[a, c],
led[x_, y_] Odd[b_, a_, z_, x_] Odd[z_, c_, d_, y_] :>
 del[b, d] led[a, c],
led[x_, y_] Odd[x_, b_, a_, z_] Odd[z_, c_, d_, y_] :>
 del[b, d] led[a, c],
led[x_, y_] Odd[c_, d_, y_, z_] Odd[z_, x_, b_, a_] :>
 del[b, d] led[a, c],
led[x_, y_] Odd[d_, y_, z_, c_] Odd[z_, x_, b_, a_] :>
 del[b, d] led[a, c],
led[x_, y_] Odd[y_, z_, c_, d_] Odd[z_, x_, b_, a_] :>
 del[b, d] led[a, c],
led[x_, y_] Odd[z_, c_, d_, y_] Odd[z_, x_, b_, a_] :>
 del[b, d] led[a, c],
led[y_, x_] Odd[a_, z_, x_, b_] Odd[c_, d_, y_, z_] :>
 del[b, d] led[c, a],
```

Appendix B (Continued)

```
led[y_, x_] Odd[b_, a_, z_, x_] Odd[c_, d_, y_, z_] :>
 del[b, d] led[c, a],
led[y_, x_] Odd[a_, z_, x_, b_] Odd[d_, y_, z_, c_] :>
 del[b, d] led[c, a],
led[y_, x_] Odd[b_, a_, z_, x_] Odd[d_, y_, z_, c_] :>
 del[b, d] led[c, a],
led[y_, x_] Odd[c_, d_, y_, z_] Odd[x_, b_, a_, z_] :>
 del[b, d] led[c, a],
led[y_, x_] Odd[d_, y_, z_, c_] Odd[x_, b_, a_, z_] :>
 del[b, d] led[c, a],
led[y_, x_] Odd[a_, z_, x_, b_] Odd[y_, z_, c_, d_] :>
 del[b, d] led[c, a],
led[y_, x_] Odd[b_, a_, z_, x_] Odd[y_, z_, c_, d_] :>
 del[b, d] led[c, a],
led[y_, x_] Odd[x_, b_, a_, z_] Odd[y_, z_, c_, d_] :>
 del[b, d] led[c, a],
led[y_, x_] Odd[a_, z_, x_, b_] Odd[z_, c_, d_, y_] :>
 del[b, d] led[c, a],
led[y_, x_] Odd[b_, a_, z_, x_] Odd[z_, c_, d_, y_] :>
 del[b, d] led[c, a],
led[y_, x_] Odd[x_, b_, a_, z_] Odd[z_, c_, d_, y_] :>
 del[b, d] led[c, a],
led[y_, x_] Odd[c_, d_, y_, z_] Odd[z_, x_, b_, a_] :>
 del[b, d] led[c, a],
```

Appendix B (Continued)

```
   led[y_, x_] Odd[d_, y_, z_, c_] Odd[z_, x_, b_, a_] :>
    del[b, d] led[c, a],
   led[y_, x_] Odd[y_, z_, c_, d_] Odd[z_, x_, b_, a_] :>
    del[b, d] led[c, a],
   led[y_, x_] Odd[z_, c_, d_, y_] Odd[z_, x_, b_, a_] :>
    del[b, d] led[c, a]};


np[L_PD] := Count[L, _X];
nm[L_PD] := Count[L, _Y];


RawBracket[K__] :=
 Simplify[(K //. rule1 // Expand) //.
    Union[ruleParity1, ruleParityR2Equiv, rule2,
     ruleParityArrowR3Equiv] //. Union[rule3, ruleGraphical]]
rule4 = {B :> 1/A, J :> -A^2 - 1/A^2};
B[K_PD] :=
 Expand[Simplify[(RawBracket[
       RawBracket[K /. (PD[z___] :> Times[z])]]) /.
     rule4]*((-(A^3))^(-(np[K] - nm[K])))]
(*F[t_] := B[t]/.A:>1*)
ParityArrow[K_PD] := B[EvenParityPD[K]]
```

Appendix C

PARITY AND NON-PARITY BRACKET AND ARROW CATEGORIFICATION CALCULATORS

C.1 (Parity) Khovanov Homology Calculator

The following program for parity Khovanov homology is based on Dror Bar-Natan's construction (17) for Khovanov homology. Here we implement a version of Gaussian elimination for computing homology with coefficients over $\mathbb{Z}_2$ that was pointed out to us by Marc Culler and implemented by Baldwin and Gillam for computation of Heegaard-Floer knot homology in (52). This can be described graphically as in Figure Figure 56 where we reduce based on the chosen marked edge. This is equivalent to the applying Gaussian Elimination to the chain complex as in Figure Figure 57 where we assume ϕ (the equivalent of the selected edge) is invertible. Maps denoted by $\bullet$ are arbitrary and inconsequential in the final result. For more on Gaussian Elimination and homotopy equivalence we point the reader to (53).

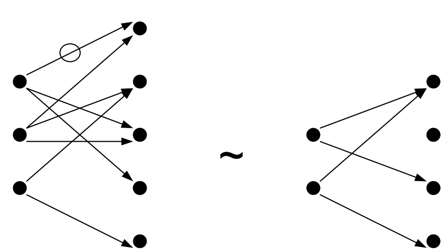

Figure 56. Graphical Reduction for Homology with $\mathbb{Z}_2$ Coefficients

Appendix C (Continued)

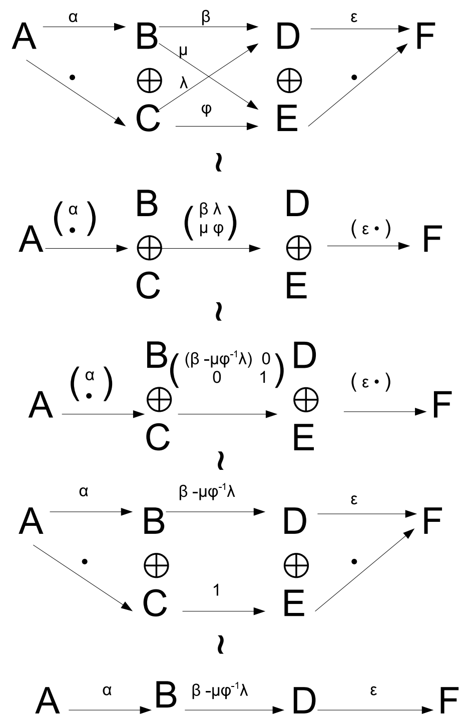

Figure 57. Gaussian Elimination for Chain Complexes

For an explanation of how this program works see the associated parts of the program for the categorification of the arrow polynomial (and its parity version) which immediately follows.

```
np[L_PD] := Count[L, _X];

nm[L_PD] := Count[L, _Y];

SetAttributes[del, Orderless]


EvenParityPD[L_PD] :=
```

Appendix C (Continued)

```
 Sort[L /. {X[i_, j_, k_, l_] :>
      Odd[i, j, k, l] /; OddQ[i - j]} /. {Y[i_, j_, k_, l_] :>
     Odd[i, j, k, l] /; OddQ[i - j]}]


SetAttributes[p, Orderless]


rule2 = {del[a_, b_][m_] del[a_, b_][m_] :> del[a, a][m],
   del[a_, b_][m_] del[b_, c_][n_] :> del[a, c][Min[m, n]]};


rule3 = {del[a_, a_][m_] :> c[m], del[a_, a_][m_]^_ :> c[m]};


ruleStar = {v___c u___ X[i_, j_, k_,
      l_] :> ((u del[i, j][Min[i, j]] del[k, l][Min[k, l]] //.
         rule2 //.
        rule3) -> (u del[l, i][Min[l, i]] del[j, k][Min[j, k]] //.
         rule2 //. rule3)),
   v___c u___ Y[i_, j_, k_,
      l_] :> ((u del[l, i][Min[l, i]] del[j, k][Min[j, k]] //.
         rule2 //.
        rule3) -> (u del[i, j][Min[i, j]] del[k, l][Min[k, l]] //.
         rule2 //. rule3))};


S[L_PD, a_List] :=
 (Times[(Times @@ (Thread[{List @@
```

Appendix C (Continued)

```
             Drop[L, Length[L] - (np[L] + nm[L])],
            a}] /. {{X[i_, j_, k_, l_], 0} :>
            del[i, j][Min[i, j]] del[k, l][Min[k, l]], {X[i_, j_, k_,
              l_], 1} :>
            del[l, i][Min[l, i]] del[j, k][Min[j, k]], {Y[i_, j_, k_,
              l_], 0} :>
            del[l, i][Min[l, i]] del[j, k][Min[j, k]], {Y[i_, j_, k_,
              l_], 1} :>
            del[i, j][Min[i, j]] del[k, l][Min[k, l]], {x_X, "*"} :>
            x, {y_Y, "*"} :> y})), (Times @@ (Take[L,
           Length[L] - (np[L] + nm[L])] /. {Odd[i_, j_, k_, l_] :>
            del[i, k][Min[i, k]] del[j, l][Min[j, l]]})))]) //.
    rule2 //. rule3 //. ruleStar
S[L_PD, s_String] := S[L, Characters[s] /. {"0" -> 0, "1" -> 1}]


Deg[expr_] := Count[expr, _v1, {0, 1}] - Count[expr, _vX, {0, 1}]
V[L_PD, s_String, deg___] :=
 V[L, Characters[s] /. {"0" -> 0, "1" -> 1}, deg]
V[L_PD, a_List] :=
 List @@ Expand[S[L, a] /. x_c :> ((v1 @@ x) + (vX @@ x))]
V[L_PD, a_List, deg_Integer] :=
 Select[V[L, a], (deg == Deg[#] + (Plus @@ a)) &]


d[L_PD, s_String] := d[L, Characters[s] /. {"0" -> 0, "1" -> 1}]
```

Appendix C (Continued)

```
d[L_PD, a_List] :=
 S[L, a] //. {(c[x_] c[y_] -> c[z_])*_. :> {v1@x v1@y -> v1@z,
      v1@x vX@y -> vX@z, vX@x v1@y -> vX@z,
      vX@x vX@y -> 0}, (c[z_] -> c[x_] c[y_])*_. :> {v1@z ->
       v1@x vX@y + vX@x v1@y,
      vX@z -> vX@x vX@y}} //. {(c[x__] -> c[y__])*_. :> {v1@x -> 0,
     vX@x -> 0}}


dif[L_PD, s_String] := dif[L, Characters[s] /. {"0" -> 0, "1" -> 1}]
dif[L_PD, a_List] :=
 Flatten[MapThread[
     ge, {V[L, a /. ("*" :> 0)],
      Expand[V[L, a /. ("*" :> 0)] /. d[L, a]]}] /. (ge[u___,
       v__ + w__] :> {ge[u, v], ge[u, w]}) /. (ge[z___, 0] :> 0)]


Comp[L_PD] :=
  Join @@ (Join @@ {Expand[
          ed[((v @@ #) /. ("*" :> 0)), ((v @@ #) /. ("*" :> 1))] dif[
            L, #]]} & /@ Perms[L]) //. (ed[a__, b__] ge[c__, d__] :>
     edge[a*c, b*d]);
Edges[L_PD] :=
 Cases[If[((# === 0) || (#[[1]] === #[[2]])), 0, #] & /@ Comp[L],
  Except[0]]
KhColumn[L_PD, r_Integer] :=
```

Appendix C (Continued)

```
  If[r < 0 || r > (np[L] + nm[L]), {0},
   Join @@ (((v @@ #) V[L, #]) & /@
      Permutations[
       Join[Table[0, {(np[L] + nm[L]) - r}], Table[1, {r}]]])];


Gens[L_PD] :=
  Cases[Flatten[{KhColumn[L, #] & /@ Range[0, (np[L] + nm[L])]}],
   Except[0]];
Perms[L_PD] :=
  Join @@ (Permutations[
       Join[{"*"}, Table[0, {(np[L] + nm[L]) - # - 1}],
        Table[1, {#}]]] & /@ Range[0, (np[L] + nm[L]) - 1]);
Height[gen___] := (gen /. {v1[a___] :> 1, vX[b___] :> 1,
     v[c___] :> Plus[c]});
EdgeHeight[e__] := If[IntegerQ[e], -1, Height[e[[1]]]];
MultGrad[e__] :=
  e /. {v[expr___] :> 1, vX[a_, b_, c_] :> K[b],
      v1[a_, b_, c_] :> K[b]} /. {K[0] :> 1} /. {K[i_]^_ :> K[i]};


AddDelEdges[edges_List, e_edge] := (Off[Part::partd];
  listfs = Select[edges, #[[2]] == e[[2]] &];
  listgs = Select[edges, #[[1]] == e[[1]] &];
  remfs = Rule[#, 0] & /@ listfs; remgs = Rule[#, 0] & /@ listgs;
  sym = edges /. remfs /. remgs /. {edge[e[[2]], ___] :> 0};
```

```
  diff = Tuples[{listfs,
      listgs}] /. {{edge[f1__, e2__], edge[e1__, g2__]} :>
      edge[f1, g2]};
  symdiff =
   If[(listfs == {}) || (listgs == {}), sym,
    Union[Complement[diff, sym], Complement[sym, diff]]];
  On[Part::partd]; symdiff)


Reduc[gens_List, edges_List,
   e_edge] := (Checks[(gens /. {e[[1]] :> 0, e[[2]] :> 0}),
    AddDelEdges[edges, e]]);
Checks[gens_List, unsortededges_List] := (
   edges = Cases[(SortBy[unsortededges, EdgeHeight[#] &]), Except[0]];
   If[edges == {}, Cases[gens, Except[0]],
    Reduc[gens, Delete[edges, 1], edges[[1]]]]);
HomReps[L_PD] :=
  Block[{$IterationLimit = Infinity, $RecursionLimit = Infinity},
   Checks[Cases[Gens[L], Except[0]], Cases[Edges[L], Except[0]]]];
QT[gen___,
   L_PD] := (r = (Height[gen] - nm[L]); (t^
      r)*(q^(r + Deg[gen] + np[L] - nm[L])));
Kh[L_PD] := Plus @@ (QT[#, L] & /@ HomReps[L]);
ParityKh[L_PD] :=
  Plus @@ (QT[#, EvenParityPD[L]] & /@ HomReps[EvenParityPD[L]]);
```

C.2 (Parity) Fully-Graded Arrow Categorification Calculator

The following program computes the categorification of the arrow categorification and the forgetful parity version for the construction which includes the full vector grading and multiple grading. It is based on the aforementioned programs. A description of the program

```
np[L_PD] := Count[L, _X];

nm[L_PD] := Count[L, _Y];

SetAttributes[del, Orderless]
```

`np` and `nm` count the number of positive and negative crossings for a given planar diagram respectively. We set `del` to be orderless to reduce the number of necessary relations.

The following lines of program perform the forgetful mapping on the odd crossings.

```
EvenParityPD[L_PD] :=

 Sort[L /. {X[i_, j_, k_, l_] :>

      Odd[i, j, k, l] /; OddQ[i - j]} /. {Y[i_, j_, k_, l_] :>

     Odd[i, j, k, l] /; OddQ[i - j]}]
```

`EvenParity` performs a simple check to determine if a given crossing is even or odd. For an odd crossing it replaces the head `X` or `Y` with `Odd`. Note this subroutine assumes that arcs of a given knot diagram are labeling consecutively.

```
OddIdentities[L_PD] :=

 ReplacePart[ ReplacePart[Reverse[Sort[

      Flatten[ReplacePart[Take[EvenParityPD[L],
```

Appendix C (Continued)

```
          Length[EvenParityPD[L]] - (np[EvenParityPD[L]] +
             nm[EvenParityPD[L]])],
         0 :> List] /. {Odd[i_, j_, k_, l_] :> {del[i, k],
           del[j, l]}}]]],
    0 :> Times] //. {del[a_, b_] del[b_, c_] :> del[a, c]}, 0 :> List]
```

`OddIdentities` creates a collection of arc relations displayed in terms of Kronecker deltas based on the odd crossings.

```
EvenCross[L_PD] :=
 Drop[EvenParityPD[L],
  Length[EvenParityPD[L]] - (np[EvenParityPD[L]] +
     nm[EvenParityPD[L]])]
```

`EvenCross` collects the even crossings from a given PD code.

```
PDReduction[L_PD, d_del] := (mm := Min[d[[1]], d[[2]]];
  nn = Max[d[[1]], d[[2]]]; L /. {nn :> mm})
```

`PDReduction` turns a single identity produced by `OddIdentities` into a reduction relation and applies this relation.

```
ForgetfulEvenParityPD[L_PD] := (RedPD = EvenCross[L];
  Do[RedPD = PDReduction[RedPD, OddIdentities[L][[i]]], {i,
    Length[OddIdentities[L]]}]; RedPD)
```

Appendix C (Continued)

`ForgetfulEvenParityPD` applies `PDReduction` for all of the relations in `OddIdentities` and returns the resulting PD code.

```
rule2 = {del[a_, b_][m_] del[a_, b_][m_] :> del[a, a][m],
   del[a_, b_][m_] del[b_, c_][n_] :> del[a, c][Min[m, n]],
   del[a_, b_][m_] led[b_, c_][n_] :> led[a, c][Min[m, n]],
   del[a_, b_][m_] led[c_, b_][n_] :> led[c, a][Min[m, n]],
   led[a_, b_][m_] del[b_, c_][n_] :> led[a, c][Min[m, n]],
   led[a_, b_][m_] del[c_, b_][n_] :> led[a, c][Min[m, n]],
   led[a_, b_][m_] led[b_, c_][n_] :> del[a, c][Min[m, n]]};
rule3 = {del[a_, a_][m1_] :> c[m1, 0, 0],
   del[a_, a_][m1_]^_ :> c[m1, 0, 0],
   led[a_, b_][m1_]^2 :> c[m1, 1, 1],
   led[a_, b_][m1_] led[a_, b_][m2_] :> c[Min[m1, m2], 1, 1],
   led[a_, b_][m1_] led[x_, b_][m2_] led[x_, d_][m3_] led[a_, d_][
      m4_] :> c[Min[m1, m2, m3, m4], 2, 2],
   led[a_, b_][m1_] led[x_, b_][m2_] led[x_, d_][m3_] led[e_, d_][
      m4_] led[e_, f_][m5_] led[a_, f_][m6_] :>
    c[Min[m1, m2, m3, m4, m5, m6], 3, 1],
   led[a_, b_][m1_] led[x_, b_][m2_] led[x_, d_][m3_] led[e_, d_][
      m4_] led[e_, f_][m5_] led[g_, f_][m6_] led[g_, h_][
      m7_] led[a_, h_][m8_] :>
    c[Min[m1, m2, m3, m4, m5, m6, m7, m8], 4, 3],
   led[a_, b_][m1_] led[x_, b_][m2_] led[x_, d_][m3_] led[e_, d_][
```

Appendix C (Continued)

```
      m4_] led[e_, f_][m5_] led[g_, f_][m6_] led[g_, h_][
      m7_] led[y_, h_][m8_] led[y_, z_][m9_] led[a_, z_][m10_] :>
    c[Min[m1, m2, m3, m4, m5, m6, m7, m8, m9, m10], 5, 1]};
```

`rule2` and `rule3` are reduction relations used by `S`. `rule2` joins arcs and cusps while `rule3` produces the labeled circles for a basic (unenhanced) state. We follow the convention `c[m, p,k]` is circle `m` with arrow number `p` and dot of order `k`. Where `p = l*2^(k - 1)` for `l` odd.

```
ruleStar = {v___c u___ X[i_, j_, k_,
      l_] :> ((u del[i, j][Min[i, j]] del[k, l][Min[k, l]] //.
         rule2 //.
        rule3) -> (u led[l, i][Min[l, i]] led[j, k][Min[j, k]] //.
         rule2 //. rule3)),
   v___c u___ Y[i_, j_, k_,
      l_] :> ((u led[l, i][Min[l, i]] led[j, k][Min[j, k]] //.
         rule2 //.
        rule3) -> (u del[i, j][Min[i, j]] del[k, l][Min[k, l]] //.
         rule2 //. rule3))};
```

`ruleStar` is a reduction relations used by `S` which produces notation corresponding to a bifurcation on an edge denoted by `*` on the cube complex.

```
S[L_PD, a_List] :=
 Times[(Times @@ (Thread[{List @@
           Drop[L, Length[L] - (np[L] + nm[L])],
```

Appendix C (Continued)

```
            a}] /. {{X[i_, j_, k_, l_], 0} :>
            del[i, j][Min[i, j]] del[k, l][Min[k, l]], {X[i_, j_, k_,
              l_], 1} :>
            led[l, i][Min[l, i]] led[j, k][Min[j, k]], {Y[i_, j_, k_,
              l_], 0} :>
            led[l, i][Min[l, i]] led[j, k][Min[j, k]], {Y[i_, j_, k_,
              l_], 1} :>
            del[i, j][Min[i, j]] del[k, l][Min[k, l]], {x_X, "*"} :>
            x, {y_Y, "*"} :> y})), (Times @@ (Take[L,
           Length[L] - (np[L] + nm[L])] /. {Odd[i_, j_, k_, l_] :>
            del[i, k][Min[i, k]] del[j, l][Min[j, l]]}))] //.
    rule2 //. rule3 //. ruleStar
S[L_PD, s_String] := S[L, Characters[s] /. {"0" -> 0, "1" -> 1}]
```

`S` produces the unenhanced state of the cube complex for `L` corresponding to the vertex `a`.

```
MG[expr_] :=
 expr //. {c[m_, 0, k_] :> 1} //. {c[m_, p_, k_] :>
     a[p]} //. {a[i_]^_ :> a[i]}
```

`MG` computes the multiple grading for an given unenhanced state. If there is no arrow numbers `MG` returns 1. If there are arrow numbers `MG` returns a product of the form $a[i_1]a[i_2]\dots a[i_n]$, where the i_j are the distinct arrow numbers (ie $i_j = i_k$ iff $j = k$).

```
Deg[expr_] := Count[expr, _v1, {0, 1}] - Count[expr, _vX, {0, 1}]
```

Appendix C (Continued)

```
V[L_PD, s_String, deg___] :=
 V[L, Characters[s] /. {"0" -> 0, "1" -> 1}, deg]
V[L_PD, a_List] :=
 List @@ Expand[S[L, a] /. x_c :> ((vX @@ x) + (v1 @@ x))]
V[L_PD, a_List, deg_Integer] :=
 Select[V[L, a], (deg == Deg[#] + (Plus @@ a)) &]
```

The above subroutines provide information on the enhanced states. `V` replaces `c[m,p,k]` by `vX[m,p,k]+v1[m,p,k]` throughout then expands each expression. Each summand corresponds to an enhanced (labeled by X and 1) state, which we separate into a list of enhanced states at each vertex. `Deg` computes (# X's - #1's)) and when given to V returns enhanced states with a given bi-degree. ((bi-degree) = (homological degree) + (# X's - #1's))

```
VG[expr_] :=
 expr //. {vX[m_, 0, k_] :> 1} //. {v1[m_, 0, k_] :> 1} //. {vX[m_,
         p_, k_] :> vg[k, 1]} //. {v1[m_, p_, k_] :>
       vg[k, -1]} //. {vg[a_, i_]^m_ :>
      vg[a, i*m]} //. {vg[a_, i_] vg[a_, j_] :> vg[a, i + j]} //. {vg[
     a_, 0] :> 1}
```

We need to compute the vector grading of an enhanced state. Recall that this (inf. dim.) vector is the sum over the labeling in the enhanced state where, for $i > 0$, we transform `vX[*,*,i]` into the vector that is 1 in the i^th position and 0 elsewhere and similarly we transform `v1[*,*,i]` into the vector that is -1 in the i^th position and 0 elsewhere. `VG` returns 1 if the vector grading is the zero vector else it returns the product of terms of the form `v[k, n]` corresponding to the k^th position in the vector grading having

Appendix C (Continued)

value n.

```
d[L_PD, s_String] := d[L, Characters[s] /. {"0" -> 0, "1" -> 1}]

d[L_PD, a_List] :=

 S[L, a] //. {(c[x__] c[y__] -> c[z__])*_. :> {v1@x v1@y -> 0,

        v1@x vX@y -> 0, vX@x v1@y -> 0,

        vX@x vX@y -> 0} /; (MG[S[L, a //. {"*" -> 0}]] =!=

         MG[S[L, a //. {"*" -> 1}]]), (c[z__] ->

         c[x__] c[y__])*_. :> {v1@z -> 0,

        vX@z -> 0} /; (MG[S[L, a //. {"*" -> 0}]] =!=

         MG[S[L, a //. {"*" -> 1}]])} //. {(c[x__] c[y__] ->

        c[z__])*_. :> {v1@x v1@y -> v1@z, v1@x vX@y -> vX@z,

       vX@x v1@y -> vX@z,

       vX@x vX@y ->

        0} /; (VG[v1@x v1@y] === VG[v1@z]) && (VG[v1@x vX@y] ===

         VG[vX@z]) && (VG[vX@x v1@y] === VG[vX@z]), (c[x__] c[y__] ->

        c[z__])*_. :> {v1@x v1@y -> 0, v1@x vX@y -> vX@z,

       vX@x v1@y -> vX@z,

       vX@x vX@y ->

        0} /; (VG[v1@x v1@y] =!= VG[v1@z]) && (VG[v1@x vX@y] ===

         VG[vX@z]) && (VG[vX@x v1@y] === VG[vX@z]), (c[x__] c[y__] ->

        c[z__])*_. :> {v1@x v1@y -> v1@z, v1@x vX@y -> 0,

       vX@x v1@y -> vX@z,

       vX@x vX@y ->
```

Appendix C (Continued)

```
 0} /; (VG[v1@x v1@y] === VG[v1@z]) && (VG[v1@x vX@y] =!=
  VG[vX@z]) && (VG[vX@x v1@y] === VG[vX@z]), (c[x__] c[y__] ->
 c[z__])*_. :> {v1@x v1@y -> v1@z, v1@x vX@y -> vX@z,
vX@x v1@y -> 0,
vX@x vX@y ->
 0} /; (VG[v1@x v1@y] === VG[v1@z]) && (VG[v1@x vX@y] ===
  VG[vX@z]) && (VG[vX@x v1@y] =!= VG[vX@z]), (c[x__] c[y__] ->
 c[z__])*_. :> {v1@x v1@y -> 0, v1@x vX@y -> 0,
vX@x v1@y -> vX@z,
vX@x vX@y ->
 0} /; (VG[v1@x v1@y] =!= VG[v1@z]) && (VG[v1@x vX@y] =!=
  VG[vX@z]) && (VG[vX@x v1@y] === VG[vX@z]), (c[x__] c[y__] ->
 c[z__])*_. :> {v1@x v1@y -> 0, v1@x vX@y -> vX@z,
vX@x v1@y -> 0,
vX@x vX@y ->
 0} /; (VG[v1@x v1@y] =!= VG[v1@z]) && (VG[v1@x vX@y] ===
  VG[vX@z]) && (VG[vX@x v1@y] =!= VG[vX@z]), (c[x__] c[y__] ->
 c[z__])*_. :> {v1@x v1@y -> v1@z, v1@x vX@y -> 0,
vX@x v1@y -> 0,
vX@x vX@y ->
 0} /; (VG[v1@x v1@y] === VG[v1@z]) && (VG[v1@x vX@y] =!=
  VG[vX@z]) && (VG[vX@x v1@y] =!= VG[vX@z]), (c[x__] c[y__] ->
 c[z__])*_. :> {v1@x v1@y -> 0, v1@x vX@y -> 0, vX@x v1@y -> 0,
 vX@x vX@y ->
```

Appendix C (Continued)

```
 0} /; (VG[v1@x v1@y] =!= VG[v1@z]) && (VG[v1@x vX@y] =!=
  VG[vX@z]) && (VG[vX@x v1@y] =!= VG[vX@z]), (c[z__] ->
 c[x__] c[y__])*_. :> {v1@z -> v1@x vX@y + vX@x v1@y,
vX@z ->
 vX@x vX@y} /; (VG[v1@z] === VG[v1@x vX@y]) && (VG[v1@z] ===
  VG[vX@x v1@y]) && (VG[vX@z] === VG[vX@x vX@y]), (c[z__] ->
 c[x__] c[y__])*_. :> {v1@z -> vX@x v1@y,
vX@z ->
 vX@x vX@y} /; (VG[v1@z] =!= VG[v1@x vX@y]) && (VG[v1@z] ===
  VG[vX@x v1@y]) && (VG[vX@z] === VG[vX@x vX@y]), (c[z__] ->
 c[x__] c[y__])*_. :> {v1@z -> v1@x vX@y,
vX@z ->
 vX@x vX@y} /; (VG[v1@z] === VG[v1@x vX@y]) && (VG[v1@z] =!=
  VG[vX@x v1@y]) && (VG[vX@z] === VG[vX@x vX@y]), (c[z__] ->
 c[x__] c[y__])*_. :> {v1@z -> v1@x vX@y + vX@x v1@y,
vX@z ->
 0} /; (VG[v1@z] === VG[v1@x vX@y]) && (VG[v1@z] ===
  VG[vX@x v1@y]) && (VG[vX@z] =!= VG[vX@x vX@y]), (c[z__] ->
 c[x__] c[y__])*_. :> {v1@z -> 0,
vX@z ->
 vX@x vX@y} /; (VG[v1@z] =!= VG[v1@x vX@y]) && (VG[v1@z] =!=
  VG[vX@x v1@y]) && (VG[vX@z] === VG[vX@x vX@y]), (c[z__] ->
 c[x__] c[y__])*_. :> {v1@z -> vX@x v1@y,
vX@z ->
```

Appendix C (Continued)

```
 0} /; (VG[v1@z] =!= VG[v1@x vX@y]) && (VG[v1@z] ===
  VG[vX@x v1@y]) && (VG[vX@z] =!= VG[vX@x vX@y]), (c[z__] ->
 c[x__] c[y__])*_. :> {v1@z -> v1@x vX@y,
vX@z ->
 0} /; (VG[v1@z] === VG[v1@x vX@y]) && (VG[v1@z] =!=
  VG[vX@x v1@y]) && (VG[vX@z] =!= VG[vX@x vX@y]), (c[z__] ->
 c[x__] c[y__])*_. :> {v1@z -> 0,
vX@z ->
 0} /; (VG[v1@z] =!= VG[v1@x vX@y]) && (VG[v1@z] =!=
  VG[vX@x v1@y]) && (VG[vX@z] =!= VG[vX@x vX@y])} //. {(c[
 x__] -> c[y__])*_. :> {v1@x -> 0, vX@x -> 0}}
```

`d` computes the edge morphism for the edge corresponding to the label `a`. Here `a` is a list of 0's and 1's along with a single `*` where `*` corresponds to the crossing we are resmoothing and 0 and 1 correspond to $A-$ and A^{-1}-smoothings at the remaining crossings.

We now have enough to construct the cube complex. The following collection of routines together collect this information and constructs a graph. We then preform the previously mentioned graphical reduction algorithm to compute the homology.

```
dif[L_PD, s_String] := dif[L, Characters[s] /. {"0" -> 0, "1" -> 1}]
dif[L_PD, a_List] :=
 Flatten[MapThread[
     ge, {V[L, a /. ("*" :> 0)],
      Expand[V[L, a /. ("*" :> 0)] /. d[L, a]]}] /. (ge[u___,
```

```
      v__ + w__] :> {ge[u, v], ge[u, w]}) /. (ge[z___, 0] :> 0)]
Comp[L_PD] :=
  Join @@ (Join @@ {Expand[
          ed[((v @@ #) /. ("*" :> 0)), ((v @@ #) /. ("*" :> 1))] dif[
            L, #]]} & /@ Perms[L]) //. (ed[a__, b__] ge[c__, d__] :>
     edge[a*c, b*d]);
Edges[L_PD] :=
 Cases[If[((# === 0) || (#[[1]] === #[[2]])), 0, #] & /@ Comp[L],
  Except[0]]
```

`dif` constructs the set of directed edges for the graph corresponding to an edge of the cube complex. It does the locally by applying the differential `d` to the tail of each edge. `Comp` produces the full set of vertices for the graph and connected the heads and tails of the directed edges formed by `dif`. Some zero differentials remain. `Edges` removes these from the list.

```
KhColumn[L_PD, r_Integer] :=
  If[r < 0 || r > (np[L] + nm[L]), {0},
   Join @@ (((v @@ #) V[L, #]) & /@
      Permutations[
       Join[Table[0, {(np[L] + nm[L]) - r}], Table[1, {r}]]])];
Gens[L_PD] :=
  Cases[Flatten[{KhColumn[L, #] & /@ Range[0, (np[L] + nm[L])]}],
   Except[0]];
```

Appendix C (Continued)

`Gens` produces the collection of enhanced states corresponding to the enhanced states of the complex (i.e. the nodes in the graph) by calling `KhColumn` for each homological degree of the planar diagram for the knot.

```
Perms[L_PD] :=
  Join @@ (Permutations[
       Join[{"*"}, Table[0, {(np[L] + nm[L]) - # - 1}],
        Table[1, {#}]]] & /@ Range[0, (np[L] + nm[L]) - 1]);
```

`Perms` generates the lists of 0's, 1's and a single * corresponding to the edges of the cube complex.

```
Height[gen___] := (gen /. {v1[a___] :> 1, vX[b___] :> 1,
     v[c___] :> Plus[c]});
EdgeHeight[e__] := If[IntegerQ[e], -1, Height[e[[1]]]];

MultGrad[e__] :=
  e /. {v[expr___] :> 1, vX[a_, b_, c_] :> K[b],
      v1[a_, b_, c_] :> K[b]} /. {K[0] :> 1} /. {K[i_]^_ :> K[i]};
```

`MultGrad` takes a homology class representative and outputs its multiple grading.

```
AddDelEdges[edges_List, e_edge] := (Off[Part::partd];
  listfs = Select[edges, #[[2]] == e[[2]] &];
  listgs = Select[edges, #[[1]] == e[[1]] &];
  remfs = Rule[#, 0] & /@ listfs; remgs = Rule[#, 0] & /@ listgs;
  sym = edges /. remfs /. remgs /. {edge[e[[2]], ___] :> 0};
  diff = Tuples[{listfs,listgs}] /.
    {{edge[f1__, e2__], edge[e1__, g2__]} :> edge[f1, g2]};
```

Appendix C (Continued)

```
  symdiff =
   If[(listfs == {}) || (listgs == {}), sym,
    Union[Complement[diff, sym], Complement[sym, diff]]];
  On[Part::partd]; symdiff)
```

Given an edge `e`, `AddDelEdges` looks for all local subgraphs which share the same head as `e`. It then computes a symmetric difference with collection of edges whose tail is the same as `e`.

```
Reduc[gens_List, edges_List,
   e_edge] := (Checks[(gens /. {e[[1]] :> 0, e[[2]] :> 0}),
    AddDelEdges[edges, e]]);
Checks[gens_List, unsortededges_List] := (
   edges = Cases[(SortBy[unsortededges, EdgeHeight[#] &]), Except[0]];
   If[edges == {}, Cases[gens, Except[0]],
    Reduc[gens, Delete[edges, 1], edges[[1]]]]);
```

`Checks` looks for the remaining edge whose head is in the highest homological degree. It then applies `Reduc` to remove the edge and apply the symmetric difference algorithm in `AddDelEdges`.

```
HomReps[L_PD] :=
  Block[{$IterationLimit = Infinity, $RecursionLimit = Infinity},
   Checks[Cases[Gens[L], Except[0]], Cases[Edges[L], Except[0]]]];
```

`HomReps` takes a planar diagram code, repeatedly applies `Checks` to run the graph reduction algorithm and outputs representatives for the homology classes.

Appendix C (Continued)

```
QT[gen___, L_PD] :=
  (r = (Height[gen] - nm[L]); (t^r)
      *(q^(r + Deg[gen] + np[L] - nm[L])));
```

`QT` computes the associated powers of q and t for a given representative of a homology class.

```
AKh[L_PD] :=
  Plus @@ (QT[#, L]*VG[# /. {v[a___] :> 1}]*
       MultGrad[# /. {v[a___] :> 1}] & /@ HomReps[L]);
ParityAKh[L_PD] :=
  If[Length[ForgetfulEvenParityPD[L]] == 1 ||
    Head[ForgetfulEvenParityPD[L]] === PDReduction, q + q^(-1),
   Plus @@ (QT[#, ForgetfulEvenParityPD[L]]*VG[# /. {v[a___] :> 1}]*
        MultGrad[# /. {v[a___] :> 1}] & /@
      HomReps[ForgetfulEvenParityPD[L]])];
```

Finally, `AKh` and `ParityAKh` compute the corresponding categorifications for a given planar diagram L.

Appendix D

SAWOLLEK POLYNOMIALS AND Z-PARITY ALEXANDER POLYNOMIALS FOR KNOTS WITH AT MOST FOUR CLASSICAL CROSSINGS

TABLE III: Sawollek and z-Parity Alexander Polynomial Calculations

Knot	Sawollek	z-Parity Alexander
2.1	$\left(s^2-s\right)t^2+\left(1-s^2\right)t+s-1$	0
3.1	$\frac{1-\frac{1}{s^2}}{t}+\frac{1}{s^2}+\left(s-\frac{1}{s}\right)t-s+\frac{1}{s}-1$	$\frac{\frac{1}{st}-1}{z^2}-\frac{1}{st}+1$
3.2	$\frac{\frac{1}{s}-\frac{1}{s^2}}{t^2}+\frac{\frac{1}{s^2}-1}{t}-\frac{1}{s}+1$	0
3.3	$\frac{\frac{1}{s^3}-1}{t}-\frac{1}{s^2}+\frac{\frac{1}{s^2}-\frac{1}{s^3}}{t^3}+1$	$\frac{\frac{1}{st}-1}{z^2}-\frac{1}{st}+1$
3.4	$\frac{\frac{1}{s}-\frac{1}{s^2}}{t}+\frac{1}{s^2}+\left(1-\frac{1}{s}\right)t-1$	$\frac{1-st}{z^2}+st-1$
3.5	$\frac{\frac{1}{s}-\frac{1}{s^3}}{t^3}+\frac{\frac{1}{s^3}-\frac{1}{s}}{t}+\frac{\frac{1}{s^2}-1}{t^2}-\frac{1}{s^2}+1$	$-\frac{1}{s^3t^3}+\frac{1}{s^3t}+\frac{1}{s^2t^2}-\frac{1}{s^2}+\frac{1}{st^3}-\frac{1}{st}-\frac{1}{t^2}+1$
3.6	0	0
3.7	$\frac{1-\frac{1}{s^2}}{t^2}+\frac{1}{s^2}+\left(s-\frac{1}{s}\right)t+\frac{\frac{1}{s}-s}{t}-1$	$-\frac{1}{s^2t^2}+\frac{1}{s^2}+st-\frac{s}{t}-\frac{t}{s}+\frac{1}{st}+\frac{1}{t^2}-1$
4.1	$\frac{\frac{2}{s^3}-\frac{2}{s}}{t}-\frac{1}{s^2}+\frac{-\frac{1}{s^4}+\frac{2}{s^3}-\frac{1}{s^2}}{t^4}+\frac{\frac{2}{s^4}-\frac{2}{s^3}-\frac{2}{s^2}+\frac{2}{s}}{t^3}+\frac{-\frac{1}{s^4}-\frac{2}{s^3}+\frac{4}{s^2}-1}{t^2}+1$	0

Appendix D (Continued)

Knot	Sawollek	z-Parity Alexander
4.2	$\left(-s^2+2s-\frac{2}{s}+1\right)t + \frac{-\frac{1}{s^2}-2s+\frac{2}{s}+1}{t} + s^2+\frac{1}{s^2}+(1-s)t^2+\frac{1-\frac{1}{s}}{t^2}+s+\frac{1}{s}-4$	0
4.3	$\frac{-\frac{2}{s^3}+\frac{1}{s}+1}{t}+\frac{1}{s^2}+\frac{\frac{1}{s^4}-\frac{1}{s^3}}{t^4}+\frac{-\frac{2}{s^4}+\frac{1}{s^3}+\frac{1}{s^2}}{t^3}+\frac{\frac{1}{s^4}+\frac{2}{s^3}-\frac{2}{s^2}-\frac{1}{s}}{t^2}-1$	0
4.4	$\frac{\frac{1}{s^2}-\frac{1}{s}}{t^3}+\frac{2-\frac{2}{s^2}}{t^2}+\frac{\frac{1}{s^2}-s+\frac{2}{s}-2}{t}+s-\frac{1}{s}$	0
4.5	$\frac{\frac{1}{s}-\frac{1}{s^3}}{t^2}-\frac{2}{s^2}+\frac{\frac{1}{s^3}+\frac{2}{s^2}-\frac{2}{s}-1}{t}+\left(\frac{1}{s}-1\right)t+2$	0
4.6	$\left(s^2-s\right)t-s^2+\frac{\frac{1}{s}-1}{t^2}+\frac{2s-\frac{1}{s}-1}{t}-s+2$	0
4.7	$\frac{\frac{1}{s}-\frac{1}{s^3}}{t^2}+\frac{\frac{1}{s^2}-1}{t}+\frac{\frac{1}{s^3}-\frac{1}{s^4}}{t^4}+\frac{\frac{1}{s^4}-\frac{1}{s^2}}{t^3}-\frac{1}{s}+1$	0
4.8	0	0
4.9	$\frac{\frac{2}{s^3}-\frac{2}{s}}{t^2}+\frac{-\frac{2}{s^2}+\frac{1}{s}+1}{t}+\frac{\frac{1}{s^4}-\frac{1}{s^3}}{t^4}+\frac{-\frac{1}{s^4}-\frac{1}{s^3}+\frac{2}{s^2}}{t^3}+\frac{1}{s}-1$	$\frac{1}{s^2t^2}+z\left(\frac{1}{s}-\frac{1}{s^2t}\right)+\frac{\frac{1}{t}-\frac{1}{st^2}}{z}-1$
4.10	$\frac{\frac{1}{s}-\frac{1}{s^3}}{t^2}-\frac{1}{s^2}+\frac{\frac{1}{s^3}+\frac{1}{s^2}-\frac{1}{s}-1}{t}+1$	$\frac{\frac{1}{s^2t}+\frac{1}{st^2}-\frac{1}{s}-\frac{1}{t}}{z}-\frac{1}{s^2t^2}+1$
4.11	$\frac{\frac{1}{s^2}-\frac{1}{s}}{t^3}-\frac{1}{s^2}+\frac{-\frac{1}{s^3}-\frac{2}{s^2}+\frac{1}{s}+2}{t^2}+\frac{\frac{1}{s^3}+\frac{2}{s^2}-s+\frac{1}{s}-3}{t}+s-\frac{1}{s}+1$	$\frac{\frac{1}{s}-t}{z}+z\left(t-\frac{1}{s}\right)$
4.12	$\left(s^2-\frac{2}{s}+1\right)t+\frac{-\frac{1}{s^2}+2s-1}{t}-s^2+\frac{1}{s^2}+(1-s)t^2+\frac{\frac{1}{s}-1}{t^2}-s+\frac{1}{s}$	0
4.13	$\frac{\frac{1}{s^2}-\frac{1}{s}}{t}-\frac{1}{s^2}+(s-1)t^2+\left(-s+\frac{2}{s}-1\right)t-\frac{1}{s}+2$	0
4.14	$\frac{-\frac{1}{s^2}-s+\frac{1}{s}+1}{t}+\frac{1}{s^2}+\frac{1-\frac{1}{s}}{t^2}+\left(s-\frac{1}{s}\right)t+\frac{1}{s}-2$	$s^2t^2+z\left(s-s^2t\right)+\frac{t-st^2}{z}-1$

Appendix D (Continued)

Knot	Sawollek	z-Parity Alexander
4.15	$\frac{\frac{1}{s^3}-\frac{1}{s^4}}{t^4} + \frac{\frac{1}{s^3}-\frac{1}{s^2}}{t^3} + \frac{-\frac{1}{s^3}+\frac{2}{s^2}-1}{t} + \frac{\frac{1}{s^4}-\frac{1}{s^3}-\frac{1}{s^2}+\frac{1}{s}}{t^2} - \frac{1}{s} + 1$	$\frac{\frac{1}{s^2t}+\frac{1}{st^2}-\frac{1}{s}-\frac{1}{t}}{z} - \frac{1}{s^2t^2} + 1$
4.16	0	$\frac{1}{s^2t^2} + z\left(\frac{1}{s} - \frac{1}{s^2t}\right) + \frac{\frac{1}{t}-\frac{1}{st^2}}{z} - 1$
4.17	$(s-1)t^2 + \left(\frac{1}{s}-1\right)t + \frac{1-\frac{1}{s}}{t} - s + 1$	$\frac{\frac{1}{s}-t}{z} + z\left(t - \frac{1}{s}\right)$
4.18	$\frac{\frac{1}{s^2}-\frac{1}{s}}{t^2} + \frac{1-\frac{1}{s^2}}{t} + \frac{1}{s} - 1$	0
4.19	$\frac{1-\frac{1}{s}}{t^2} + (s-1)t + \frac{1-s}{t} + \frac{1}{s} - 1$	$\frac{s-\frac{1}{t}}{z} + z\left(\frac{1}{t} - s\right)$
4.20	$\frac{\frac{1}{s^2}-\frac{1}{s}}{t} - \frac{1}{s^2} + \left(\frac{1}{s}-1\right)t + 1$	$\frac{s^2t+st^2-s-t}{z} - s^2t^2 + 1$
4.21	$\left(s^2-s\right)t^3 + \left(s^2-2s+1\right)t^2 + \left(1-s^2\right)t - s^2 + \frac{s-1}{t} + 2s - 1$	$s^2t^2 + z\left(s - s^2t\right) + \frac{t-st^2}{z} - 1$
4.22	$\left(\frac{1}{s^2}+\frac{1}{s}-2\right)t - \frac{1}{s^2} + \left(s-\frac{1}{s}\right)t^2 + \frac{1-\frac{1}{s}}{t} - s + \frac{1}{s} + 1$	$\frac{s^2t+st^2-s-t}{z} - s^2t^2 + 1$
4.23	$\frac{\frac{1}{s^2}-\frac{1}{s}}{t^3} + \frac{\frac{1}{s}-\frac{1}{s^2}}{t} + \frac{1-\frac{1}{s}}{t^2} + \frac{1}{s} - 1$	$z\left(-\frac{1}{s^2t} - \frac{1}{st^2} + \frac{1}{s} + \frac{1}{t}\right) + \frac{1}{s^2t^2} - 1$
4.24	$\left(s^2-1\right)t^3 + \left(s^2-2s+\frac{1}{s}\right)t^2 + \left(-s^2-s+2\right)t - s^2 + \frac{s-1}{t} + 2s - \frac{1}{s}$	$z\left(s^2(-t) - st^2 + s + t\right) + s^2t^2 - 1$
4.25	$\frac{\frac{1}{s}-\frac{1}{s^2}}{t^2} + \frac{\frac{1}{s^2}-\frac{1}{s}}{t} + \frac{\frac{1}{s^4}-\frac{1}{s^3}}{t^4} + \frac{\frac{1}{s^3}-\frac{1}{s^4}}{t^3}$	0
4.26	$\left(\frac{1}{s}-s^2\right)t^2 + \left(s^2-\frac{1}{s^2}+s-1\right)t + \frac{\frac{1}{s^2}-\frac{1}{s}}{t} - s + 1$	0
4.27	$\frac{\frac{1}{s^3}-\frac{1}{s}}{t^2} + \frac{\frac{1}{s}-\frac{1}{s^2}}{t} + \frac{\frac{1}{s^2}-\frac{1}{s^3}}{t^3}$	0
4.28	$\left(1-s^2\right)t^3 + \left(s^2-s\right)t + \left(s-\frac{1}{s}\right)t^2 + \frac{\frac{1}{s}-1}{t}$	0

Appendix D (Continued)

Knot	Sawollek	z-Parity Alexander
4.29	$\frac{\frac{2}{s^2}-\frac{2}{s}}{t^3}+\frac{\frac{1}{s^3}-\frac{2}{s^2}+\frac{1}{s}}{t}+\frac{\frac{1}{s^4}-\frac{2}{s^3}+\frac{1}{s^2}}{t^4}+\frac{-\frac{1}{s^4}+\frac{1}{s^3}-\frac{1}{s^2}+1}{t^2}+\frac{1}{s}-1$	$\frac{-\frac{1}{s^2t}-\frac{1}{st^2}+\frac{1}{s}+\frac{1}{t}}{z}+\frac{1}{s^2t^2}-1$
4.30	$\frac{-\frac{1}{s^3}+\frac{2}{s}-1}{t}+\frac{2}{s^2}+\frac{\frac{1}{s^3}-\frac{2}{s^2}+\frac{1}{s}}{t^2}+\left(1-\frac{1}{s}\right)t-\frac{2}{s}$	0
4.31	$\frac{\frac{1}{s}-\frac{1}{s^2}}{t^3}+\frac{\frac{1}{s^2}+\frac{1}{s}-2}{t^2}+\frac{s-\frac{2}{s}+1}{t}-s+1$	$-\frac{1}{s^2t^2}+z\left(\frac{1}{s^2t}-\frac{1}{s}\right)+\frac{\frac{1}{st^2}-\frac{1}{t}}{z}+1$
4.32	$\frac{\frac{1}{s^2}-1}{t}-\frac{1}{s^2}+\left(\frac{1}{s}-s\right)t+s-\frac{1}{s}+1$	$\frac{t-\frac{1}{s}}{z}+z\left(\frac{1}{s}-t\right)$
4.33	$\frac{\frac{1}{s}-\frac{1}{s^2}}{t^2}+\frac{\frac{1}{s^2}-1}{t}-\frac{1}{s}+1$	0
4.34	$\frac{\frac{1}{s}-\frac{1}{s^2}}{t}+\frac{1}{s^2}+\left(1-\frac{1}{s}\right)t-1$	$\frac{s^2(-t)-st^2+s+t}{z}+s^2t^2-1$
4.35	$\frac{\frac{1}{s}-1}{t^2}+(1-s)t+\frac{s-1}{t}-\frac{1}{s}+1$	$\frac{\frac{1}{t}-s}{z}+z\left(s-\frac{1}{t}\right)$
4.36	$\left(s-s^2\right)t^3+\left(-s^2+2s-1\right)t^2+\left(s^2-1\right)t+s^2+\frac{1-s}{t}-2s+1$	$-s^2t^2+z\left(s^2t-s\right)+\frac{st^2-t}{z}+1$
4.37	$\frac{1-\frac{1}{s^4}}{t^2}+\frac{\frac{1}{s^2}-\frac{1}{s}}{t^3}+\frac{\frac{1}{s^4}-\frac{1}{s^3}}{t^4}+\frac{\frac{1}{s^3}-\frac{1}{s^2}}{t}+\frac{1}{s}-1$	$\frac{1}{s^2t^2}+\frac{\frac{1}{s}-\frac{1}{s^2t}}{z}+z\left(\frac{1}{t}-\frac{1}{st^2}\right)-1$
4.38	$\frac{\frac{1}{s}-1}{t^2}+\frac{s-\frac{1}{s}}{t}-s+1$	$\frac{\frac{1}{t}-s}{z}+z\left(s-\frac{1}{t}\right)$
4.39	$\frac{1}{s^3}+\frac{\frac{1}{s}-\frac{1}{s^2}}{t^2}+\left(1-\frac{1}{s^2}\right)t+\frac{1}{s^2}+\frac{-\frac{1}{s^3}+\frac{1}{s^2}+\frac{1}{s}-1}{t}-\frac{2}{s}$	$\frac{t-\frac{1}{s}}{z}+z\left(\frac{1}{s}-t\right)$
4.40	$\frac{\frac{1}{s}-1}{t}+(1-s)t+s-\frac{1}{s}$	$s^2t^2+\frac{s-s^2t}{z}+z\left(t-st^2\right)-1$
4.41	0	$-\frac{1}{s^2t^2}+z\left(\frac{1}{s^2t}-\frac{1}{s}\right)+\frac{\frac{1}{st^2}-\frac{1}{t}}{z}+1$
4.42	$\left(\frac{1}{s^2}-\frac{1}{s}\right)t+\frac{\frac{1}{s}-\frac{1}{s^2}}{t}+\left(1-\frac{1}{s}\right)t^2+\frac{1}{s}-1$	$\frac{t-\frac{1}{s}}{z}+z\left(\frac{1}{s}-t\right)$
4.43	$\frac{\frac{2}{s^3}-\frac{2}{s}}{t^2}+\frac{\frac{2}{s}-\frac{2}{s^2}}{t}+\frac{\frac{2}{s^2}-\frac{2}{s^3}}{t^3}$	0
4.44	$\frac{\frac{1}{s}-\frac{1}{s^3}}{t^2}+\frac{\frac{1}{s^2}-\frac{1}{s}}{t}+\frac{\frac{1}{s^3}-\frac{1}{s^2}}{t^3}$	0

Appendix D (Continued)

Knot	Sawollek	z-Parity Alexander
4.45	$-\frac{1}{s^3}+\frac{\frac{1}{s}-\frac{1}{s^2}}{t^2}+\left(\frac{1}{s^2}-s\right)t+\frac{\frac{1}{s^2}-1}{t}+\frac{\frac{1}{s^3}-\frac{1}{s^2}}{t^3}+s-\frac{1}{s}+1$	0
4.46	$\frac{\frac{1}{s^2}-\frac{1}{s}}{t^2}+\frac{-\frac{1}{s^2}-\frac{1}{s}+2}{t}+(s-1)t-s+\frac{2}{s}-1$	0
4.47	$\left(1-\frac{1}{s^2}\right)t+\frac{\frac{1}{s^2}-1}{t}+\left(\frac{1}{s}-s\right)t^2+s-\frac{1}{s}$	0
4.48	$\frac{\frac{1}{s^3}-\frac{1}{s}}{t}-\frac{1}{s^2}+\frac{\frac{1}{s^3}-\frac{1}{s^4}}{t^4}+\frac{-\frac{1}{s^3}+\frac{2}{s^2}-1}{t^2}+\frac{\frac{1}{s^4}-\frac{1}{s^3}-\frac{1}{s^2}+\frac{1}{s}}{t^3}+1$	$-\frac{1}{s^2t^2}+\frac{\frac{1}{s^2t}-\frac{1}{s}}{z}+z\left(\frac{1}{st^2}-\frac{1}{t}\right)+1$
4.49	$\frac{\frac{1}{s}-\frac{1}{s^2}}{t^3}+\frac{\frac{1}{s^2}-1}{t^2}+\frac{1-\frac{1}{s}}{t}$	$\frac{s-\frac{1}{t}}{z}+z\left(\frac{1}{t}-s\right)$
4.50	$\frac{\frac{1}{s^3}-\frac{1}{s}}{t^2}+\frac{1}{s^2}+\frac{-\frac{1}{s^3}-\frac{1}{s^2}+\frac{1}{s}+1}{t}-1$	$\frac{-\frac{1}{s^2t}-\frac{1}{st^2}+\frac{1}{s}+\frac{1}{t}}{z}+\frac{1}{s^2t^2}-1$
4.51	$\left(s-s^2\right)t+s^2+\frac{1-\frac{1}{s}}{t^2}+\frac{-2s+\frac{1}{s}+1}{t}+s-2$	0
4.52	$\frac{1-\frac{1}{s}}{t}+(s-1)t-s+\frac{1}{s}$	$-s^2t^2+\frac{s^2t-s}{z}+z\left(st^2-t\right)+1$
4.53	$\frac{\frac{1}{s^3}-\frac{1}{s}}{t^2}+\frac{1-\frac{1}{s^2}}{t}+\frac{\frac{1}{s^4}-\frac{1}{s^3}}{t^4}+\frac{\frac{1}{s^2}-\frac{1}{s^4}}{t^3}+\frac{1}{s}-1$	0
4.54	$\frac{\frac{1}{s^2}-\frac{1}{s}}{t^3}+\frac{2-\frac{2}{s^2}}{t^2}+\frac{\frac{1}{s^2}-s+\frac{2}{s}-2}{t}+s-\frac{1}{s}$	0
4.55	0	0
4.56	0	0
4.57	$\frac{\frac{1}{s}-\frac{1}{s^2}}{t^2}+\frac{1}{s^2}+\frac{\frac{1}{s}-1}{t}+\left(1-\frac{1}{s}\right)t-\frac{1}{s}$	$\frac{\frac{1}{s^2t}+\frac{1}{st^2}-\frac{1}{s}-\frac{1}{t}}{z}-\frac{1}{s^2t^2}+1$
4.58	0	0
4.59	0	0
4.60	$\frac{\frac{1}{s}-1}{t}+(1-s)t+s-\frac{1}{s}$	$s^2t^2+\frac{s-s^2t}{z}+z\left(t-st^2\right)-1$

Appendix D (Continued)

Knot	Sawollek	z-Parity Alexander
4.61	$\frac{\frac{2}{s^3}-\frac{2}{s}}{t^2}+\frac{-\frac{2}{s^2}+\frac{1}{s}+1}{t}+\frac{\frac{1}{s^4}-\frac{1}{s^3}}{t^4}+\frac{-\frac{1}{s^4}-\frac{1}{s^3}+\frac{2}{s^2}}{t^3}+\frac{1}{s}-1$	$\frac{1}{s^2t^2}+z\left(\frac{1}{s}-\frac{1}{s^2t}\right)+\frac{\frac{1}{t}-\frac{1}{st^2}}{z}-1$
4.62	$\frac{1}{s^3}+\left(1-\frac{1}{s^2}\right)t+\frac{\frac{3}{s^2}-s+\frac{1}{s}-3}{t}+\frac{-\frac{1}{s^3}-\frac{2}{s^2}+\frac{2}{s}+1}{t^2}+s-\frac{3}{s}+1$	$\frac{s-\frac{1}{t}}{z}+z\left(\frac{1}{t}-s\right)$
4.63	$-\frac{1}{s^2}+\frac{-\frac{1}{s^3}-\frac{1}{s^2}+\frac{2}{s}}{t^2}+\frac{\frac{1}{s^3}+\frac{2}{s^2}-\frac{1}{s}-2}{t}-\frac{1}{s}+2$	$\frac{\frac{1}{s}-t}{z}+z\left(t-\frac{1}{s}\right)$
4.64	$\left(s^2-\frac{1}{s}\right)t+\frac{s-\frac{1}{s^2}}{t}-s^2+\frac{1}{s^2}-s+\frac{1}{s}$	$s^2t^2+z\left(s-s^2t\right)+\frac{t-st^2}{z}-1$
4.65	$\frac{\frac{1}{s}-\frac{1}{s^2}}{t^3}+\frac{-\frac{1}{s^2}+\frac{2}{s}-1}{t^2}+\frac{\frac{1}{s^2}-1}{t}+\frac{1}{s^2}+\left(1-\frac{1}{s}\right)t-\frac{2}{s}+1$	$-\frac{1}{s^2t^2}+\frac{\frac{1}{s^2t}-\frac{1}{s}}{z}+z\left(\frac{1}{st^2}-\frac{1}{t}\right)+1$
4.66	$\left(\frac{1}{s^2}+s-2\right)t+\frac{-\frac{1}{s^2}-s+2}{t}+\left(s-\frac{1}{s}\right)t^2+\frac{1-\frac{1}{s}}{t^2}-s+\frac{2}{s}-1$	$\frac{s-\frac{1}{t}}{z}+z\left(\frac{1}{t}-s\right)$
4.67	$(s-1)t^2+\left(\frac{1}{s}-1\right)t+\frac{1-\frac{1}{s}}{t}-s+1$	$\frac{\frac{1}{s}-t}{z}+z\left(t-\frac{1}{s}\right)$
4.68	0	$-s^2t^2+\frac{s^2t-s}{z}+z\left(st^2-t\right)+1$
4.69	$\frac{\frac{2}{s}-\frac{2}{s^3}}{t^2}+\frac{\frac{2}{s^2}-\frac{1}{s}-1}{t}+\frac{\frac{1}{s^3}-\frac{1}{s^4}}{t^4}+\frac{\frac{1}{s^4}+\frac{1}{s^3}-\frac{2}{s^2}}{t^3}-\frac{1}{s}+1$	$-\frac{1}{s^2t^2}+z\left(\frac{1}{s^2t}-\frac{1}{s}\right)+\frac{\frac{1}{st^2}-\frac{1}{t}}{z}+1$
4.70	$\frac{\frac{1}{s^3}-\frac{1}{s}}{t^2}+\frac{1}{s^2}+\frac{-\frac{1}{s^3}-\frac{1}{s^2}+\frac{1}{s}+1}{t}-1$	$\frac{-\frac{1}{s^2t}-\frac{1}{st^2}+\frac{1}{s}+\frac{1}{t}}{z}+\frac{1}{s^2t^2}-1$
4.71	0	0
4.72	0	0
4.73	$\frac{1-\frac{1}{s^4}}{t^2}+\frac{\frac{2}{s^2}-\frac{2}{s}}{t^3}-\frac{1}{s^2}+\frac{\frac{2}{s^3}-\frac{2}{s^2}}{t}+\frac{\frac{1}{s^4}-\frac{2}{s^3}+\frac{1}{s^2}}{t^4}+\frac{2}{s}-1$	0

Appendix D (Continued)

Knot	Sawollek	z-Parity Alexander
4.74	$\frac{\frac{1}{s}-\frac{1}{s^2}}{t^3}+\frac{\frac{1}{s^2}+s-\frac{2}{s}}{t}+\frac{\frac{2}{s}-2}{t^2}-s-\frac{1}{s}+2$	0
4.75	0	0
4.76	0	0
4.77	0	0
4.78	$\frac{\frac{1}{s^4}-\frac{1}{s}}{t}-\frac{1}{s^3}+\frac{\frac{1}{s}-\frac{1}{s^2}}{t^3}+\frac{\frac{1}{s^2}-1}{t^2}+\frac{\frac{1}{s^3}-\frac{1}{s^4}}{t^4}+1$	$z\left(\frac{1}{s^2t}+\frac{1}{st^2}-\frac{1}{s}-\frac{1}{t}\right)-\frac{1}{s^2t^2}+1$
4.79	$\frac{1}{s^3}+\left(\frac{1}{s}-\frac{1}{s^2}\right)t+\frac{\frac{1}{s^2}-\frac{1}{s}}{t}-\frac{1}{s^2}+\frac{\frac{1}{s^2}-\frac{1}{s^3}}{t^2}$	$\frac{-\frac{1}{s^2t}-\frac{1}{st^2}+\frac{1}{s}+\frac{1}{t}}{z}+\frac{1}{s^2t^2}-1$
4.80	$\frac{1-\frac{1}{s^4}}{t}+\frac{1}{s^3}+\frac{\frac{1}{s^4}-\frac{1}{s^3}}{t^4}-1$	0
4.81	$-\frac{1}{s^3}+\left(\frac{1}{s^2}-1\right)t+\frac{\frac{1}{s^3}-\frac{1}{s^2}}{t^2}+1$	0
4.82	$\frac{\frac{1}{s}-\frac{1}{s^2}}{t^3}+\frac{\frac{1}{s^4}-\frac{1}{s^2}}{t^4}+\frac{\frac{1}{s^3}+\frac{1}{s^2}-\frac{2}{s}}{t}+\frac{-\frac{1}{s^4}-\frac{1}{s^3}+\frac{1}{s^2}+\frac{1}{s}}{t^2}$	$z^2\left(\frac{1}{st}-\frac{1}{s^2t^2}\right)+\frac{\frac{1}{st}-\frac{1}{s^2t^2}}{z^2}+\frac{2}{s^2t^2}-\frac{2}{st}$
4.83	$\frac{1}{s^3}+\frac{1-\frac{1}{s^2}}{t^2}+\left(s-\frac{1}{s^2}\right)t+\frac{1}{s^2}+\frac{-\frac{1}{s^3}+\frac{1}{s^2}-s+\frac{1}{s}}{t}-\frac{1}{s}-1$	$z^2(1-st)+\frac{1-\frac{1}{st}}{z^2}+st+\frac{1}{st}-2$
4.84	$\frac{\frac{1}{s^2}-1}{t^2}-\frac{1}{s^2}+\left(\frac{1}{s}-1\right)t+\frac{s-\frac{2}{s}+1}{t}-s+\frac{1}{s}+1$	$z^2\left(\frac{1}{st}-\frac{1}{s^2t^2}\right)+\frac{\frac{1}{st}-\frac{1}{s^2t^2}}{z^2}+\frac{2}{s^2t^2}-\frac{2}{st}$
4.85	$\frac{\frac{1}{s^2}-1}{t^2}-\frac{1}{s^2}+\left(\frac{1}{s}-s\right)t+\frac{s-\frac{1}{s}}{t}+1$	$\frac{1}{s^2t^2}-\frac{1}{s^2}+s(-t)+\frac{s}{t}+\frac{t}{s}-\frac{1}{st}-\frac{1}{t^2}+1$
4.86	$\frac{1-\frac{1}{s^2}}{t^2}+\frac{1}{s^2}+\left(s-\frac{1}{s}\right)t+\frac{\frac{1}{s}-s}{t}-1$	$-\frac{1}{s^2t^2}+\frac{1}{s^2}+st-\frac{s}{t}-\frac{t}{s}+\frac{1}{st}+\frac{1}{t^2}-1$
4.87	$\frac{\frac{1}{s^3}-1}{t^2}-\frac{1}{s^3}+\frac{\frac{1}{s^2}-\frac{1}{s^4}}{t^4}+\frac{\frac{1}{s^4}-\frac{1}{s^2}}{t}+1$	$z^2\left(\frac{1}{s^2t^2}-1\right)-\frac{1}{s^2t^2}+1$
4.88	$\left(1-\frac{1}{s^2}\right)t+\frac{1}{s^2}+\left(\frac{1}{s}-1\right)t^2-\frac{1}{s}$	$\frac{\frac{1}{s^2t^2}-1}{z^2}-\frac{1}{s^2t^2}+1$

Appendix D (Continued)

Knot	Sawollek	z-Parity Alexander
4.89	$\frac{1-\frac{1}{s^4}}{t^2}+\frac{1}{s^2}+\frac{\frac{1}{s^4}-\frac{1}{s^2}}{t^4}-1$	$\frac{1}{s^4t^4}-\frac{1}{s^4t^2}-\frac{1}{s^2t^4}+\frac{1}{s^2}+\frac{1}{t^2}-1$
4.90	0	0
4.91	$\frac{\frac{1}{s}-\frac{1}{s^4}}{t^4}+\frac{\frac{1}{s^3}-\frac{1}{s}}{t^2}-\frac{1}{s^3}+\frac{\frac{1}{s^2}-1}{t^3}+\frac{\frac{1}{s^4}-\frac{1}{s^2}}{t}+1$	0
4.92	$\frac{\frac{1}{s^4}-\frac{1}{s}}{t^4}+\frac{\frac{1}{s}-\frac{1}{s^4}}{t}+\frac{1-\frac{1}{s^3}}{t^3}+\frac{1}{s^3}-1$	0
4.93	$\frac{\frac{1}{s^3}-1}{t}-\frac{1}{s^3}+\frac{\frac{1}{s}-\frac{1}{s^2}}{t^2}+\left(\frac{1}{s^2}-\frac{1}{s}\right)t+1$	$\frac{\frac{1}{s^2t^2}-1}{z^2}-\frac{1}{s^2t^2}+1$
4.94	$\frac{\frac{1}{s^3}-\frac{1}{s}}{t^2}+\frac{\frac{1}{s}-\frac{1}{s^2}}{t}+\frac{\frac{1}{s^2}-\frac{1}{s^3}}{t^3}$	0
4.95	$\frac{\frac{1}{s^3}-1}{t^3}-\frac{1}{s^3}+\frac{s-\frac{1}{s^2}}{t^2}+\left(\frac{1}{s^2}-s\right)t+1$	0
4.96	$\frac{\frac{1}{s^3}-\frac{1}{s}}{t^3}+\frac{\frac{1}{s}-\frac{1}{s^3}}{t}+\frac{1-\frac{1}{s^2}}{t^2}+\frac{1}{s^2}-1$	$z^2\left(\frac{1}{st}-\frac{1}{s^2t^2}\right)+\frac{\frac{1}{st}-\frac{1}{s^2t^2}}{z^2}+\frac{2}{s^2t^2}-\frac{2}{st}$
4.97	$\frac{\frac{1}{s^2}-s}{t^2}+\frac{s^2+s-\frac{2}{s}}{t}-s^2-\frac{1}{s^2}+\left(\frac{1}{s}-1\right)t+\frac{1}{s}+1$	$z^2(1-st)+\frac{1-\frac{1}{st}}{z^2}+st+\frac{1}{st}-2$
4.98	0	0
4.99	0	0
4.100	$\frac{\frac{1}{s^3}-\frac{1}{s}}{t^2}+\frac{1-\frac{1}{s^2}}{t}+\frac{\frac{1}{s^4}-\frac{1}{s^3}}{t^4}+\frac{\frac{1}{s^2}-\frac{1}{s^4}}{t^3}+\frac{1}{s}-1$	0
4.101	$\frac{1}{s^3}+\frac{1-\frac{1}{s^2}}{t^3}+\left(1-\frac{1}{s^2}\right)t+\frac{\frac{3}{s^2}-3}{t}+\frac{-\frac{1}{s^3}-\frac{1}{s^2}-s+\frac{3}{s}}{t^2}+s-\frac{3}{s}+1$	0
4.102	$\left(s^2+\frac{1}{s^2}-2\right)t+\frac{-s^2-\frac{1}{s^2}+2}{t}+\left(s-\frac{1}{s}\right)t^2+\frac{s-\frac{1}{s}}{t^2}-2s+\frac{2}{s}$	0
4.103	$\frac{\frac{1}{s^3}-1}{t^3}+\frac{s-\frac{1}{s^2}}{t^2}+\frac{\frac{1}{s^2}-\frac{1}{s^3}}{t}+\left(\frac{1}{s}-s\right)t-\frac{1}{s}+1$	$\frac{1-\frac{1}{s^2t^2}}{z^2}+\frac{1}{s^2t^2}-1$
4.104	$\left(\frac{1}{s}-s^2\right)t^2+\frac{\frac{1}{s^2}-s}{t^2}+\left(s-\frac{1}{s^2}\right)t+\frac{s^2-\frac{1}{s}}{t}$	0

Appendix D (Continued)

Knot	Sawollek	z-Parity Alexander
4.105	0	0
4.106	$\frac{\frac{1}{s}-\frac{1}{s^3}}{t^3}+\frac{\frac{1}{s^3}-\frac{1}{s}}{t}+\frac{\frac{1}{s^2}-1}{t^2}-\frac{1}{s^2}+1$	$-\frac{1}{s^3t^3}+\frac{1}{s^3t}+\frac{1}{s^2t^2}-\frac{1}{s^2}+\frac{1}{st^3}-\frac{1}{st}-\frac{1}{t^2}+1$
4.107	$\left(1-s^2\right)t^2+\frac{1-\frac{1}{s^2}}{t^2}+s^2+\frac{1}{s^2}+\left(2s-\frac{2}{s}\right)t+\frac{\frac{2}{s}-2s}{t}-2$	$s^2\left(-t^2\right)-\frac{1}{s^2t^2}+s^2+\frac{1}{s^2}+2st-\frac{2s}{t}-\frac{2t}{s}+\frac{2}{st}+t^2+\frac{1}{t^2}-2$
4.108	0	0

Appendix E

Z-PARITY ALEXANDER BIQUANDLE CALCULATORS

The following Mathematica program computes the Parity Alexander Polynomial and Sawollek Polynomial for virtual knots using the planar diagram conventions given in Section B.1. Given a planar diagram code `PD[-]`, for a virtual knot run `SawollekPoly[PD[-]]` for the Sawollek Polynomial and `ParityBiquandle[PD[-]]` for the z-Parity Alexander Biquandle.

```
np[L_PD] := Count[L, _X];

nm[L_PD] := Count[L, _Y];


rule1 = {X[a_, b_, c_, d_] :> {c == (t*a + (1 - s*t) d), b == s d},

   Y[a_, b_, c_, d_] :> {c == (1/s) a,

     b == ((1/t) d + (1 - (1/s) (1/t)) a)}};


ruleP = {Odd[a_, b_, c_, d_] :> {c == a/z, b == z* d}};


ParityPD[L_PD] :=

 Sort[L /. {X[i_, j_, k_, l_] :>

      Odd[i, j, k, l] /; OddQ[i - j]} /. {Y[i_, j_, k_, l_] :>

     Odd[i, j, k, l] /; OddQ[i - j]}]


Sawollek[s_, t_] :=
```

Appendix E (Continued)

```
 Expand[Det[
   Extract[Normal[ CoefficientArrays[Flatten[s /. rule1], t]], {2}]]]
SawollekPoly[
  L_PD] := ((-1)^(np[L] - nm[L]))*(Sawollek[
    ReplacePart[L /. {x_Integer :> X[x]}, 0 -> List],
    Range[2*Length[L]] /. {x_Integer :> X[x]}])


PP[s_, t_] :=
 Expand[Det[
   Extract[Normal[
     CoefficientArrays[Flatten[s /. rule1 /. ruleP], t]], {2}]]]
ParityBiquandle[
  L_PD] := ((-1)^(np[L] - nm[L]))*(PP[
    ReplacePart[ParityPD[L] /. {x_Integer :> X[x]}, 0 -> List],
    Range[2*Length[L]] /. {x_Integer :> X[x]}])
```

CITED LITERATURE

1. Kauffman, L.: A self-linking invariant of virtual knots. Fund. Math., 184:135–158, 2004.

2. Manturov, V.: Parity in knot theory. Mat. Sb., 201(5–6):693–733, 2010.

3. Kauffman, L.: Virtual knot theory. European J. Combin., 20:663–690, 1999.

4. Goussarov, M., Polyak, M., and Viro, O.: Finite type invariants of classical and virtual knots. Topology, 39(5):1045–1068, 2000.

5. Kauffman, L.: Introduction to virtual knot theory, Jan 2011. arXiv:1101.0665v1.

6. Manturov, V.: A functorial map from knots in thickened surfaces to classical knots and generalisations of parity, Nov 2010. arXiv:1011.4640.

7. Turaev, V.: Cobordism of knots on surfaces. J. Topol., 1(2):285–305, 2008.

8. Dye, H.: Invariants from the linking number, Jul 2010. arXiv:1007.1175.

9. Ilyutko, D., Manturov, V., and Nikonov, I.: Virtual knot invariants arising from parities, Feb 2011. arXiv:1102.5081.

10. Krylov, D. and Manturov, V.: Parity and relative parity in knot theory, Dec 2010. arXiv:1101.0128.

11. Kauffman, L.: New invariants in the theory of knots. Amer. Math. Monthly, 95(3):195–242, 1988.

12. Kauffman, L.: On Knots. Princeton, NJ, Princeton University Press, 1987.

13. Kauffman, L.: An extended bracket polynomial for virtual knots and links. J. Knot Theory Ramifications, 18(10):1369–1422, 2009.

14. Dye, H. and Kauffman, L.: Minimal surface representations of virtual knots and links. Algebr. Geom. Topol., 5:509–535, 2005.

15. Dye, H. and Kauffman, L.: Virtual crossing number and the arrow polynomial. J. Knot Theory Ramifications, 18(10):1335–1357, 2009.

16. Khovanov, M.: A categorification of the jones polynomial. Duke Math. J., 101(3):359–426, 2000.

17. Bar-Natan, D.: On Khovanov's categorification of the Jones polynomial. Algebr. Geom. Topol., 2:337–370, 2002.

18. Bar-Natan, D.: Khovanov's homology for tangles and cobordisms. Geom. Topol., 9:1443–1499, 2005.

19. Rasmussen, J.: Khovanov homology and the slice genus. Invent. Math., 182(2):419–447, 2010.

20. Lee, E.: An endomorphism of the Khovanov invariant. Adv. Math., 197(2):554–586, 2005.

21. Kronheimer, P. and Mrowka, T.: Khovanov homology is an unknot-detector, May 2010. arXiv:1005.4346.

22. Viro, O.: Virtual links, orientations of chord diagrams and Khovanov homology. Proceedings of 12th Gokova Geometry-Topology Conference, pages 184–209, 2006.

23. Asaeda, M., Przytycki, J., and Sikora, A.: Categorification of the Kauffman bracket skein module of I-bundles over surfaces. Algebr. Geom. Topol., 4:1177–1210, 2004.

24. Manturov, V.: Khovanov homology for virtual knots with arbitrary coefficients. J. Knot Theory Ramifications, 16(3):345–377, 2007.

25. Dye, H., Kauffman, L., and Manturov, V.: On two categorifications of the arrow polynomial for virtual knots. In The Mathematics of Knots, eds. M. Banagl and V. D., volume 1, pages 95–124. Contributions in Mathematical and Computational Sciences, 2011.

26. Sawollek, J.: On Alexander-Conway polynomials for virtual knots and links, Jan 2001. arXiv:math/9912173v2.

27. Nelson, S.: Link invariants from finite biracks, Dec 2010. arXiv:1002.3842.

28. Fenn, R., Jordan-Santana, M., and Kauffman, L.: Biquandles and virtual links. Topology and its Applications, 145:157–175, 2004.

29. Kauffman, L. and Manturov, V.: Virtual biquandles. Fundamenta Mathematicae, 188:103–146, 2005.

30. Hrencecin, D. and Kauffman, L.: Biquandles for virtual knots. J. Knot Theory Ramifications, 16(10):1361–1382, 2007.

31. Kauffman, L. and Radford, D.: Bi-oriented quantum algebras, and a generalized Alexander polynomial for virtual links. In Diagrammatic morphisms and applications, volume 318 of Contemp. Math., pages 113–140, Providence, RI, 2003. Amer. Math. Soc.

32. Bartholomew, A. and Fenn, R.: Biquandles of small size and some invariants of virtual and welded knots, Jan 2010. arXiv:1001.5127.

33. Bartholomew, A. and Fenn, R.: Quaternionic invariants of virtual knots and links. J. Knot Theory Ramifications, 17(2):231–251, 2008.

34. Green, J.: A table of virtual knots, Aug 2010. `http://www.math.toronto.edu/~drorbn/Students/GreenJ/`.

35. Khovanov, M.: A functor-valued invariant of tangles. Algebr. Geom. Topol., 2:66541, 2002.

36. Wehrli, S.: A spanning tree model for Khovanov homology. J. Knot Theory Ramifications, 17(12):1561–1574, 2008.

37. Shumakovitch, A.: Torsion of the Khovanov homology, May 2004. arXiv:math.GT/0405474.

38. Elliot, A.: State cycles, quasipositive modification, and constructing H-thick knots in Khovanov homology. Doctoral dissertation, Rice University, 2010.

39. Hatcher, A.: Pants decompositions of surfaces, Jun 1999. arXiv:math/9906084.

40. Manturov, V.: Knot theory. Boca Raton, FL, Chapman & Hall / CRC, 2004.

41. Manturov, V.: Minimal diagrams of classical and virtual links, Jan 2005. arXiv:math/0501393.

42. Kauffman, L. and Lambropoulou., S.: Classifying and applying rational knots and rational tangles. In Physical knots: knotting, linking, and folding geometric objects in $\mathbb{R}^3$, volume 304, pages 223–259. Providence, RI, Amer. Math. Soc., 2002.

43. Jablan, S. and Sazdanovic, R.: LinKnot, Sep 2010. http://math.ict.edu.rs:8080/webMathematica/LinkSL/.

44. Kauffman, L.: Knots and Physics. Series on Knots and Everything. River Edge, NJ, World Scientific Publishing Co, 3 edition, 2001.

45. Crowell, R. and Fox, R.: Introduction to Knot Theory. Boston, MA, Ginn and Co, 1963.

46. Jaeger, F., Kauffman, L., and Saleur, H.: The Conway polynomial in r^3 and in thickened surfaces: A new determinant formulation. J. Combin. Theory Ser. B, 61:237–259, 1994.

47. Bar-Natan, D.: The jones polynomial - the knot atlas, Dec 2008. http://katlas.org/wiki/The_Jones_Polynomial.

48. Manturov, V.: On invariants of virtual links. Acta Appl. Math., 72(3):295–309, 2002.

49. Dye, H.: Unitary solutions to the yang-baxter equation in dimension four. Quantum Inf. Process, 2(1–2):117–151, 2002.

50. Wada, M.: Twisted Alexander polynomial for finitely presentable groups. Topology, 33(2):241–256, 1994.

51. Silver, D. and Williams, S.: Alexander groups and virtual links. J. Knot Theory Ramifications, 10(1):151–160, 2001.

52. Baldwin, J. and Gillam, W.: Computations of Heegaard-Floer knot homology, Jan 2007. arXiv:math.GT/0610167.

53. Clark, D., Morrison, S., and Walker, K.: Fixing the functoriality of Khovanov homology. Geom. Topol., 13(3):1499–1582, 2009.

VITA

Curriculum Vitae for Aaron Kaestner

Contact Information

Address:	Department of Mathematics, Statistics, and Computer Science (MC 249)
	University of Illinois at Chicago
	851 S. Morgan St.
	Chicago, IL 60607
Telephone:	(314)-368-1998
E-mail:	akaestne@math.uic.edu
URL:	`http://www.math.uic.edu/~akaestne`

Personal Data

Date of Birth:	20 November 1980
Place of Birth:	St. Louis, MO
Nationality:	US

Education

1998–2002	BS	Mathematics	Indiana University
2002–2004	MA	Mathematics	St. Louis University
2006–2011	PhD	Mathematics	University of Illinois at Chicago

Dissertation Adviser: Louis Kauffman

Dissertation Title: Applications of Parity in Virtual Knot Theory

Employment History

- 2002 - 2004 Teaching Assistant - St. Louis University
- 2004 - 2005 Mathematics Instructor - St. Joseph's College Prep - Westchester, IL
- 2005 - 2006 Asst. Tech. Director - St. Joseph's College Prep - Westchester, IL
- 2006 - 2011 Teaching Assistant - University of Illinois at Chicago

Research Publications

1. (with L. Kauffman) *A Categorification of the Arrow Polynomial: Computations and Examples.* In preparation.
2. (with L. Kauffman) *Parity, Khovanov Homology and Categorifications of the Arrow Polynomial.* In preparation.
3. (with L. Kauffman) *Parity Biquandles.* Submitted.

Conference Talks

1. A Categorification of the Arrow Polynomial: Computations and Examples, Knots In Chicago, September 2010
2. On the Khovanov Homology of Virtual Knots, AMS Sectional Meeting #1063: Special Session on Algebraic Structures in Knot Theory, October 2010
3. Applications of Parity in Virtual Knot Theory, Joint Math Meeting, New Orleans, LA January 2011

Invited Talks

1. An Introduction to Knot Theory, Webster University Math Club, December 2010.

Teaching Experience

- Spring 2011: MTHT 430 - Formal Logic I: Logic Across the High School Curriculum
- Fall 2010: Math 181 - Calculus II
- Summer 2010: MTHT 490 - Topics in Teaching Secondary Mathematics: Making Sense of Numbers and Symbols
- Spring 2010: Grader for Math 320 - Linear Algebra
- Fall 2009: Math 180 - Calculus I
- Summer 2009: Math 160 - Finite Math for Business
- Spring 2009: Math 160 - Finite Math for Business
- Fall 2008: Math 165 - Business Calculus
- Spring 2008: Math 180 - Calculus I
- Fall 2007: Math 165 - Business Calculus
- Summer 2007: Math 118 - Mathematical Reasoning
- Spring 2007: Math 160 - Finite Math for Business
- Fall 2006: Math 075 - Beginning Algebra

- Fall 2003: MT-A120 - College Algebra
- Spring 2003: MT-A120 - College Algebra
- Fall 2002: MT-A120 - College Algebra

Other Professional Experiences & Skills

1. Assisted Prof. Bonnie Saunders and Prof. John Baldwin in developing on-line curriculum for MTHT 490 and MTHT 430
2. Familiarity with programming in Mathematica

Major areas of research interest

Knot Theory, Virtual Knot Theory, Categorification, Knot and Link Homology Theories, Quandles and Biquandles